1-1-1993

Melt crystallization of ferroelectric copolymers of poly(vinylidene fluoride-trifluoroethylene)/

Katherine Antolin Bakeev
University of Massachusetts Amherst

MELT CRYSTALLIZATION OF FERROELECTRIC COPOLYMERS OF POLY(VINYLIDENE FLUORIDE-TRIFLUOROETHYLENE)

A Dissertation Presented

by

KATHERINE ANTOLIN BAKEEV

Submitted to the Graduate School of the
University of Massachusetts in partial fulfillment
of the requirements for the degree of

DOCTOR OF PHILOSOPHY

September 1993

Polymer Science and Engineering

MELT CRYSTALLIZATION OF FERROELECTRIC COPOLYMERS OF POLY(VINYLIDENE FLUORIDE-TRIFLUOROETHYLENE)

A Dissertation Presented

by

KATHERINE ANTOLIN BAKEEV

Approved as to style and content by:

Shaw Ling Hsu, Chair

William J. MacKnight, Member

Bret E. Jackson, Member

William J. MacKnight, Department Head
Polymer Science and Engineering

ACKNOWLEDGEMENTS

I would like to thank my advisor Professor Shaw Ling Hsu for his guidance during the course of this research. I thank him also for the opportunity to work in several interesting areas of research during my graduate work. I am also thankful to Professors William MacKnight and Bret Jackson for serving on my committee and for their valuable comments to my work.

I wish to acknowledge the help of Professor Yinkang Wang and Dr. Alan Waddon in teaching me about X-ray and giving so unselfishly of their time in helping me to carry out and analyze many of the experiments. I also thank Professor N. F. Bakeev of the Karpov Institute of Physical Chemistry for his help in carrying out the variable temperature X-ray experiments.

I also thank the members of my research group for the fruitful discussions that we've had over the years. Especially I would like to acknowledge Wanda Walczak and Nick Reynolds for their valuable experimental assistance, comments and criticisms. Thanks go to Jennifer Hsu and Su-Yen for their help in writing the temperature controller program.

For his efforts in the critical reading of my manuscript and interesting scientific discussions, I thank Mohan Srinivosarao.

I thank my friends Geni Dessipri, Susan Dawson, and Brian Milas for making my stay in Amherst enjoyable and memorable, and for all the chocolate chip cookies. I thank the many friends whom I have met and have helped me to maintain a balance of life and taught me so many things in addition to science, especially Denis Melot, Karen Winey, Jürgen Pionteck, Mardye Lindway, Jim Thomas and Afranio Torres.

I give the warmest thanks for my husband Kirill and my family for their love and encouragement throughout my work.

ABSTRACT

MELT CRYSTALLIZATION OF FERROELECTRIC COPOLYMERS OF POLY(VINYLIDENE FLUORIDE-TRIFLUOROETHYLENE)

SEPTEMBER 1993

KATHERINE ANTOLIN, B.S., CASE WESTERN RESERVE UNIVERSITY

Ph.D., UNIVERSITY OF MASSACHUSETTS AMHERST

Directed by: Professor Shaw Ling Hsu

This dissertation is a study of the phase transition and melt crystallization of ferroelectric copolymers of poly(vinylidene fluoride-trifluoroethylene) [P(VDF-TrFE)] containing 83 mol% poly(vinylidene fluoride). The microstructure of crystallized P(VDF-TrFE) are characterized by vibrational spectroscopy to determine their chain conformation distribution, wide-angle X-ray diffraction (WAXD) to measure the crystal structure and determine the content of α and β crystal phases. Differential scanning calorimetry (DSC) is used to measure the transition temperatures and their enthalpies.

P(VDF-TrFE) is a polymorphic system exhibiting a Curie transition below its melting temperature, at which the copolymer undergoes a long range conformational change from a predominantly trans structure (β phase) which can be ferroelectric, to a structure which has a mixture of trans and gauche conformations and is called the paraelectric α phase. Variable temperature FTIR studies have been made to follow the phase transition and to understand the multiple phase behavior that has been suggested for these copolymers. Factor analysis has been applied to the FTIR data to determine the number of crystal phases present for this copolymer composition.

Melt crystallization under nonisothermal and isothermal conditions has been used to modify the structure of the copolymers and change both the Curie and melting temperatures. It is found that with slow cooling rates from the melt through the crystallization temperature, there is a stabilization of the paraelectric α phase which is then retained to different degrees on passing through the Curie transition on cooling. Under all crystallization conditions the copolymers exhibit two Curie transitions on cooling whose temperatures and intensities vary with cooling rate and crystallization time. The Curie temperature on cooling and subsequent heating is decreased upon slower cooling, reflecting an increase in the gauche chain conformers as evidenced by FT-Raman spectroscopy. WAXD data show that there are α and β phase crystals present in samples that have been cooled slowly, accompanied by an increase in interplanar spacing which indicates that the β phase also contains gauche defects. Longer isothermal crystallization at 135°C shows also that there is an increase in α phase content with longer crystallization time, though when crystallization is carried out at 135°C there is always a coexistence of α and β phases in the final room temperature structure.

Highly oriented P(VDF-TrFE) copolymers were prepared by solid-state coextrusion to aid in understanding the vibrational assignments in the copolymer. Infrared dichroism and WAXD were used to assess the sample orientation and measure the transition moment angles for some of the vibrations in the spectrum.

TABLE OF CONTENTS

LIST OF TABLES

LIST OF FIGURES

CHAPTER I

INTRODUCTION

Poly(vinylidene fluoride)

In the 1980's electrically active organic polymers emerged as a new class of materials, challenging technologies previously limited to inorganic materials. Ferroelectrics are a subgroup of pyroelectrics and piezoelectrics, and like pyroelectric materials exhibit a spontaneous polarization in the absence of an electric field and polarization switching by application of a field (1). Polymer ferroelectrics are attractive materials because they are tough, flexible, and lightweight materials. Though they have a lower piezoelectric activity than ceramic ferroelectrics, they can be easily obtained as ultrathin films, fibers, and liquid crystals. Polymers that have been identified as ferroelectrics include polyvinylidene fluoride (PVDF) and its copolymers with trifluoroethylene (P(VDF-TrFE) or tetrafluoroethylene, polyvinyl fluoride, poly(vinyl cyanide-vinyl acetate), and the odd nylons (2-4).

PVDF and its copolymers with trifluoroethylene are some of the most extensively studied systems, exhibiting, ferroelectric, piezoelectric, and pyroelectric properties that find various technological applications including sensors and transducers (2, 5-7). Piezoelectric and pyroelectric materials exhibit a change in polarization with small changes in stress and temperature respectively (1). The exact origin of the piezoelectric and ferroelectric properties of the polymers is still unknown but there are believed to be contributions from electrostriction, dipole libration, dimensional changes of the whole sample, and dimensional changes in the crystallite. Electrostriction is due to changes in the dielectric constant of the crystal, and dipole libration causes changes in the net polarization. The maximum

contribution to the piezoelectricity and ferroelectricity arises from the change in the density of CF_2 dipoles in the crystalline regions that can undergo a polarization reversal in response to a mechanical stress or electric field (1, 8). The ferroelectric properties of PVDF and its copolymers are due to the presence of a polar crystalline structure among its four polymorphic phases. The polymorphism of PVDF is by now known to include four distinct crystal phases (Figure 1.1) which have been characterized by Raman and infrared spectroscopy and shown to differ in chain conformation. The all trans chain conformation is a ferroelectric polymer crystal and exhibits the highest polarization of the crystal structures (9-11).

Though several studies have been made on the crystallization of PVDF and P(VDF-TrFE) copolymers, a thorough characterization of the crystalline structures formed under different crystallization conditions has not been carried out to date. It is known that the crystalline structure, and therefore the ferroelectric properties, depend on the crystallization conditions, but details of different crystalline structures of the copolymers prepared under various crystallization conditions have not been presented. It is the objective of this research to focus on the structural characterization of P(VDF-TrFE) copolymers that have been purified and then crystallized under different conditions. A controversy exists whether there are three unique crystalline phases or an intermediary state that is more disordered than the ferroelectric or paraelectric state.

The most important polymorph of PVDF, which possesses piezoelectric and pyroelectric properties, is the all trans β phase, packed in an orthorhombic unit cell with lattice constants a = 8.58Å, b = 4.91Å, and c = 2.56Å. In the β phase the CH_2 and CF_2 dipoles are perpendicularly oriented to the chain axis, thus making it a polar phase. The other crystal phases are referred to as α, α_p, and γ. The α phase, with a trans-gauche-trans-gauche' (TGTG') chain conformation packed in a monoclinic unit cell, is the most common form obtained by crystallization from the

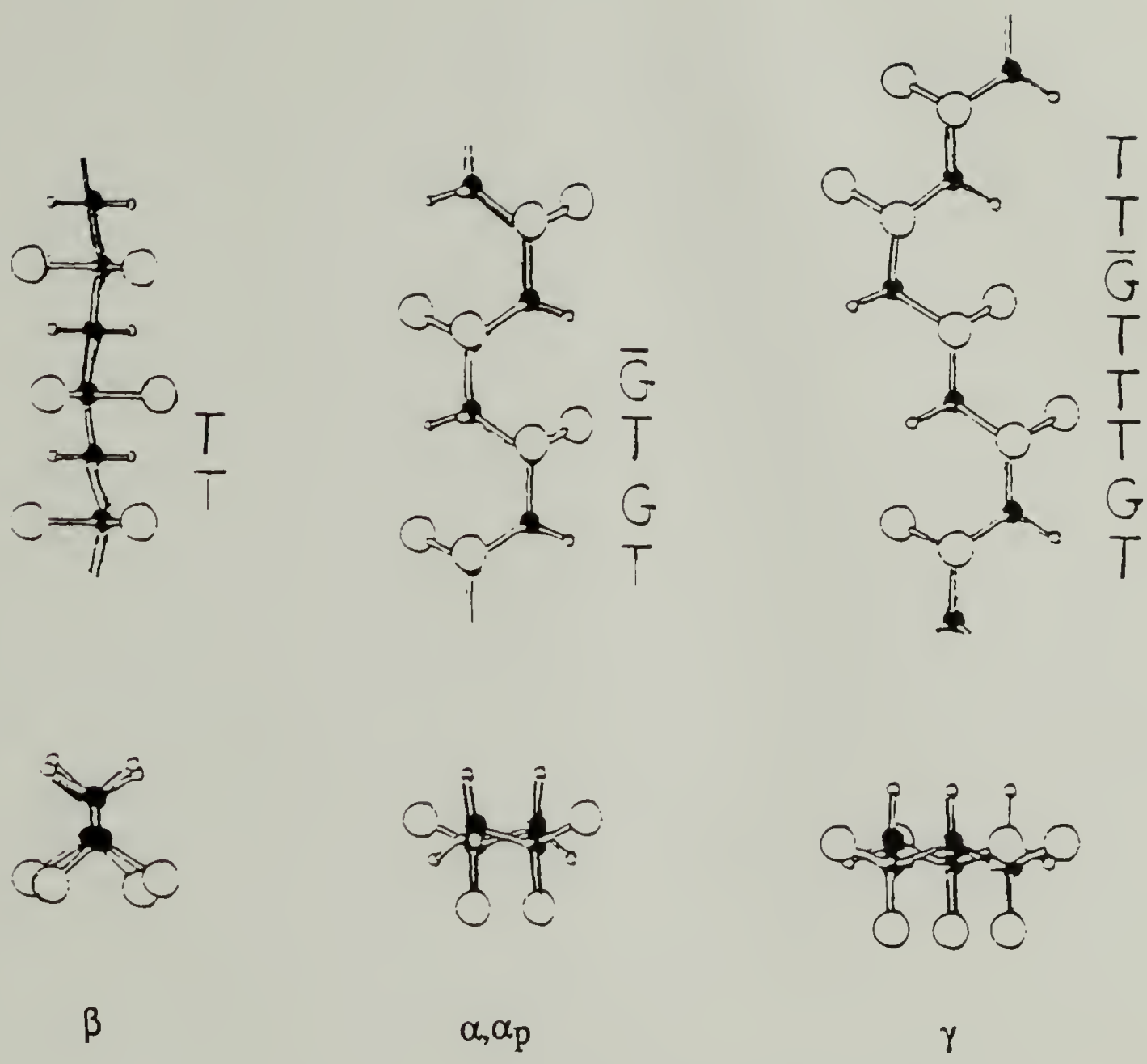

Figure 1.1 Molecular structures of the crystal phases of Poly(vinylidene fluoride). (from ref. 5)

melt. The α phase is paraelectric and has no net dipole moment though each monomer unit has a dipole moment of 2.1D. The γ phase, also packed in a monoclinic unit cell, has a conformation between that of the α and β phases with T_3GT_3G' segments and can be formed by high temperature crystallization (12), high-pressure crystallization (13), crystallization under an applied field (14, 15), or by a solid-solid transformation from the α phase (16, 17). The α_p phase is the polar counterpart of the α phase, having the same chain conformation in a 180° rotation, with a slight difference in its interchain packing.

The piezoelectric activity of a polymer film is measured by its remanent polarization, P_r, which is the polarization that remains after the removal of an electric field from a material. P_r is given by the following relation (18):

$$P_r = f_x f_\beta f_\theta P \qquad (1.1)$$

where f_x = the fraction of crystallinity

f_β = fraction of the polar β phase

f_θ = factor associated with the mean crystal orientation with respect to the film plane

P = polarization arising from the inherent dipole alignment of molecules.

From this it can be seen that by increasing the sample crystallinity, orientation, or fraction of β phase crystals an improved piezoelectric material may be obtained. The piezoelectric constants of P(VDF-TrFE) copolymers are higher than those for PVDF (d_{31} = 25-50pC/N and 15-25pC/N respectively), mainly because higher degrees of crystallinity can be attained (80-90% in P(VDF-TrFE) as opposed to ~50% in PVDF) and the dipolar alignment is retained better in the crystalline phase than in the amorphous (2, 6, 19).

To form the ferroelectric β phase in PVDF, the α crystal can be poled by applying an electric field, which results in the orientation of dipoles in the direction of the electric field. Mechanical deformation such as drawing or otherwise

uniaxially orienting the molecular chains of the paraelectric crystal phase causes an $\alpha \rightarrow \beta$ phase transformation resulting in the formation of the oriented β phase (2, 5, 20). The interconversion of the crystalline phases is shown in the diagram in Figure 1.2. From studies of the formation of the different polymorphs it is believed that the β form is thermodynamically the most stable because it is the predominant polymorph obtained as crystallization rate is lowered in melt cooling and solution casting, with the α crystalline form being kinetically favored (5, 21).

Three regions for the crystallization of PVDF from the melt have been identified from microscopic observations of spherulitic growth (22). At crystallization temperatures higher than 160°C, γ phase crystals are grown since in this temperature range the growth rate of γ phase crystals is faster than for the α phase. In the range of 150 - 160°C a mixture of α and γ phase crystals is formed, but the growth rate of the α phase crystallites is greater. At temperatures below 150°C only α phase crystals are formed due to the larger nucleation and growth rates of this phase as compared with the γ phase. Crystallization performed under a static electric field results in an increase in the nucleation rate of the γ phase and therefore the γ phase content is increased (14, 15). Detailed studies of the crystallization of PVDF have found that the resultant crystal form is very sensitive to the crystallization conditions (23). The relative amount of each phase of PVDF can be modified by applying a high electric field to the material (2).

Poly(vinylidene fluoride-trifluoroethylene) Copolymers

A major characteristic of most ferroelectric materials is a Curie transition at which polarization is lost through an order-disorder transition rendering the material paraelectric. PVDF does not exhibit such a transition as it has a melting temperature that occurs below the temperature of the Curie transition. The P(VDF-TrFE) copolymers have received much attention since Yagi et. al. (24) observed a phase transition in copolymers containing 55

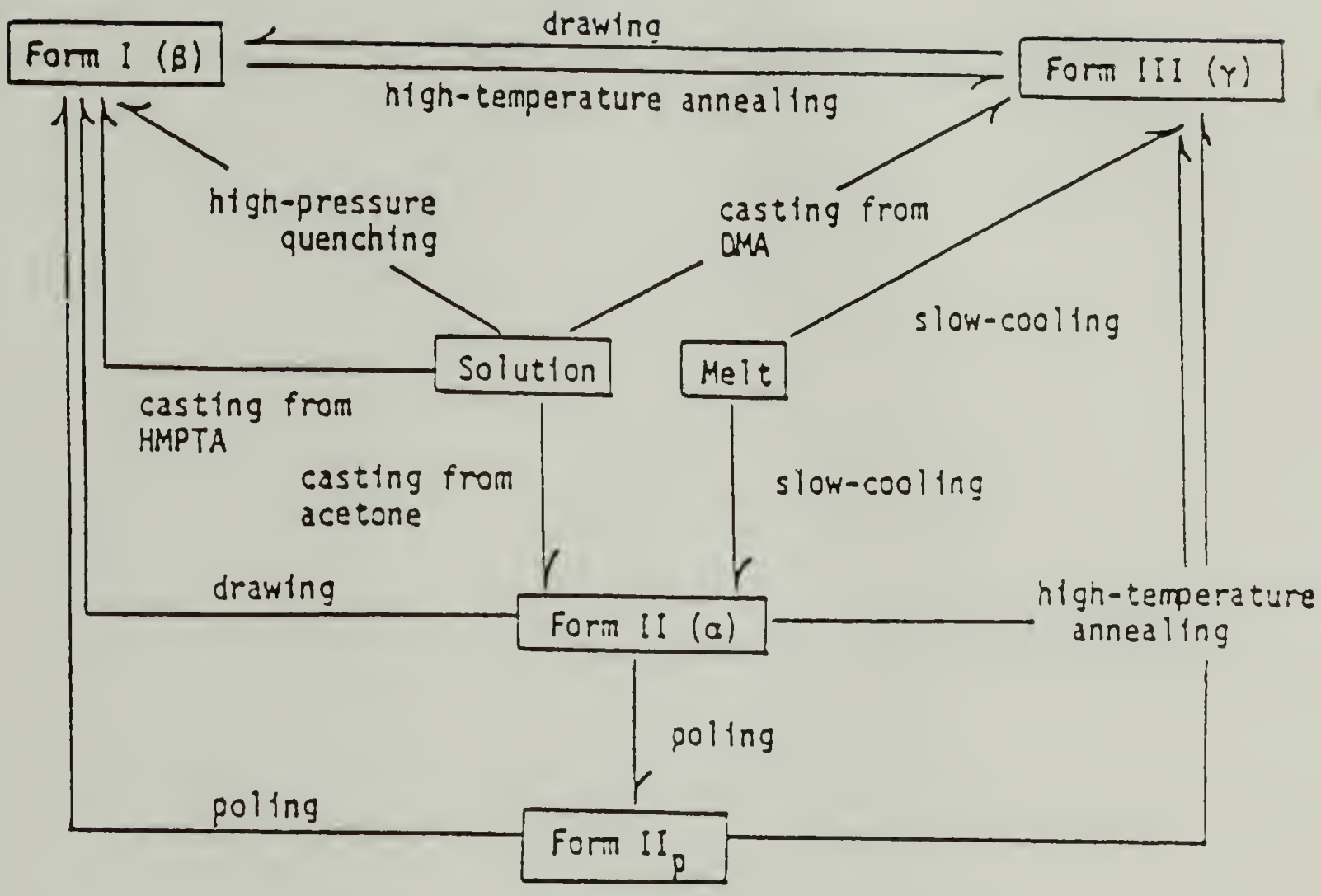

Figure 1.2 Transformation among the various crystal modifications of Poly(vinylidene fluoride). (from ref. 5)

mol % VDF and found the Curie transition to be copolymer composition dependent (5, 6, 24, 25) (Figure 1.3). At the phase transition the copolymers undergo a large scale conformational transition from the extended trans zigzag form, the ferroelectric phase, to a more contracted paraelectric crystalline phase that consists of TT, TG, and TG' rotational isomers but the details of the transition are not understood.

The transition behavior of P(VDF-TrFE) copolymers has proven to be rather complex with many factors influencing the transition temperatures and the formation of crystal phases. The trifluoroethylene unit in the copolymer favors the crystallization into the extended trans chain conformation unlike the PVDF homopolymer that requires stretching or poling of the paraelectric phases to form the β phase. This preference for the β phase can be related to the van der Waal's radii of fluorine (1.35Å) and hydrogen (1.2Å) which allow the copolymers to pack better in the β phase than the α phase (26). The copolymer composition has a strong influence on the transition behavior, with the Curie transition temperature increasing towards the melting temperature as the VDF content is increased, with a coincidence of the transitions in PVDF (5, 27-29). The Curie transition for copolymers with a high VDF content (> 70%) is a first-order transition, with a wide region of coexistence of the crystal phases, and exhibits a large expansion of the crystal lattice at the transition. The cooperative Curie transition also has a large hysteresis between heating and cooling, typical of a first-order transition (5).

The copolymer unit serves as a defect to the PVDF structure, hence changing its crystal structure as head-to-head structures do in PVDF (26, 30). The trifluorethylene units cocrystallize with the vinylidene fluoride with a preference for the ferroelectric β phase structure (26). Conformational defects such as gauche linkages in the P(VDF-TrFE) copolymer have an important role in the mechanism of the Curie transition of the system (31).

The different crystal phases of the P(VDF-TrFE) copolymer vary depending on the copolymer composition, with three crystal phases proposed for copolymers

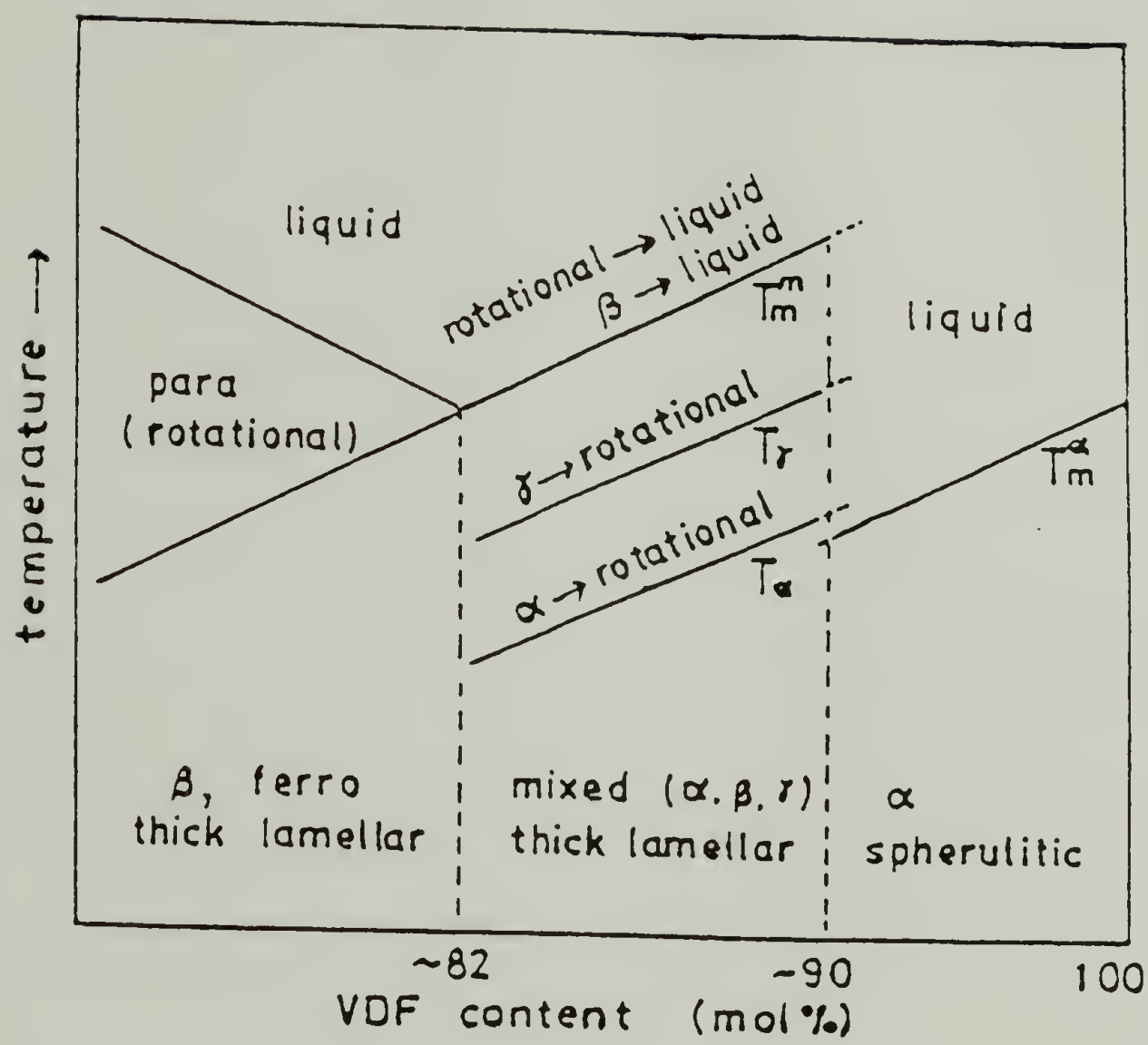

Figure 1.3 Schematic drawing of the phase diagram of Poly(vinylidene fluoride-trifluoroethylene) copolymers crystallized by annealing near the melting point or crystallized slowly from the melt. (from ref. 25)

in the range of 50-90% VDF (5, 7, 20, 25, 29, 32). These crystal phases are referred to as the low temperature phase, which is approximately the β phase of PVDF but with a monoclinic unit cell, the paraelectric high temperature phase which is comprised of a statistical combination of TT, TG, and TG' segments, and the cooled phase which may also be non-ferroelectric and has a similar chain conformation to the low temperature phase. Due to the presence of skew bonds, the cooled phase has a more disordered structure with different interplanar spacings than the low temperature phase (5, 32). Suggestions have also been made that the three crystalline phases of P(VDF-TrFE) copolymers are analogous to the α, β, and γ phases of PVDF (25, 33). A conflicting analysis has been presented by Lovinger (34) for copolymers with 52 mol % VDF, for which he claims that the copolymers do not have three distinct crystal phases, but rather at some temperatures form a mixed crystal of the α and β phases. The structural transitions between the various crystal phases depend on the processing conditions including extrusion techniques, the solvents used for film casting and their rate of evaporation, degree of molecular orientation, thermal history and polarization time, temperature and field strength used in preparing the copolymers (5, 6, 14, 18, 23, 25, 29, 33, 35-43). A phase diagram for copolymers with 80 mol % VDF and higher, proposed to have three crystal phases, is shown in Figure 1.3.

The conformational change at the Curie transition is common to all the copolymer compositions, and the transition behavior is composition dependent. For intermediate VDF content copolymers (50-60%), the transition on heating is from the low temperature phase, through the cooled phase, to the high temperature phase. For copolymers with a high VDF content only the low temperature and high temperature phases are observed with change of temperature (20). A typical DSC thermogram for the P(VDF-TrFE) copolymer with 83 mol % VDF is shown in Figure 1.4.

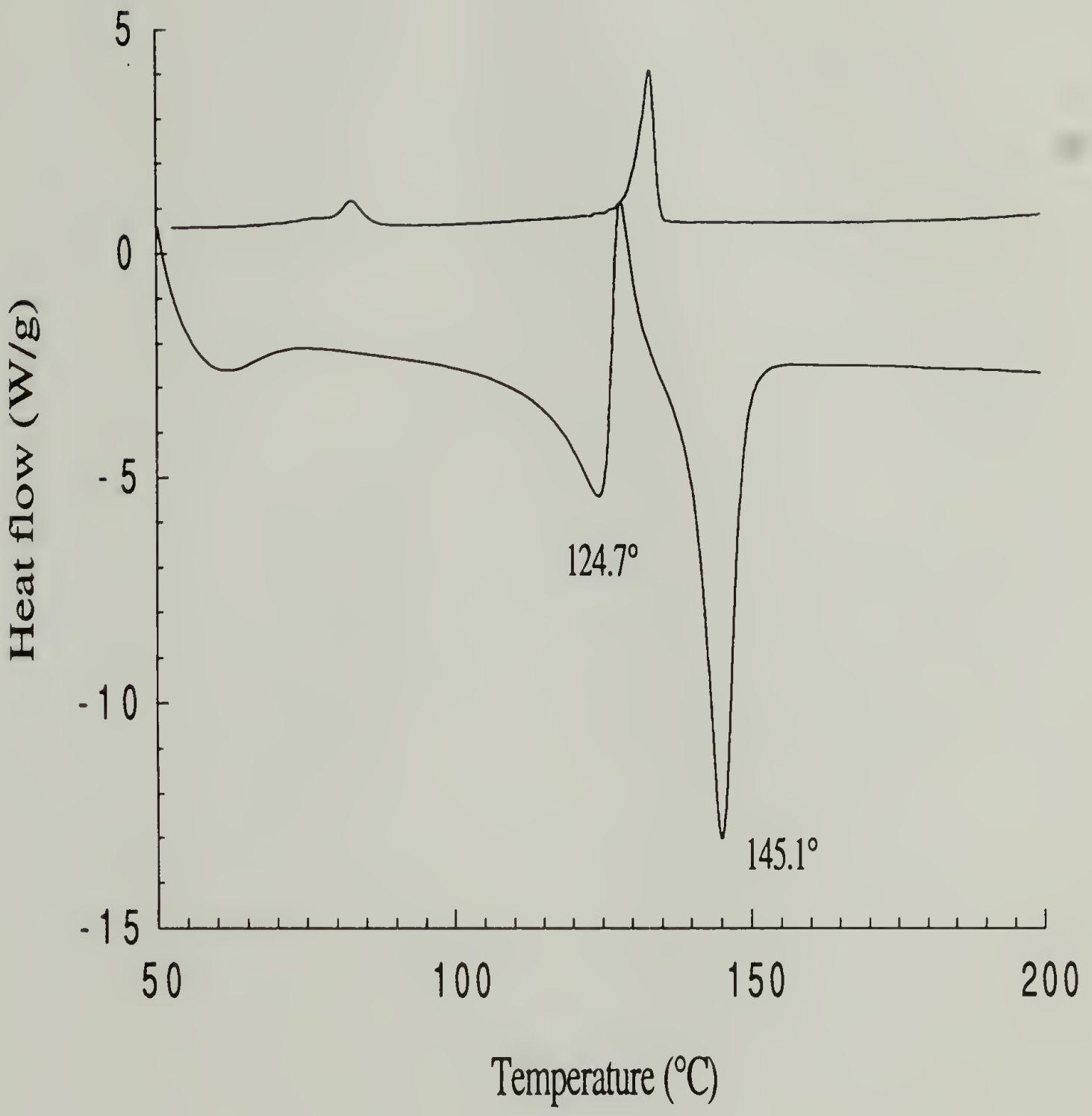

Figure 1.4 DSC Thermogram of P(VDF-TrFE) copolymer with 83/17 molar content.

Crystallization

Polymer crystallization conditions are important in dictating the final morphology of a semicrystalline polymer including its lamellar thickness, crystallite dimensions, and defect content. The most important parameter controlling the crystallization process is the degree of supercooling, $\Delta T(= T_m^\circ - T_{cry})$ (44). Under favorable crystallization conditions well-ordered crystalline states may be formed in polymers, with the degree of perfection of a state depending on the thermal treatment. In a polymorphic system in which there is competitive growth of the different crystalline states, the final phase content can be modified by varying the crystallization conditions which will change the supercooling for the different polymorphs, and with it their nucleation and growth rates.

The crystallization processes that occur in real processing conditions require a knowledge of the nonisothermal conditions, which are more realistic than isothermal experiments. Several studies have been made to try to model and analyze the nonisothermal crystallization of polymers (45, 46). To describe fully the nonisothermal process requires a knowledge of the thermal history of the polymer and many material characteristics including the time and temperature dependent nucleation and growth rates. To date the material characteristics of crystallization, even for a single polymer, have not been determined (46).

It is known that P(VDF-TrFE) copolymers may possess up to three crystal phases but the crystallization of these phases andthe process of interconversion between them still remains uncertain. It is also known that by a control of the crystallinity, orientation, and the phase content improved piezoelectric polymers can be formed.

In studies of the thermal history and kinetic effects on the phase transition of P(VDF-TrFE) copolymers, Moriera et al. (33) used DSC and dielectric techniques and observed anomalies at the phase transition in their experiments on copolymers with 70

mol% VDF. On comparing the thermal transitions of copolymers that had been air-quenched with those cooled at 320°C/min, it was observed that the thermal treatment affects the transition temperature, with a decrease in the melting temperature for rapidly cooled samples. There were also multiple transitions observed in the DSC cooling thermograms. It was proposed that the complex transitions observed could be due to an intermediate crystalline phase, which is most likely the γ phase, or to inhomogeneities in the crystal such as conformational defects but no structural analysis was performed.

A study was made of the correlation between the crystallization behavior and ferroelectric phase transition of several compositions of P(VDF-TrFE) copolymers (36) by annealing the copolymers above and below the Curie temperature and curve fitting X-ray diffraction patterns to calculate the amorphous and crystalline contributions. In this study it was found that the crystallization rate rises abruptly at the Curie transition temperature for the paraelectric or ferroelectric phase accordingly as the crystallization is above or below the Curie temperature. The abrupt crystallization is assumed to be because crystallization occurs at the interface between the crystal and amorphous regions of the copolymer and at the Curie transition the crystal conformation expands into the amorphous phase.

The effect of thermal history of 80/20 copolymers on their phase transitions was studied by Stack and Ting (42) who found that the rate of cooling from the melt through the paraelectric to ferroelectric phase affected the temperature at which the transition occurred on subsequent heating. Even greater effects on the transition temperatures were observed when the conditions under which the polymer initially crystallized into the paraelectric phase were modified by changing the rate of cooling through the crystallization temperature. Slowly cooled materials showed a higher final melting temperature and a lower Curie transition temperature. Their results show that the effect of thermal treatment on the transition can be mainly attributed to the initial crystallization into the paraelectric phase and not to changes in the rate of passing through the Curie transition. In their work they were not able to indicate the structural differences in the ferroelectric crystals having

different transition temperatures, though it is known that both melting and Curie transitions depend strongly on crystallite size and defect content (8).

Tanaka et al. (41) determined that the crystalline structure and the ferroelectric phase transition of P(VDF-TrFE) copolymers are strongly dependent on the crystallization temperature. A copolymer crystallized above the Curie transition in its paraelectric phase cannot perfectly transform to the ordered ferroelectric phase as it is cooled through the Curie transition temperature resulting in conformational defects in the ferroelectric phase. These defects then result in a lower Curie temperature of samples crystallized at higher temperatures. For copolymers with 65 or 73 mol % VDF the cooling process shows two peaks for the Curie transition that are believed to be attributable to the presence of two kinds of ferroelectric phases of different degrees of order.

In a real-time X-ray diffraction study of the melt crystallization of 60/40 copolymers Lopez Cabarcos et al. (32) found from the lattice spacings and crystallite dimensions that there is a breakdown of the paraelectric crystals into smaller ferroelectric domains mixed with paraelectric ones at the Curie transition on cooling. In the low-temperature region there are predominantly ferroelectric crystals, though about 25% of the material is still in the paraelectric state. Their data clearly show that there is a coexistence of crystal phases in the copolymer below the Curie transition.

It appears that the crystallization behavior of P(VDF-TrFE) copolymers is difficult to generalize because of its strong composition dependence, making comparisons among literature results impracticable. The crystallization behavior of different resins of PVDF has also been shown to vary due to the complex polymorphism and differences in defect content, making absolute measurement of equilibrium melting values impossible (2). One can conclude that the phase formation and phase transitions do vary under various thermal treatments for PVDF and P(VDF-TrFE) copolymers.

A complete structural characterization of the crystal phases of P(VDF-TrFE) formed under different crystallization conditions requires the use of several

techniques that enable one to probe the structure at different levels. The localized conformational structure can be measured by vibrational spectroscopy, particularly Fourier transform Raman and infrared spectroscopy. It is anticipated that vibrational spectroscopy will help to clarify the controversy on the variations of crystalline phases that are present in the copolymers since very localized structures are measured. The crystal phases and their dimensions can be probed on a longer range with wide-angle X-ray diffraction (WAXD). It seems that the use of WAXD has not been able to provide the detail necessary to discern between unique crystal phases or a mixture of crystal phases in studies of P(VDF-TrFE) copolymers with ~50 mol % VDF (5, 20, 34) The coherence of the conformational differences between the crystalline phases may be too small to be detected by diffraction. Thermal analysis is important in the measure of the transition temperatures and their enthalpies, both of which can be related to structural measurements obtained by other techniques.

A limitation in all of these approaches is that a unique feature characteristic of the crystal phases cannot be isolated. By FTIR and the analytical method of factor analysis on the spectral data, one can determine the number of independent factors that contribute to a set of data. Factor analysis enables one to determine the number of linearly independent components contributing to data. It is particularly useful in analyzing spectral data because it is a method based on standard theorems of linear algebra with no assumptions concerning band shape (47, 48). The vibrational band assignments for the different crystal phases have been made (10, 11), but a better understanding of the assignments for the CF_2 stretching is needed as virtually all the CF vibrations are coupled delocalized vibrations involving many vibrations. The drawback in the use of vibrational spectroscopy is that even the PVDF vibrational spectra have more bands than have been calculated from the normal coordinate analysis, and they are attributed to disordered structures in the

crystal lattice (10). There are four types of disorder that can contribute to the vibrational spectra: disorder in the molecular structure, disorder in molecular packing, conformational disorder, and disorder in chain structure (e.g. head-to-head, tail-to-tail defects). Because it is a copolymer, P(VDF-TrFE) has an even more disordered structure than PVDF, including sequence distribution, thus making its complete characterization difficult.

The goal of this research is to investigate the influence of thermal history on the crystalline structure of P(VDF-TrFE) copolymers with an 83/17 molar composition, a composition not previously studied. Since the crystalline structure is believed to determine the piezoelectric and ferroelectric properties, it is of interest to have a better understanding of the formation of the different crystalline phases, which are to date still disputed. This entails crystallizing the purified copolymers under different conditions and characterizing the final room temperature structures that are formed. The simultaneous preparation of samples used for all the structural characterization ensures uniform crystallization.

This dissertation is divided into four chapters discussing different experimental approaches that have been taken in order to better understand the phase transition behavior, crystalline structure and crystallization of poly(vinylidene fluoride-trifluoroethylene) copolymers with a molar composition of 83% VDF. In the first part, variable temperature infrared spectroscopic studies are made to follow the phase transition behavior. Factor analysis is applied to the data to try to determine the number of crystal phases present under various conditions. Nonisothermal crystallization studies were made on the copolymers and the resulting structures were characterized by vibrational spectroscopy and WAXD, with thermal analysis used to understand the phase transition behavior. In the fourth chapter isothermal crystallization experiments and their influence on the copolymer structure are described. Orientation by coextrusion is described in the fifth chapter. The preparation of a highly oriented sample from which transition moment angles can be

measured may aid in vibrational assignments for P(VDF) and P(VDF-TrFE) for which the force fields are poorly defined. The orientation measured by infrared dichroism and WAXD and spectroscopically measured structural changes due to the orientation in the copolymer upon coextrusion are presented.

References

1. Das-Gupta, D. K. *Ferroelectrics*, **1991**, *118*, 165.

2. Lovinger, A. J.; *Developments in Crystalline Polymers-1;* D. C. Bassett, ed.; Applied Science: London, 1982; p 195.

3. Davis, G. T.; *The Applications of Ferroelectric Polymers;* T. T. Wang, J. M. Herbert and A. M. Glass, ed.; Chapman and Hall: New York, 1988; p 37.

4. Nalwa, H. S. *J.M.S.-Rev. Macromol. Chem. Phys.*, **1991**, *C31*, 341.

5. Tashiro, K.; Kobayashi, M. *Phase Transitions*, **1989**, *18*, 213.

6. Higashihata, Y.; Sako, J.; Yagi, T. *Ferroelectrics*, **1981**, *32*, 85.

7. Tashiro, K.; Takano, K.; Kobayashi, M.; Chatani, Y.; Tadokoro, H. *Polymer*, **1984**, *25*, 195.

8. Sessler, G. M.; Das-Gupta, D. K.; DeReggi, A. S.; Eisenmenger, W.; Furukawa, T.; Giacometti, J. A.; Gerhard-Multhaupt, R. *IEEE Trans. Electr. Insul.*, **1992**, *27*, 872.

9. Boerio, F. J.; Koenig, J. L. *J. Polym. Sci.*, **1971**, *A2*, 1517.

10. Kobayashi, M.; Tashiro, K.; Tadokoro, H. *Macromolecules*, **1975**, *8*, 158.

11. Tashiro, K.; Itoh, Y.; Kobayashi, M.; Tadokoro, H. *Macromolecules*, **1985**, *18*, 2600.

12. Prest, W. M., Jr.; Luca, D. J. *J. Appl. Phys.*, **1975**, *46*, 4136.

13. Doll, W. W.; Lando, J. B. *J. Macromol. Sci.- Phys.*, **1968**, *B2*, 219.

14. Marand, H. L.; Stein, R. S.; Stack, G. M. *J. Polym. Sci., Polym. Phys. Ed.*, **1988**, *26*, 1361.

15. Marand, H.; Stein, R. S. *J. Poly. Sci., Polym. Phys. Ed.*, **1989**, *27*, 1089.

16. Lovinger, A. J. *Polymer*, **1980**, *21*, 1317.

17. Prest, W. M., Jr.; Luca, D. J. *J. Appl. Phys.*, **1978**, *49*, 5042.

18. Bongianni, W. *Ferroelectrics*, **1990**, *103*, 57.

19. Furukawa, T. *IEEE Trans. El. Ins.*, **1989**, *24*, 375.

20. Tashiro, K.; Takano, K.; Kobayashi, M.; Chatani, Y.; Tadokoro, H. *Ferroelectrics*, **1984**, *57*, 297.

21. Bartenev, G. M.; Remizova, A. A.; Kuleshov, I. V.; Martynov, M. A.; Sarminskaya, T. N. *Polym. Sci., USSR*, **1975**, *17*, 2381.

22. Lovinger, A. J. *J. Polym. Sci., Polym. Phys. Ed.*, **1980**, *18*, 793.

23. Tashiro, K.; Kobayashi, M. *Rep. Prog. Polym. Phys. Jpn.*, **1987**, *30*, 119.

24. Yagi, T.; Tatemoto, M.; Sako, J. *Polym. J.*, **1980**, *12*, 209.

25. Koga, K.; Nakano, N.; Hattori, T.; Ohigashi, H. *J. Appl. Phys.*, **1990**, *67*, 965.

26. Lando, J. B.; Doll, W. W. *J. Macromol. Sci.-Phys.*, **1968**, *B2*, 205.

27. Lovinger, A. J.; Furukawa, T.; Davis, G. T.; Broadhurst, M. G. *Polymer*, **1983**, *24*, 1225.

28. Lovinger, A. J.; Furukawa, T.; Davis, G. T.; Broadhurst, M. G. *Polymer*, **1983**, *24*, 1233.

29. Koga, K.; Ohigashi, H. *J. Appl. Phys.*, **1986**, *59*, 2142.

30. Lovinger, A. J.; Davis, D. D.; Cais, R. E.; Kometani, J. M. *Polymer*, **1987**, *28*, 617.

31. Latour, M.; Almairac, R.; Moreira, R. L. *IEEE Trans. Electrical Insul.*, **1989**, *24*, 443.

32. Lopez Cabarcos, E.; Gonzalez Arche, A.; Baltá Calleja, F. J.; Bösecke, P.; Röber, S.; Bark, M.; Zachmann, H. G. *Polymer*, **1991**, *32*, 3097.

33. Moreira, R. L.; Saint-Gregoire, P.; Lopez, M.; Latour, M. *J. Polym. Sci., Polym. Phys. Ed.*, **1989**, *27*, 709.

34. Lovinger, A. J.; Davis, G. T.; Furukawa, T.; Broadhurst, M. G. *Macromolecules*, **1982**, *15*, 323.

35. Green, J. S.; Farmer, B. L.; Rabolt, J. F. *J. Appl. Phys.*, **1986**, *60*, 2690.

36. Ikeda, S.; Shimojima, Z.; Kutani, M. *Ferroelectrics*, **1990**, *109*, 297.

37. Oka, Y.; Murata, Y.; Koizumi, N. *Polymer J.*, **1986**, *18*, 417.

38. Moreira, R. L.; Saint-Gregoire, P.; Latour, M. *Phase Transitions*, **1989**, *14*, 243.

39. Moreira, R. L.; Almairac, R.; Latour, M. *J. Phys.: Condens. Matter*, **1989**, *1*, 4273.

40. Legrand, J. F. *Ferroelectrics*, **1989**, *91*, 303.

41. Tanaka, H.; Yukawa, H.; Nishi, T. *Macromolecules*, **1988**, *21*, 2469.

42. Stack, G. M.; Ting, R. Y. *J. Polym. Sci., Polym. Phys. Ed.*, **1988**, *26*, 55.

43. Ohigashi, H.; Kagami, N.; Li, G. R. *J. Appl. Phys.*, **1992**, *71*, 506.

44. Wunderlich, B.; *Macromolecular Physics Vol. 2*; Academic Press: New York, 1976.

45. Ozawa, T. *Polymer*, **1971**, *12*, 150.

46. Walsiak, A. *Chemtracts-Macro. Chem.*, **1991**, *2*, 211.

47. Maliknowski, E. R.; Howery, D. G.; *Factor Analysis in Chemistry*; Wiley-Interscience: New York, 1980.

48. Kim, K. J.; Reynolds, N. M.; Hsu, S. L. *Macromolecules*, **1989**, *22*, 4395.

CHAPTER II

PHASE TRANSITION BEHAVIOR OF POLY(VINYLIDENE FLUORIDE - TRIFLUOROETHYLENE) MEASURED BY FTIR

Introduction

The Curie transition in P(VDF-TrFE) copolymers has been identified as a long range conformational transition from a predominantly trans conformation to one also having gauche conformations. The different crystal phases of P(VDF-TrFE) copolymers are known to vary depending on the copolymer composition and crystallization conditions, but the precise identity of the phases remains unclear (1-6). Phase diagrams have been proposed showing three crystal phases for copolymers possessing from 55-90 mol % VDF (see Figure 1.3), with the structure of the crystal phases remaining largely unidentified (3, 6). A mixture of crystalline phases is expected to occur in copolymers with a high VDF content because the gauche conformation has greater stability in this case than in copolymers with lower VDF content (3, 7). The cooled phase proposed by Tashiro et al. (3) for copolymers with 55 mol % VDF is said to have a rather disordered structure with skew linkages within long trans sequences. It has similar X-ray and infrared spectra to the low temperature ferroelectric phase, with the only difference being a tilting in the X-ray fiber diagram. The interconversion of the crystal phases is also uncertain though several authors have observed two Curie transitions in DSC cooling thermograms that suggest the presence of two paraelectric phases transforming to the ferroelectric phase (6, 8, 9). Real-time wide-angle X-ray diffraction (WAXD) experiments using synchrotron radiation (10) have shown that in 70/30 copolymers there is an increase in crystallinity and a change in structure for samples cycled through the Curie transition.

The principal advantage of using vibrational spectroscopy in the study of ferroelectric copolymers of P(VDF-TrFE) is that it is sensitive to localized chain conformation, orientation, and packing. It is therefore expected that FTIR can discern between different crystal phases that have localized structural differences. Vibrational spectroscopy is also ideal in following the phase transition in P(VDF-TrFE) copolymers that is a conformational transition.

Vibrational band assignments for the α, β, and γ phases of PVDF have been made from normal coordinate calculations, but a definitive identification of the γ or some other third crystalline phase by vibrational spectroscopy has not been made because a unique characteristic vibration for it has not been identified (11, 12). The many types of disorder that contribute to the vibrational spectra further complicate vibrational assignments (11). Because it is a random copolymer, P(VDF-TrFE) has an even more disordered structure than PVDF thus making its complete characterization difficult. Because of this uncertainty in vibrational assignments in the copolymer, extensive spectroscopic studies have not been made (1, 2, 13-15).

Due to the lack of a unique vibration by which to identify a third crystalline phase the factor analysis method will be applied to FTIR data to determine the number of independent factors that contribute to the spectral data. Factor analysis has been applied to FTIR data to determine the number of components contributing to a spectral region within a mixture and to determine the concentration of each pure component (14, 16-18). The number of factors determined by factor analysis will be assumed to be the number of crystal phases that are present in the P(VDF-TrFE) copolymer with 83 mol % VDF.

Factor analysis is particularly well suited to spectroscopic analysis of polymers in which conformational changes result in the formation of new crystal phases. It has successfully been used in the analysis of P(VDF-TrFE) copolymers with 75 mol % VDF that have been annealed at various temperatures, or temperature cycled through the Curie transition. Using factor analysis the pure crystal and amorphous spectra for this copolymer

were calculated as were spectra of the low and high temperature phases in this copolymer. There was no suggestion made of three crystalline phases in this copolymer composition from the spectroscopic data (14).

Factor Analysis

Factor analysis is based on expressing a data point as a linear sum of product functions and is thus well suited to spectroscopic data that follows the Beer's law relationship that has such a form.

$$A_{\nu j}=\sum_{k}\varepsilon_{\nu k}c_{kj} \qquad (2.1)$$

where $A_{\nu j}$ = absorbance at frequency ν for the j^{th} mixture

$\varepsilon_{\nu k}$ = extinction coefficient of the k^{th} species

c_{kj} = concentration of the k^{th} species in the j^{th} mixture

Because factor analysis is a method based on the standard theorems of linear algebra, there are no assumptions about band shape (17, 18).

In the method of factor analysis one defines a data matrix [X] of dimension r x c where r is the number of data points over the spectral region under study and c is the number of mixture spectra used in the analysis. The rank of [X], n, is equal to the number of linearly independent components in the set of spectra chosen to define [X]. The number of spectra used for the analysis must be greater than the number of components to ensure that the correct number of components is determined. Because the number of points in the spectral region being analyzed is typically large (i.e., 832 points for 800 cm^{-1} region) computation can be cumbersome. To facilitate computation the covariance matrix is defined:

$$[Z] = [X][X]^T \qquad (2.2)$$

This is a square matrix with dimensions equal to the number of spectra used in the analysis. The number of components in the data, n, is equal to the rank of [Z], which is determined from the number of nonzero eigenvalues in the eigenvalue matrix [λ] calculated from the eigenvector matrix [E] by the following

$$[E]^{-1}[Z][E] = [\lambda] \qquad (2.3)$$

Factor analysis invariably results in an excessive number of factors because of experimental error. Due to computational and measurement inaccuracies, there is never a true zero eigenvalue so other methods of determining the number of factors are used. One such method is to compute the empirical Maliknowski factor indicator function, IND, which is related to the error functions. This function is at a minimum when the correct number of independent factors in the data is reached. It is defined as

$$IND = \frac{RE}{(c-n)^2} \qquad (2.4)$$

where RE is the real error, which is a measure of the difference between the pure data and raw experimental data containing experimental error, defined as (17):

$$RE = \left[\frac{\sum_{j=n+1}^{c} \lambda_j}{r(c-n)} \right]^{\frac{1}{2}} \qquad (2.5)$$

A method of determining the number of factors that is based on the experimental error is to find the point at which the residual standard deviation of the absorbance (RSD) is greater than the estimated error in the absorbance measurement. The error in the spectral absorbance is determined from the maximum absorbance deviation from 0.0 measured

from the 100% line of the spectrometer (Figure 2.1) to be 0.0005 (17-19). The residual standard deviation is defined as:

$$RSD=\frac{1}{c}\left[\frac{\text{Tr } Z-\sum_{i=1}^{n}\lambda_i}{r-n}\right]^{\frac{1}{2}} \qquad (2.6)$$

Abstract eigenspectra are constructed from the real data and the eigenvectors associated with it by

$$[A] = [X]\,[E] \qquad (2.7)$$

Factor analysis may be used to extract the pure component spectra from spectra of mixtures by constructing a regenerated data matrix from the abstract eigenspectra using a transformation matrix. This does not apply to a case with more that two pure components because a unique solution cannot be defined. Isolating the spectra of each component also requires that there be at least one unique data point for each component (17, 20).

Experimental

Random copolymers of poly(vinylidene fluoride-trifluoroethylene) with an 83/17 molar composition were supplied by Elf Atochem Sensors (Foraflon 810C) in pellet form and were reprecipitated from acetone solution to remove residual PVDF homopolymer and low molecular weight impurities. The purified copolymer has M_W = 880,00 and M_n = 154,000 as measured using GPC with polystyrene standards. Variable temperature FTIR experiments were carried out on a film cast from acetone solution that was mounted between two KBr plates to follow the microstructural changes at the Curie transition on heating and cooling. Spectra were measured on an IBM IR32 spectrometer using 256 scans at 2 cm^{-1} resolution with measurements taken from RT to 140°C and then back to RT. In addition experiments were made holding the sample isothermally at 120°C

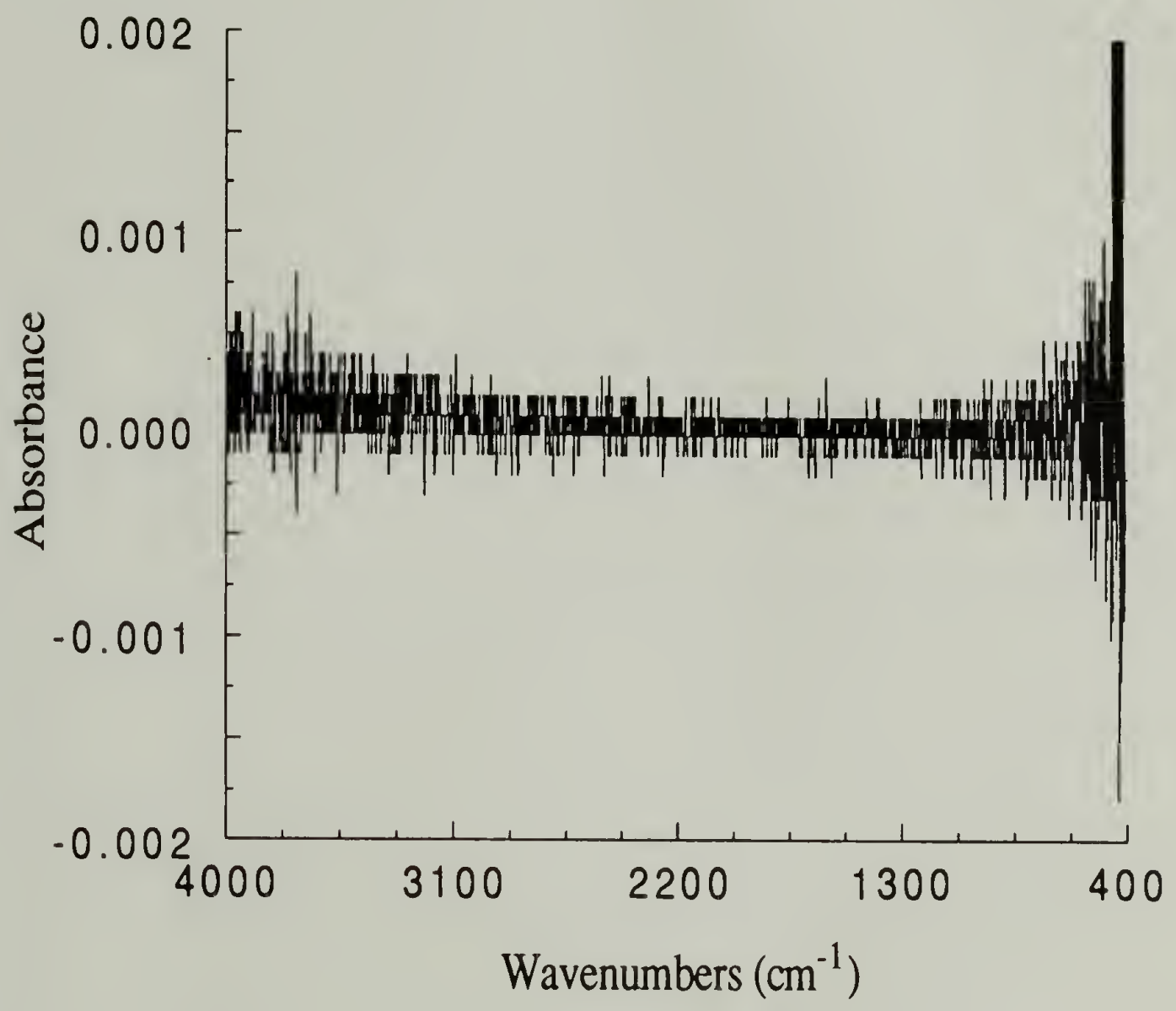

Figure 2.1 100% line; 256 scans at 2 cm^{-1} resolution.

and 135°C respectively on heating to see the annealing effects on the copolymer structure. A heating cell designed in this lab was controlled by an Omega temperature controller.

Factor analysis was carried out on 10-14 spectra measured at different temperatures with the analysis range being from 1500-700 cm^{-1}. An Array Basic computer program for principal component analysis supplied by Galactic Industries has been modified to perform the factor analysis on FTIR data of samples prepared under different thermal conditions and from variable temperature spectra (Appendix A). This program also can generate the abstract eigenspectra from the calculated eigenvectors.

Results and Discussion

The first indication that the copolymers being studied here, with 83/17 molar composition, may possess three crystal phases comes from the observation of two Curie transition peaks in the DSC cooling thermograms (Figure 2.2). This observation is agrees with previous studies on copolymers with high VDF content and deserves further study to elucidate the structure associated with the Curie transitions.

Several vibrational bands for PVDF have been assigned to specific chain conformations for the different crystalline phases (11, 13, 21). These assignments will be used in this study of P(VDF-TrFE) copolymers to understand the structural changes exhibited as a function of temperature. The assignments of the selected bands are listed in Table 2.1.

The following bands have been identified to be due to the pure crystalline phase from factor analysis on annealed copolymers with 75/25 molar composition: 1293, 1181, 1076, 884, 848, 504, and 472 cm^{-1}. Amorphous bands were identified at 1247(sh), 907(sh), 883, 830(sh), 750, 600, and 515 cm^{-1}. As is the case for the vibrational assignments of the different chain conformations of PVDF, there is also an overlap of the

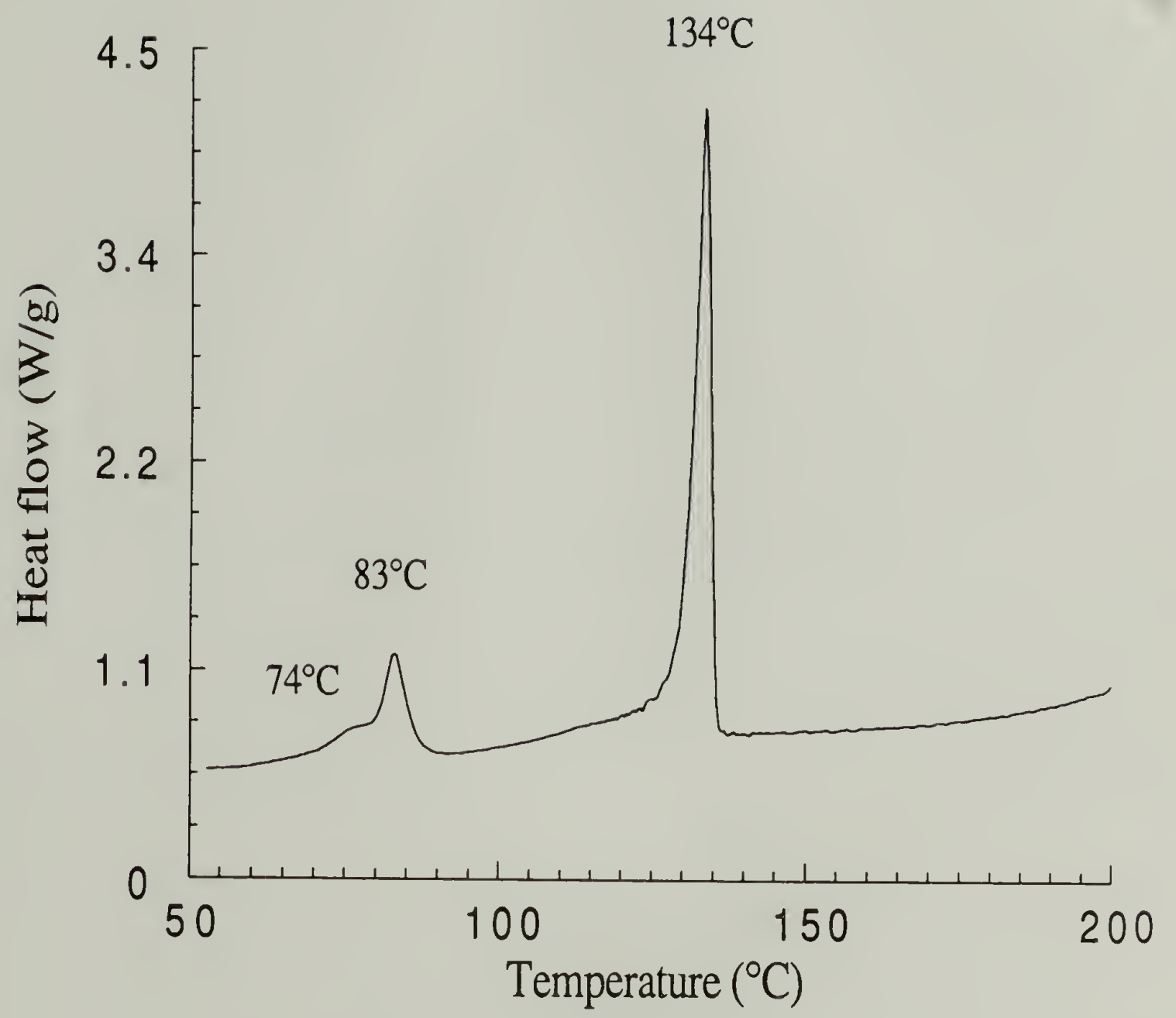

Figure 2.2 DSC cooling thermogram for cast film.

Table 2.1 Vibrational band assignments for three crystal forms of PVDF (11).

crystal phase	β	γ	α	assignment	Conformation
freq. (cm^{-1})	1428	1427	1420	$\delta(CH_2)$	
	1398	1400	1399	$w(CH_2)\nu_a(CC)$	
	1273	1269		$\nu_s(CF_2)\nu_s(CC)\delta(CCC)$	T_m (m>4)
			1290	$\nu_a(CF_2)r(CF_2)$	
	1176	1175	1182	$\nu_a(CF_2)r(CF_2)r(CH_2)$	
	1071	1073	1067	$\nu_a(CC)w(CF_2)w(CH_2)$	
	884	882	878	$\nu_a(CF_2)r(CH_2)r(CF_2)$	T
	840	838	853	$\nu_s(CC)\nu_s(CF_2)$	T_m (m>3)
			795	$\delta(CF_2)\delta(CCC)$	TG
			766	$\delta(CF_2)\delta(CCC)$	TG
			612	$\delta(CF_2)\delta'(CCC)$	TG
	508	510	531	$\delta(CF_2)$	
	468	483	489	$w(CF_2)$	
	442	440	410	$r(CF_2)r(CH_2)$	

crystalline and amorphous vibrations so that crystalline bands at 1181, 1124, 1075, 884, and 848 cm^{-1} cannot be used to measure sample crystallinity (14).

Temperature Cycling through the Curie Temperature

From the spectra measured at different temperatures structural changes attributable to the ferroelectric transition are observed (Figure 2.3). Vibrations associated with both the α and γ phase crystals increase in intensity as β phase vibrations decrease on increasing temperature. At 120°C the α phase peak at 610 cm^{-1} first begins to appear while the β

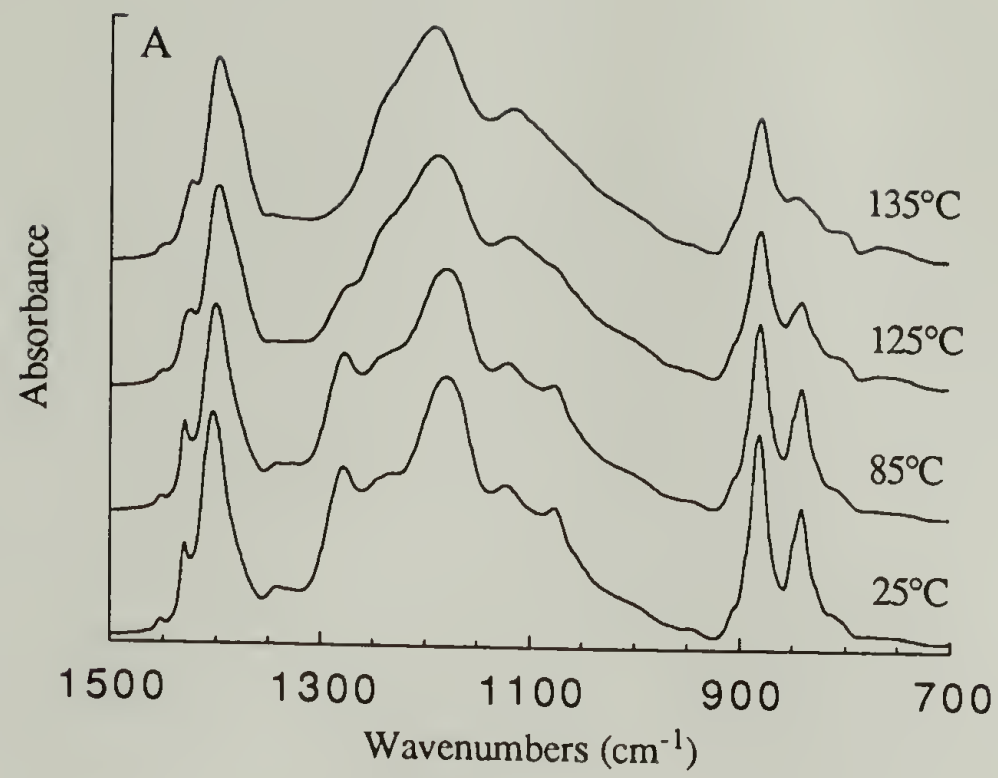

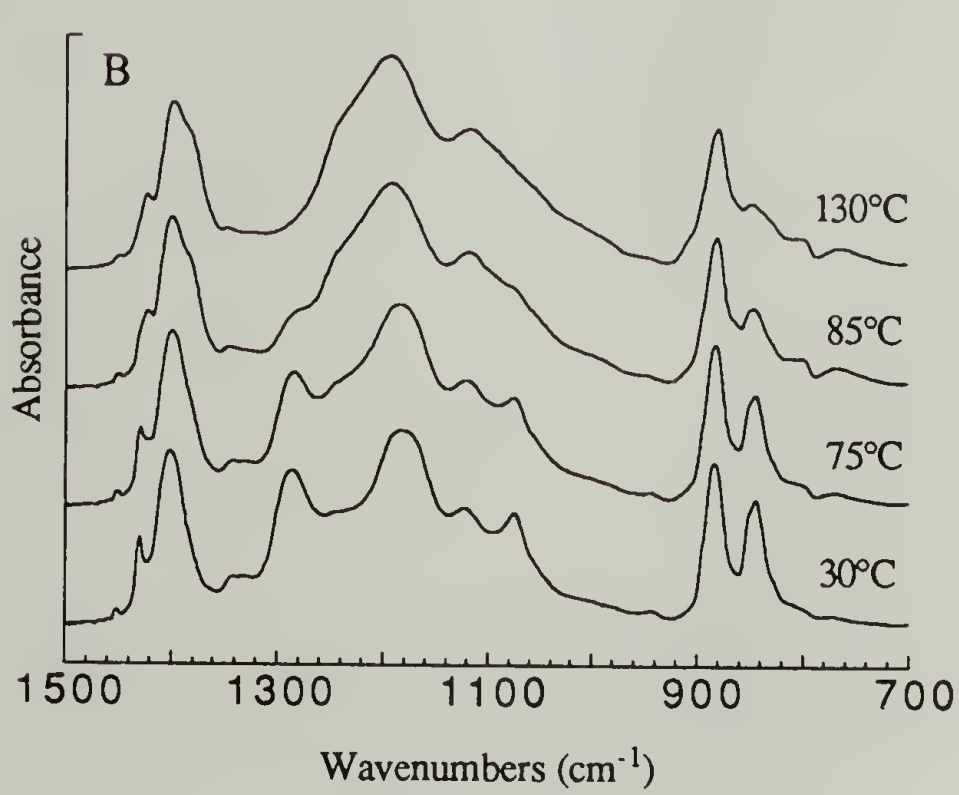

Figure 2.3 Infrared spectra in the 1500-700 cm^{-1} region of P(VDF-TrFE) 83/17 copolymer as a function of temperature. A: heating; B: cooling.

phase band at 479 cm^{-1} decreases in intensity, indicating the introduction of TGTG' conformational sequences in the copolymer chain. The intensity of this peak increases as the temperature reaches 140°C and other α phase peaks at 489, 1383, and 1248 cm^{-1} appear. The strongest β-phase all trans band at 1280 cm^{-1} disappears at 135°C as the copolymer loses long trans sequences upon undergoing the ferroelectric-to-paraelectric transition. Other trans bands at 1075, 842, 509, and 475 cm^{-1} also decrease in intensity on increasing temperature. The intensity of the 1075 cm^{-1} vibration has a higher intensity after the sample has been cycled through the Curie temperature than it did originally, as does the band at 475 cm^{-1}. On cooling the sample from the paraelectric phase a shoulder develops at 1381 cm^{-1} that decreases in intensity at 80°C and disappears by 70°C. The 1400 cm^{-1} peak does broaden considerably on heating, beginning at 120°C, but it is only on cooling that a distinctive shoulder is seen on this peak, suggesting structural changes on cooling from the paraelectric phase before undergoing the Curie transition. The hysteresis of the Curie transition observed by the band intensity changes with temperature is characteristic of a first-order phase transition. The broadening of these vibrations suggests that there is a greater disorder in the copolymers at increasing temperatures that may be associated with a change in crystal structure and with a decrease in sample crystallinity.

Upon heating the copolymer sample, it undergoes conformational changes as it goes through the Curie transition. Some of the changes are marked by the shift in band position as the temperature is increased. The $\delta(CF_2)$ vibration undergoes a frequency shift from 1430 cm^{-1} in the β phase to 1423 cm^{-1} in the α phase, with the γ phase having a band at an intermediary position. As the sample is heated, a shoulder appears at 1424 cm^{-1} at 130°C, with the 1430 cm^{-1} β phase disappearing completely at 136°C, as it is replaced by the α phase band. The frequency of the α phase band remains steady on cooling, until reaching 91°C, at which point the β phase band reappears at 1429 cm^{-1} and continues to shift until reaching 1432 cm^{-1} at 72°C. The strong band centered at 1180 cm^{-1} at room temperature [$\nu_a(CF_2)r(CF_2)r(CH_2)$] gradually increases in frequency to 1191 cm^{-1} at the

Curie transition indicating the transformation to the α phase. On the cooling cycle this band shifts back to 1180 cm^{-1} at 85°C.

Perhaps the most dramatic changes in the spectroscopic data as a function of temperature are seen in the CF_2 vibrations in the 470-530 cm^{-1} region (figure 2.4). The β phase vibration at 509 cm^{-1} diminishes to a shoulder at 136°C, with the α phase band developing as a shoulder at 530 cm^{-1} beginning at 135°C. The $\delta(CF_2)w(CF_2)$ vibration shifts with chain conformation, being at 483 cm^{-1} and 490 cm^{-1} for the α and γ phases respectively. The β phase has a vibration at 474 cm^{-1} that decreases in intensity as the α and γ phase vibrations begin to develop at 130°C. These bands show an intensity inversion as the frequency shifts to 489 cm^{-1} at 136°C, slowly shifting to 487 cm^{-1} on cooling as the β phase peak grows. From 130-80°C, the bands at 489 and 475 cm^{-1} coexist, suggesting the presence of multiple crystalline phases over this temperature range. The β phase peak at 509 cm^{-1} reappears at 82°C, but at 506 cm^{-1}, with the frequency shift attributable to increased crystallinity over the original room temperature sample.

The Curie transition in these copolymers on cooling is observed over a temperature range of 82-72°C, exhibiting the same hysteresis and multiple behavior as observed in the DSC thermograms. The two stage nature of the Curie transition on cooling is seen in the diminishment of α phase vibrations that begins at 82°C, accompanied by the appearance of β phase vibrations, which continue to increase in intensity as the α phase vibrations decrease. The α phase bands do not disappear completely until the sample reaches 70°C. The long trans band of the β phase $\nu_s(CF_2)\nu_s(CC)\delta(CCC)$ vibration reappears on cooling, but with a shift to higher frequency indicating greater order in the β phase and higher crystallinity when formed from the α phase, rather than from solution (Figure 2.5).

It is not evident from the variable temperature spectra whether three crystalline phases are present over the temperature region measured. The two stage transition that is observed may be due to a conversion of two paraelectric phases, α and γ, to the ferroelectric β phase, or to the α phase transforming to an intermediary ferroelectric phase

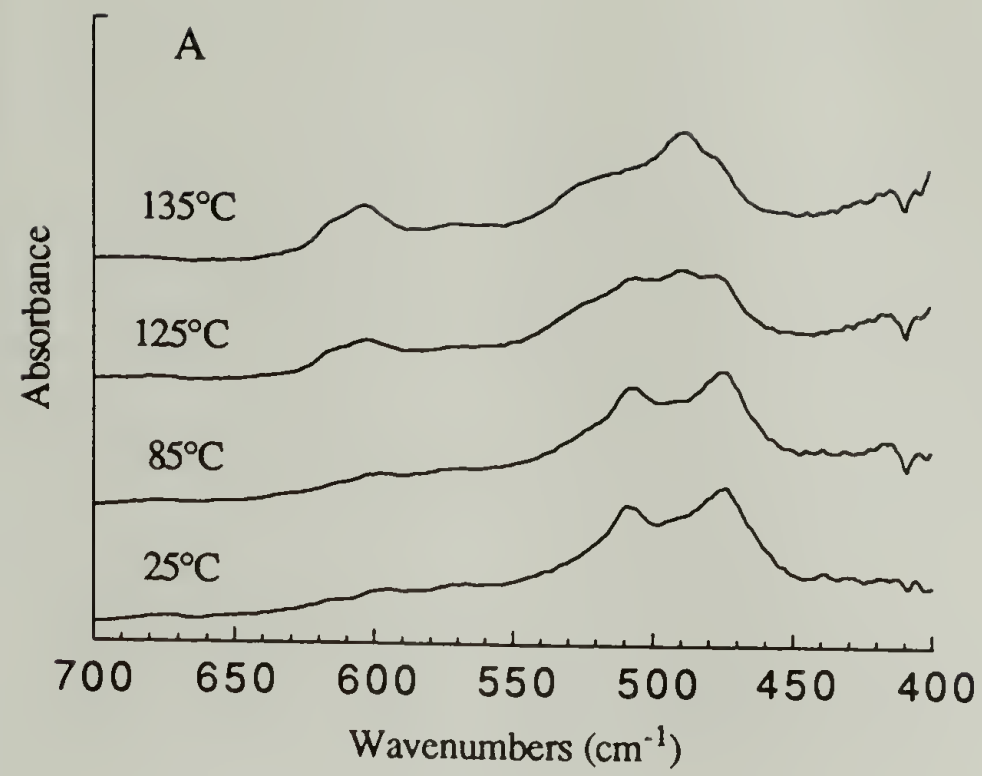

Figure 2.4 Infrared spectra in the 700-400 cm^{-1} region of P(VDF-TrFE) 83/17 copolymer as a function of temperature. A: heating; B: cooling.

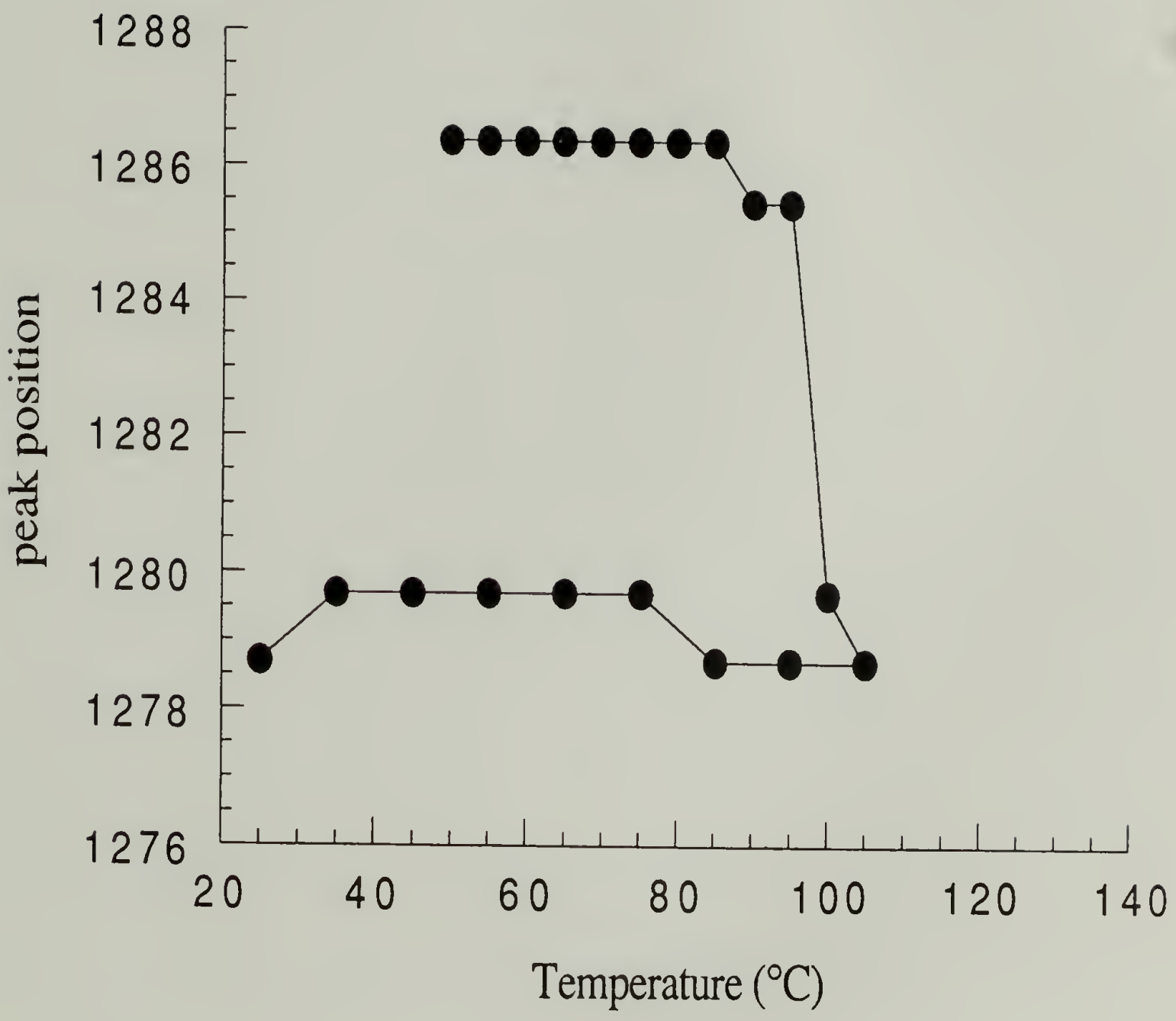

Figure 2.5 Peak position of the long trans sequence vibration as a function of temperature on cycling through the Curie transition.

that converts to the β phase. To determine whether there are three phases present 14 spectra recorded at different temperatures were analyzed by factor analysis. The results of this analysis are presented in Table 2.2.

Table 2.2 Factor analysis results for temperature cycled 83/17 P(VDF-TrFE) copolymer

component	eigenvalue	RE	IND	RSD
1	677.221	.024813	.000147	.006394
2	5.8636	.008928	.000062	.002212
3	.470939	.005958	.000049	.001414
4	.256137	.002874	.000029	.000651
5	.044058	.001815	.000022	.000390
6	.018298	.000977	.000015	.000198
7	.002588	.000804	.000016	.000153
8	.001340	.000698	.000019	.000123
9	.001135	.000558	.000022	.000089
10	.000546	.000474	.000030	.000067
11	.000308	.000420	.000047	.000052
12	.000224	.000310	.000077	.000019
13	.000129	.000298	.000298	0

The minimum in Maliknowski's indicator function is reached at six factors while the RSD criteria is met with four factors. The relative significance of a factor can be determined from the value of the eigenvalue which for n values greater than four is nearly zero. The eigenvalues for n=3 and 4 are also small so we turn to the abstract eigenspectra which are constructed from the eigenvectors to determine how many factors there are. The first five abstract eigenspectra are shown in Figure 2.6. It is observed from the

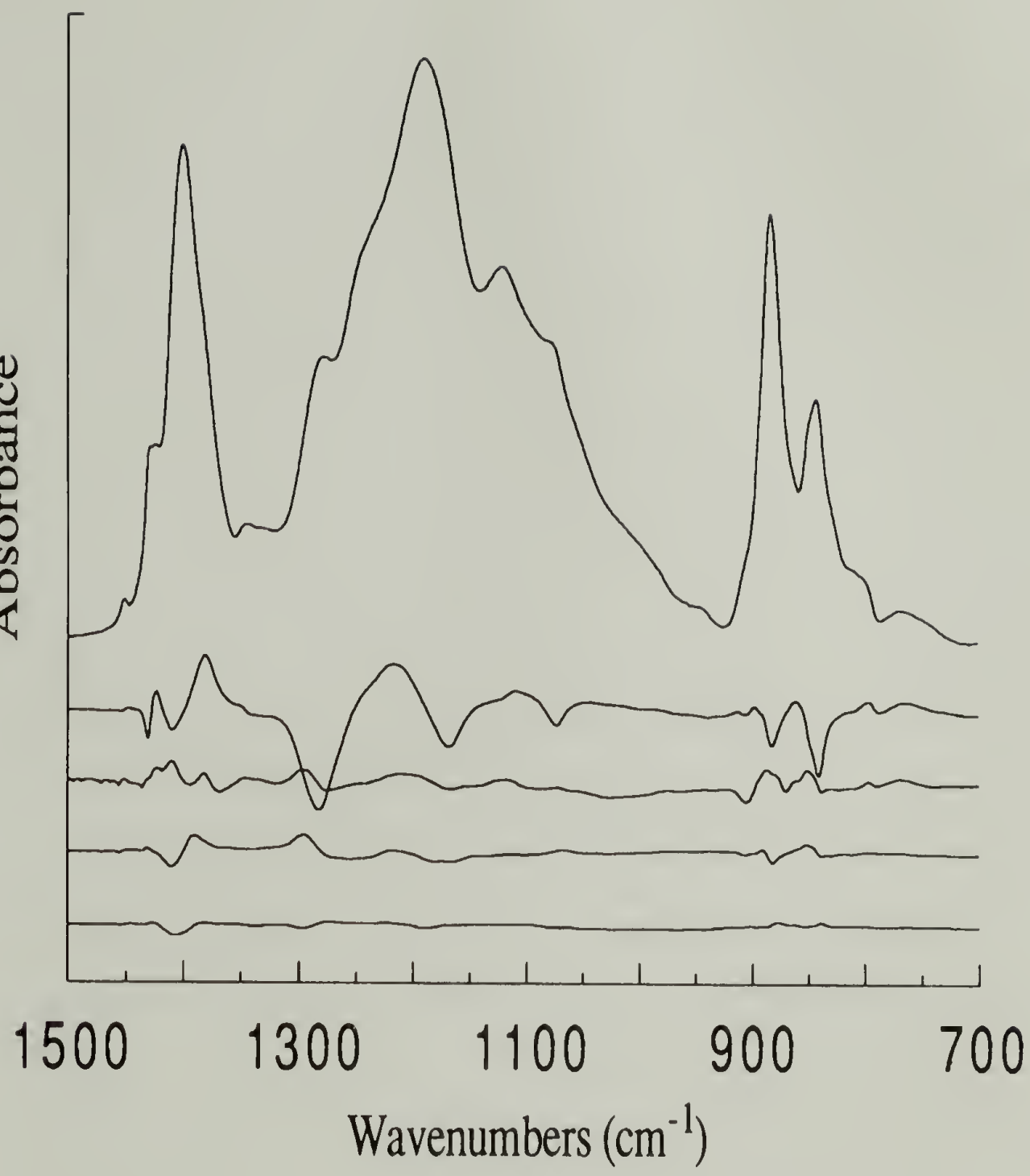

Figure 2.6 Abstract eigenspectra for infrared spectra of P(VDF-TrFE) copolymer temperature cycled through the Curie transition.

abstract eigenspectra that the first two eigenspectra are significant, with the third and fourth also having a minor component. The factor analysis does not give a definite result on the number of phases, but does indicate that there may be more than two for this system.

Annealing below and above the Curie Temperature

The Curie transition observed in the DSC for a cast film sample is very broad, going from 120-135°C and having an exotherm between T_c and T_m. In studies of P(VDF-TrFE) copolymers it was found that there is a coexistence of α, β, and γ phases in this temperature range that accounts for the diffuse Curie transition. In this mixed phase the chain molecules include many TG sequences along with all-trans sequences (5, 6). Annealing experiments at 120°C in the DSC indicate that the breadth of the Curie transition and the exotherm just above it in 83/17 copolymers are due to a distribution of ferroelectric domain sizes having different defect content in terms of G and G' linkages as suggested by Ohigashi et al. (22, 23). Annealing experiments done by Ohigashi et al. on poled and nonpoled copolymers with high VDF content showed that the Curie transition would develop into two peaks for the different domain sizes. On annealing samples for 15-60 minutes at 120°C, before heating through the melt, the Curie transition splits into two distinct transitions, with the second being at 130-132°C, depending on the annealing time (Figure 2.7). The splitting of the Curie transition observed on annealing results from the separation into domains with different defect contents that have different T_c. The T_c slightly increases with annealing time because of the perfection of the domains. T_m remains the same, meaning the overall crystallinity does not differ with annealing time from 15-60 minutes. When a sample is annealed for three hours at 120°C, then cooled back to RT, a single, sharpened Curie transition peak at 132°C is observed on subsequent heating (Figure 2.8).

To understand better the structural differences occurring over this wide temperature region, annealing studies were also done in the FTIR. By studying the changes in structure

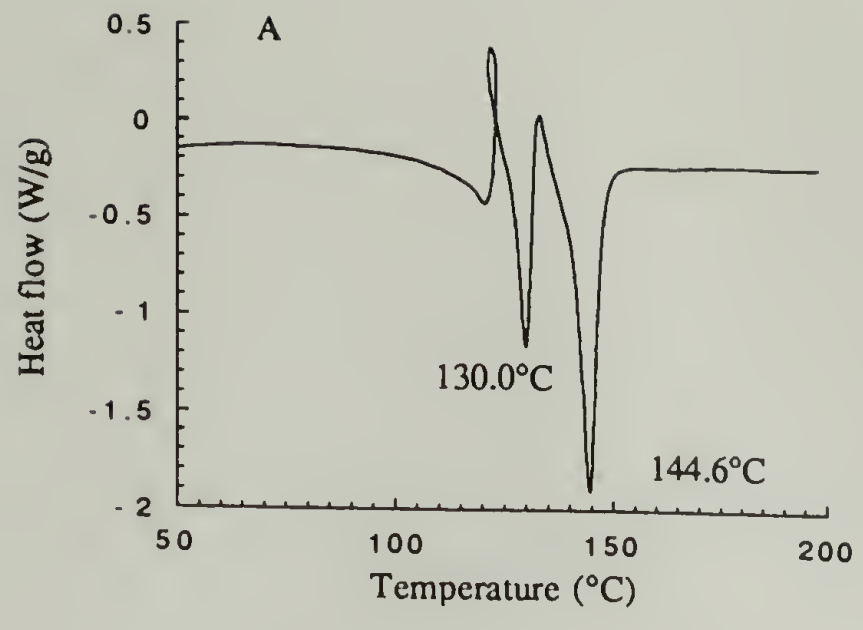

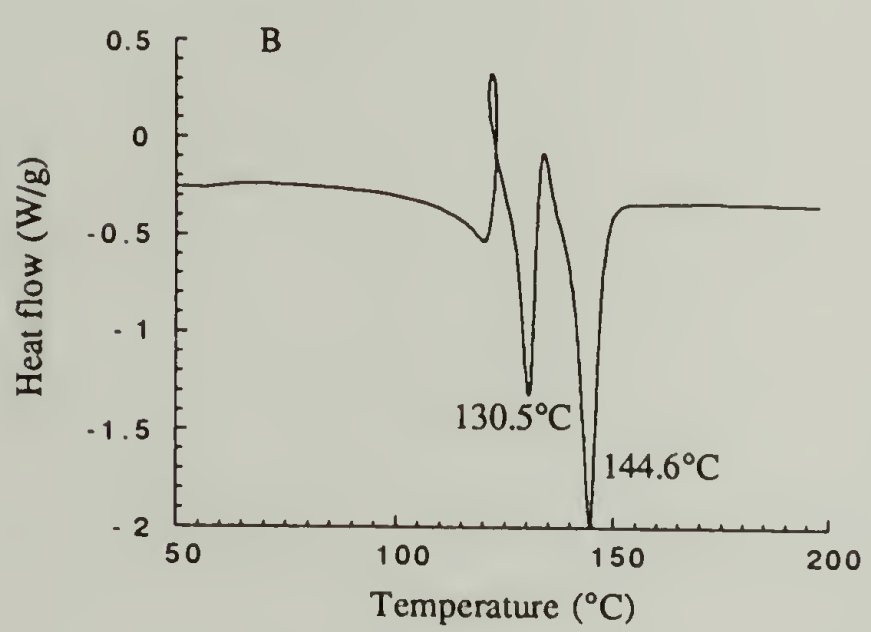

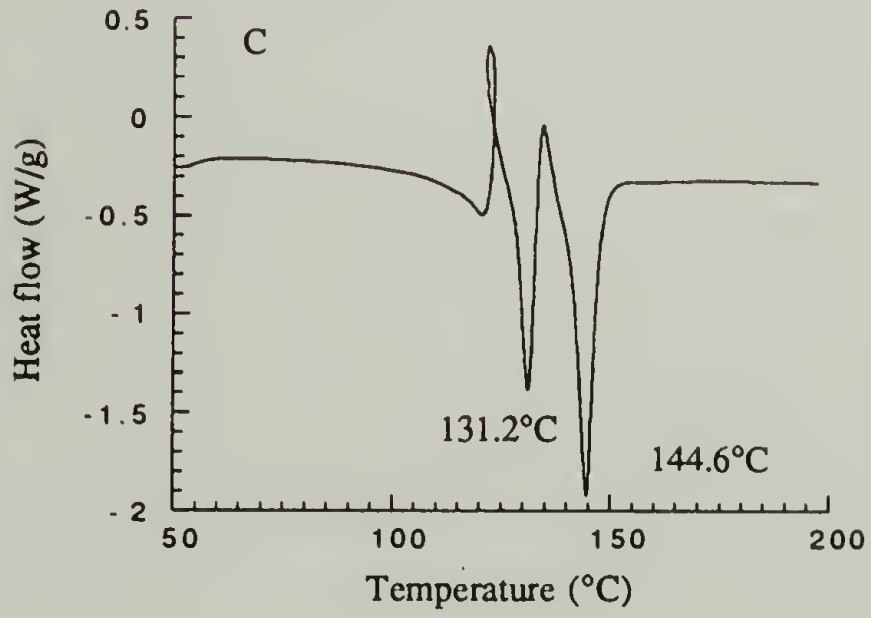

Figure 2.7 DSC thermograms for P(VDF-TrFE) copolymer annealed at 120°C for A: 15 min; B: 30 min; C: 60 min and heated to 200°C.

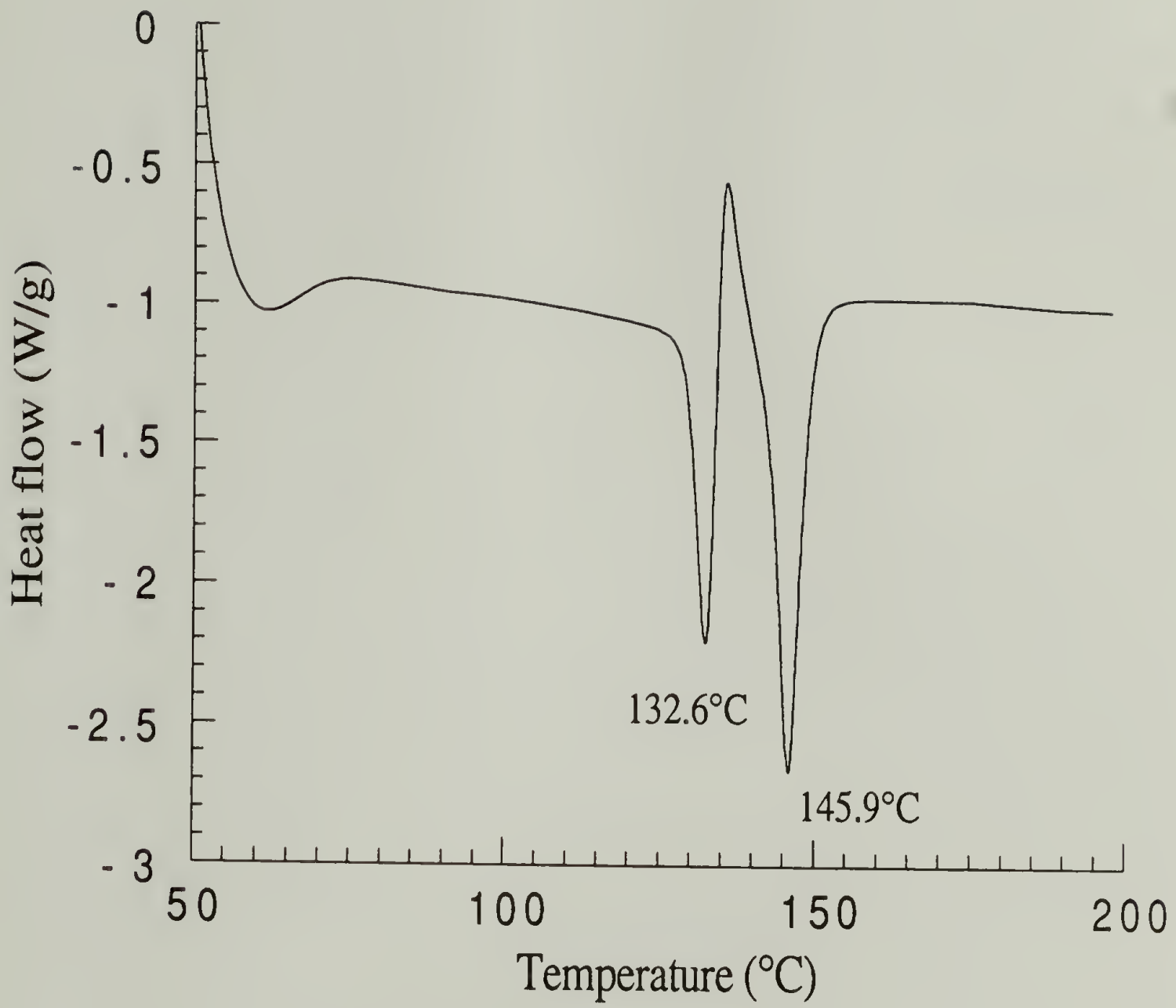

Figure 2.8 DSC thermogram for sample annealed at 120°C for three hours and cooled to RT.

for a sample held at 120°C for three hours, it can be determined if the Curie transition does occur at this temperature for the ferroelectric phase which is formed when a sample is cast from acetone solution at RT. The annealing of a sample at 135°C (above the Curie transition) will enable us to determine if thermal treatment can be used to stabilize the paraelectric phase, and change the Curie transition observed on cooling this sample.

In the case of annealing the copolymer at the onset of the Curie transition at 120°C, the vibrational spectra show that at this temperature the amorphous shoulder at 1248 cm^{-1} becomes stronger and the β phase vibration at 475 cm^{-1} has an intensity decrease (Figure 2.9). As the sample temperature is decreased to RT the amorphous shoulder again diminishes and the 475 cm^{-1} band increases in intensity. At 85°C, the Curie transition temperature on cooling, the long trans peak shifts in frequency from its original position of 1279.6 cm^{-1} and continues to shift, reaching 1281.6 cm^{-1} at RT. From these spectroscopic changes it is seen that some structural changes do occur even at the onset of the Curie transition. By annealing at 120°C, where the sample is in the ferroelectric phase, there is further ordering in this phase as seen by the increase in the 475 cm^{-1} band intensity and the shift to higher frequency of the long trans band.

When a sample is annealed at 135°C, it is already in the α phase, and during the annealing process spectroscopic changes are not observed (Figure 2.10), indicating that the annealing does not cause structural changes in the α phase. On cooling back to RT the long trans sequence band, not present at 135°C, reappears at 85°C with a frequency shift to 1286.1 cm^{-1} from its original position of 1279.6 cm^{-1}. The frequency continues to increase to 1287.5 cm^{-1} on returning to RT (Figure 2.11). The band shift occurs from increased sample crystallinity on cooling from the paraelectric state and transformation to a more ordered ferroelectric β phase. In the low frequency region the changes observed are similar to those seen for the variable temperature experiment without annealing. The β phase bands reappear at the same temperatures as in the temperature cycling experiment, signifying that the annealing does not alter the Curie transition for the copolymer.

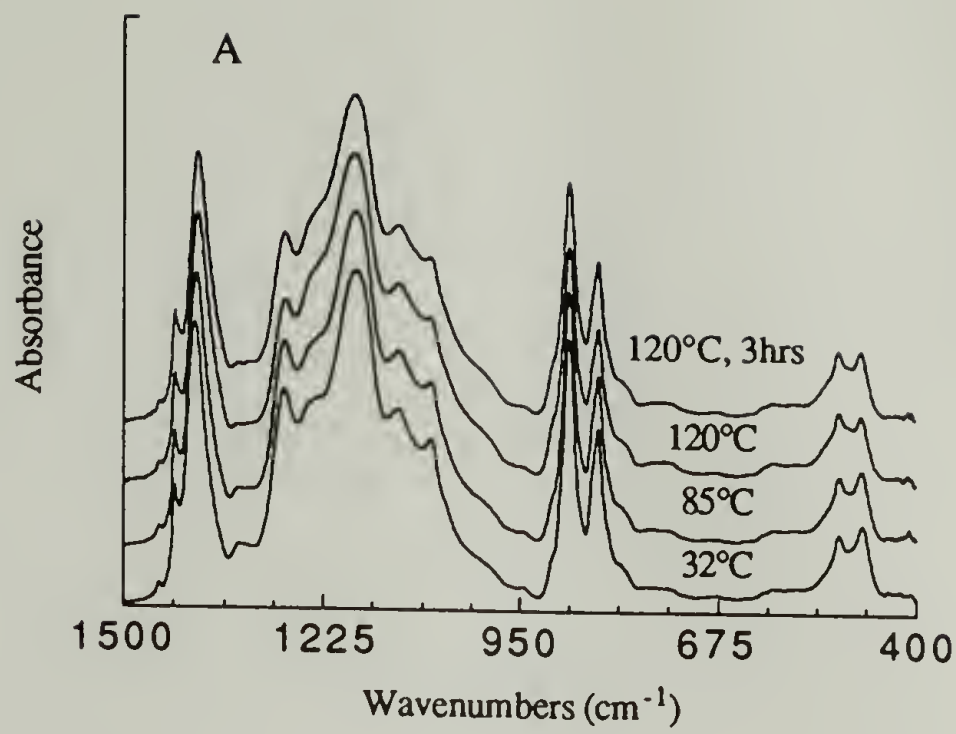

Figure 2.9 Infrared spectra as a function of temperature for sample annealed three hours at 120°C. A: heating; B: cooling.

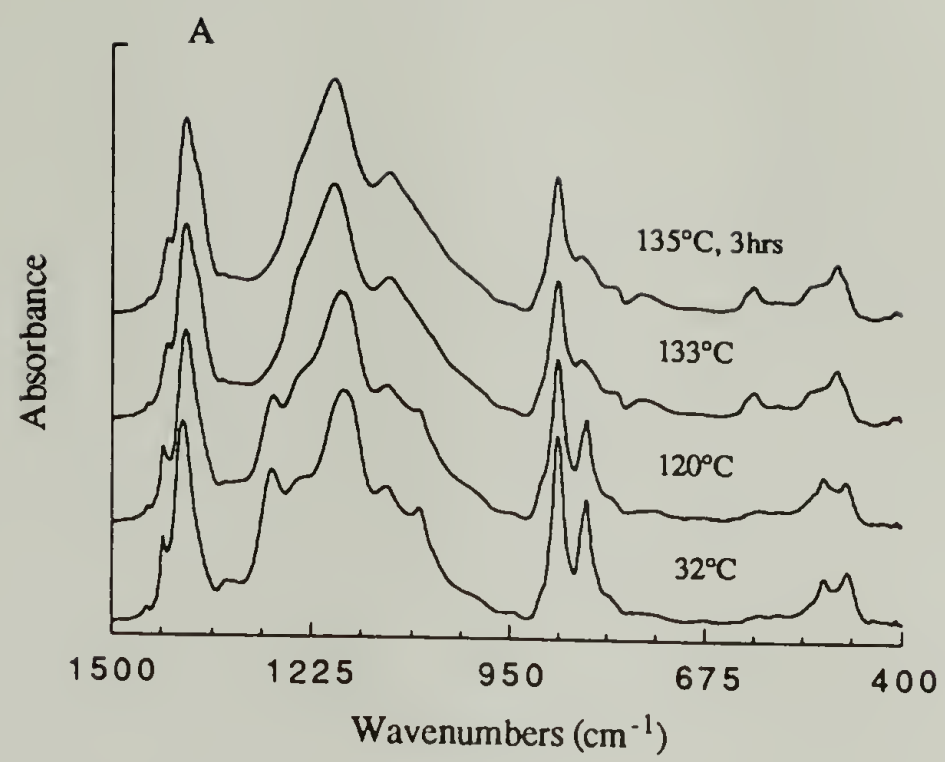

Figure 2.10 Infrared spectra as a function of temperature for sample annealed three hours at 135°C. A: heating; B: cooling.

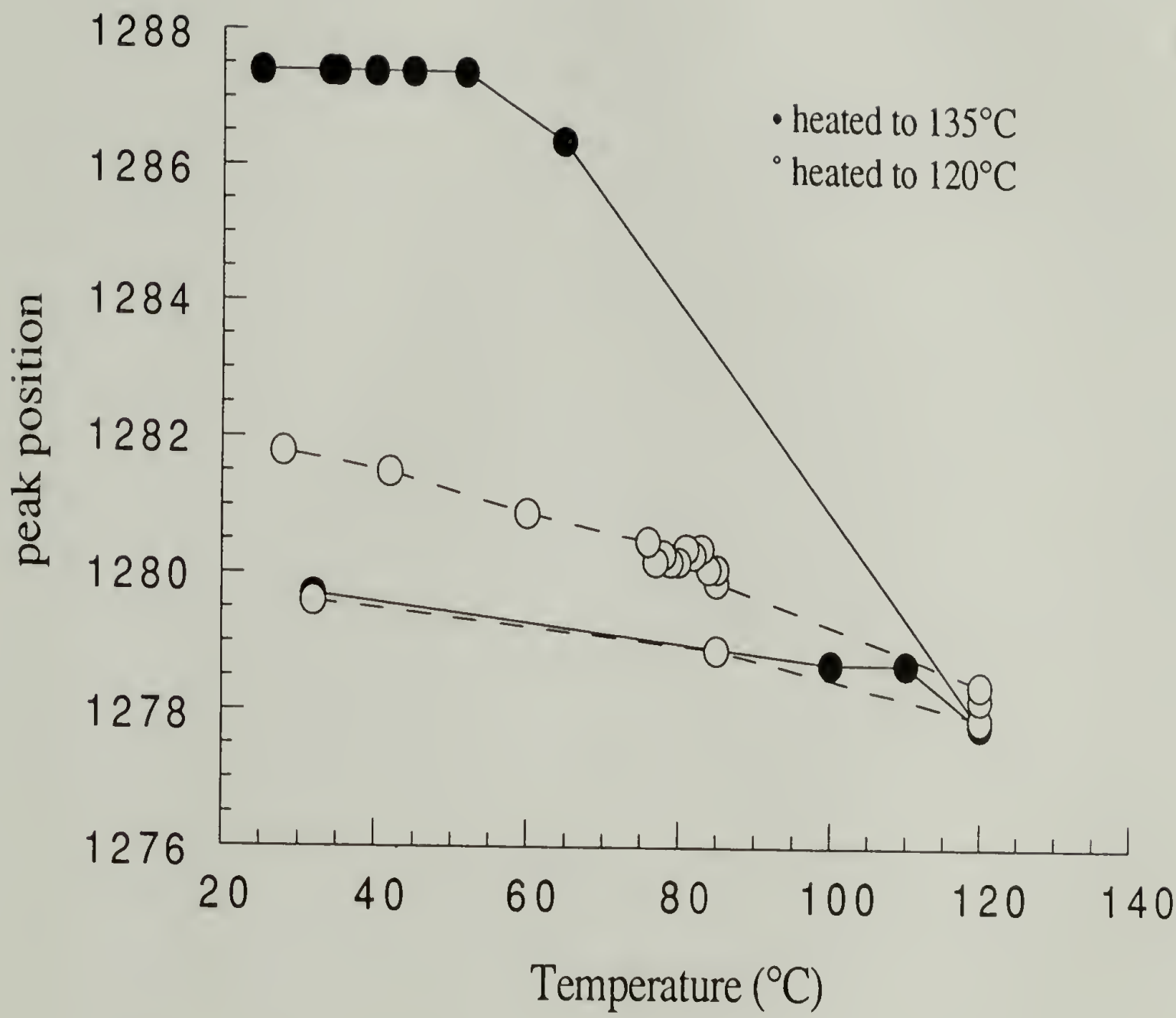

Figure 2.11 Peak position of the long trans sequence vibration as a function of temperature for samples annealed at 120°C and 135°C for three hours.

Again factor analysis was applied to the spectra of the annealing experiments to determine if it can give information about multiple crystalline phases present in these two temperature ranges which cannot be directly observed. Results are shown in Tables 2.3 and 2.4.

Table 2.3 Factor analysis results for 83/17 P(VDF-TrFE) copolymer annealed at 120°C for three hours

component	eigenvalue	RE	IND	RSD
1	2002.97	.017458	.000174	.005022
2	2.20896	.006608	.000082	.001805
3	.270445	.002914	.000046	.000752
4	.049475	.001101	.000022	.000270
5	.003628	.000830	.000023	.000191
6	.001824	.000623	.000025	.000135
7	.000475	.000585	.000036	.000116
8	.000364	.000557	.000062	.000099
9	.000341	.000510	.000128	.000078
10	.000240	.000482	.000482	.000006

Table 2.4 Factor analysis results for 83/17 P(VDF-TrFE) copolymer annealed at 135°C for three hours

component	eigenvalue	RE	IND	RSD
1	1694.32	.053822	.000664	.016156
2	18.8684	.020594	.000322	.005832
3	2.40139	.008508	.000174	.002256
4	.388919	.002559	.000071	.000630
5	.024065	.001440	.000058	.000326
6	.006598	.000781	.000049	.000163
7	.001124	.000603	.000067	.000115
8	.000550	.000464	.000116	.000077

The factor analysis results are different, as may have been expected, for the different annealing temperatures. The sample annealed at the onset of the Curie transition at 120°C shows a minimum in the Maliknowski indicator function at four factors with the RSD being greater than the error at three factors. In comparison, the sample annealed above the Curie transition has six factors following the indicator function criteria, and four factors following the RSD criteria. We must again turn to the abstract eigenspectra to determine how many factors are of significance. From the intensity of the abstract eigenspectra for the sample annealed at 120°C (Figure 2.12), it appears that only two factors are present, signifying the presence of two crystal phases. This can be described by assuming that below the Curie transition the copolymer is in the β trans state and a disordered crystal phase that has gauche conformers disrupting the all trans structure as has been suggested by other authors (6). An investigation of the abstract eigenspectra from the

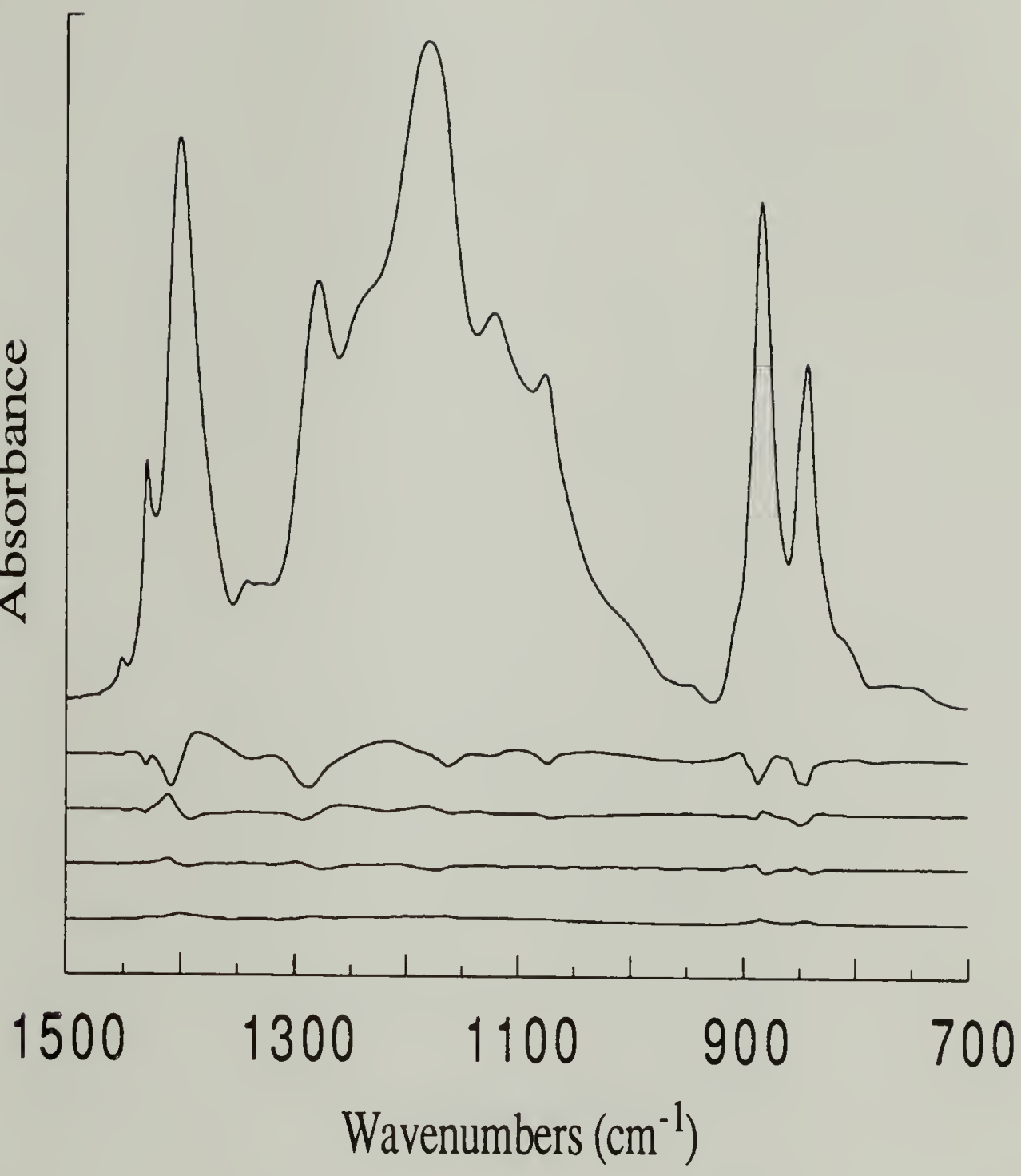

Figure 2.12 Abstract eigenspectra for infrared spectra of P(VDF-TrFE) annealed at 120°C for three hours.

factor analysis of the copolymer annealed at 135°C for three hours shows that there are three factors in this case (Figure 2.13). The values of the first three eigenvalues are much greater than zero, clearly showing that by annealing above T_C the copolymer has three crystalline phases over the temperature range from room temperature to T_C. This is interpretable by the presence of two crystalline phases below the Curie transition, the β phase and α phase possessing some gauche conformers as defects, which can then undergo the conformational change at the Curie temperature to form the paraelectric phase with a disordered TGTG' conformation, giving three crystal phases over the temperature region studied.

Conclusions

The vibrational spectra of P(VDF-TrFE) copolymer have been measured over the temperature range from RT through the Curie transition, and up to 140°C and conformational changes have been monitored. The phase transition is clearly distinguishable at 135°C on heating, and has the typical hysteresis of a first order transition, occurring at lower temperatures on cooling. As in the thermal analysis, the spectroscopic data seem to indicate that the Curie transition on cooling involves two transitions at ~82 and 72°C. The structure of samples that have been temperature cycled differs from the original room temperature material, with spectral differences suggesting a more ordered ferroelectric phase with higher crystallinity being formed from samples crystallized from the melt (Figure 2.14). The structural changes that occur from temperature cycling through the Curie transition agree with studies done on 70/30 copolymers studied by WAXD (10). There is a shift in the frequency of the long trans sequence peak to higher wavenumbers on the reformation of the β phase from the paraelectric phase.

Annealing of the copolymer below the Curie transition gives a greater order in the ferroelectric phase as is seen by the enhancement of vibrations of the β phase. Annealing

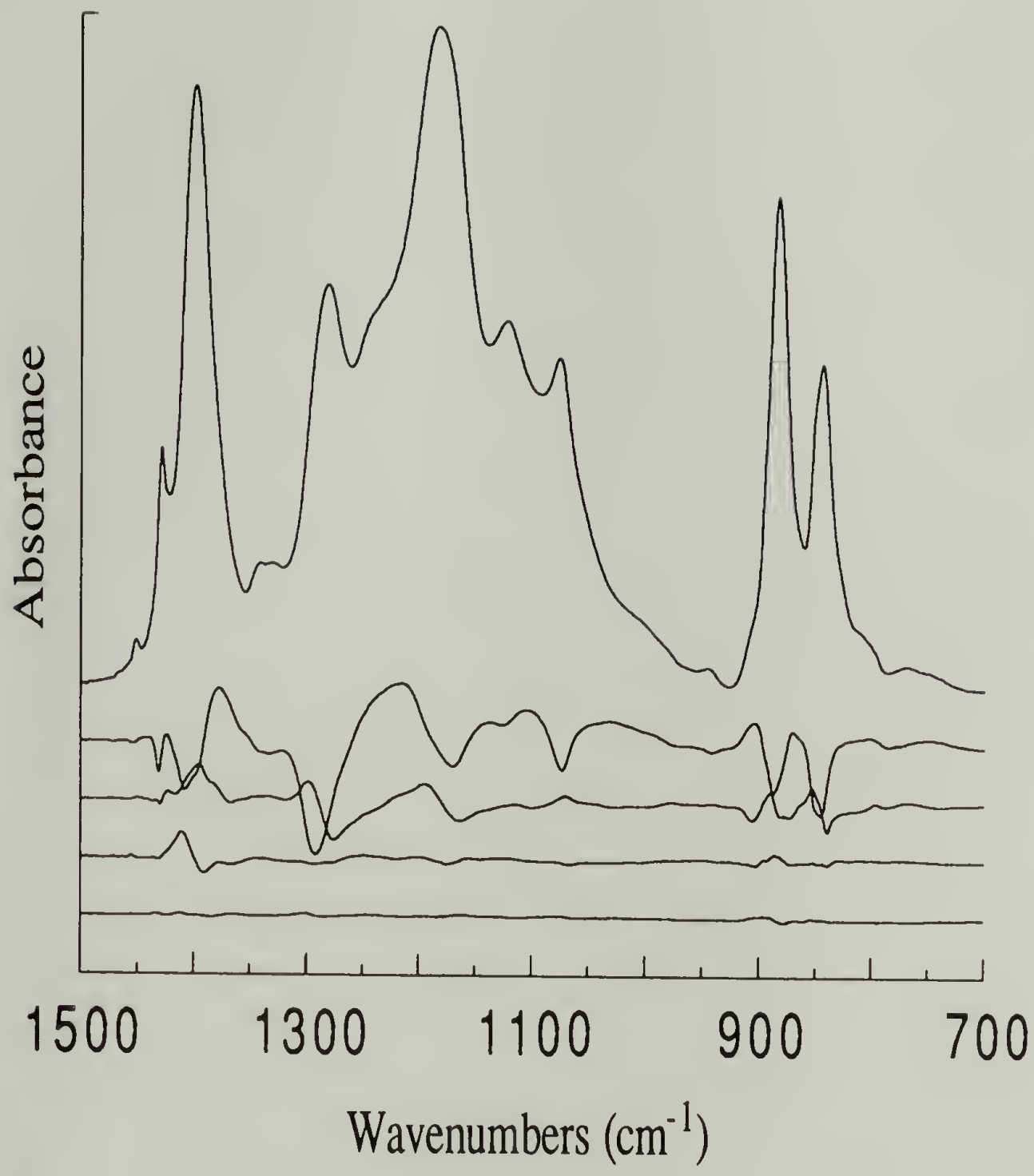

Figure 2.13 Abstract eigenspectra for infrared spectra of P(VDF-TrFE) annealed at 135°C for three hours.

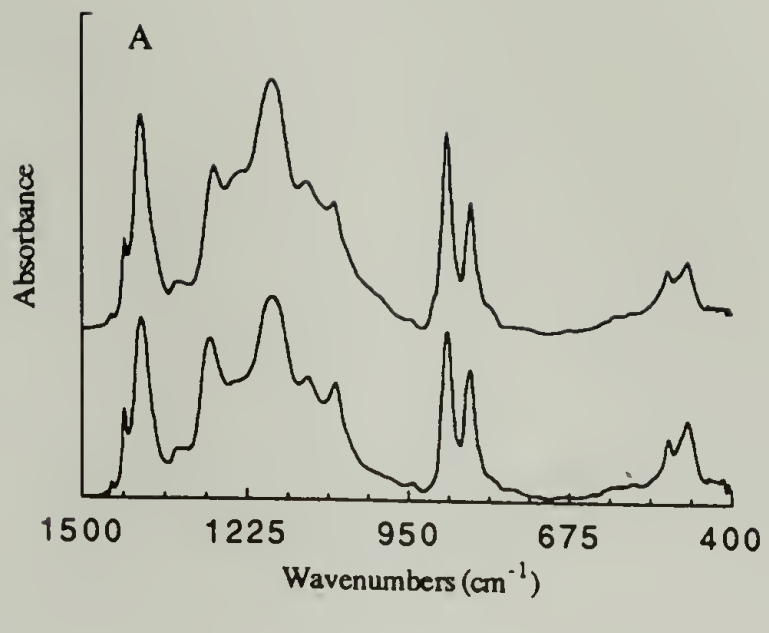

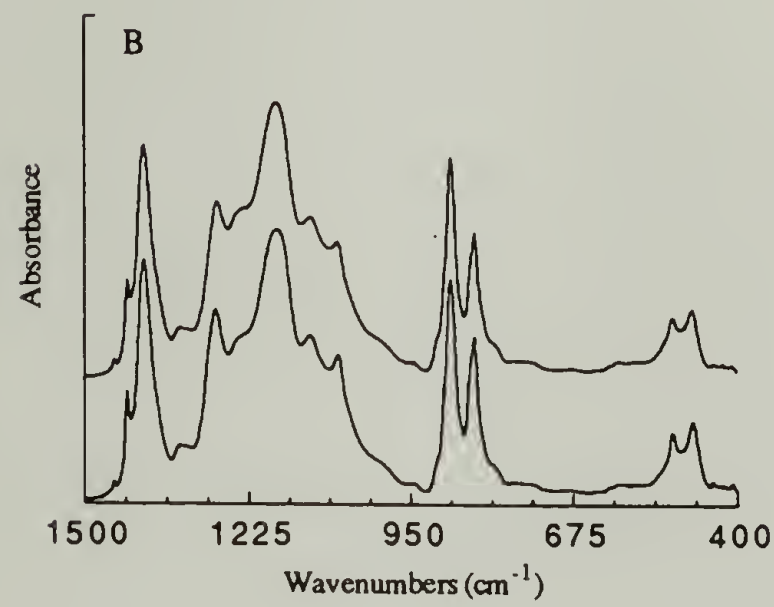

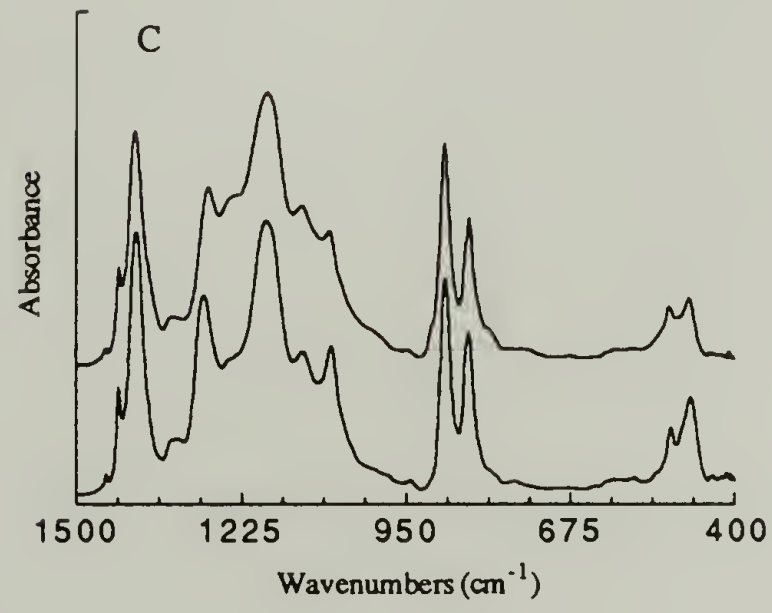

Figure 2.14 Infrared spectra of P(VDF-TrFE) copolymer measured at room temperature before (top) and after (bottom) thermal treatment. A: Temperature cycled through the Curie transition. B: Annealed three hours at 120°C. C: Annealed three hours at 135°C.

above T_C does not change the paraelectric phase or the Curie transition as measured spectroscopically. There is a substantial increase in crystallinity after the copolymers have been annealed at 120 or 135°C as evidenced by the diminishment of amorphous bands in the spectra.

The number of independent crystal phases that contribute to this data cannot be easily discerned using factor analysis. The number of linearly independent components in mixture spectra can usually be determined in factor analysis if the component spectra are not too similar (17). In this case the factor analysis proves to be inconclusive, with the different criteria giving different results. The abstract eigenspectra do suggest that there are three crystal phases present in samples cycled through the Curie temperature and those annealed above the Curie transition, and two factors for those annealed below the Curie transition. From these data three crystalline phase appear to be presentr the temperature range from room temperature to 135°C, with the multiple phase transition behavior in the cooling cycle of the FTIR and DSC being the most supportive evidence of it.

References

1. Tashiro, K.; Kobayashi, M. *Phase Transitions*, **1989**, *18*, 213

2. Tashiro, K.; Takano, K.; Kobayashi, M.; Chatani, Y.; Tadokoro, H. *Polymer*, **1984**, *25*, 195.

3. Tashiro, K.; Takano, K.; Kobayashi, M.; Chatani, Y.; Tadokoro, H. *Ferroelectrics*, **1984**, *57*, 297.

4. Lopez Cabarcos, E.; Gonzalez Arche, A.; Baltá Calleja, F. J.; Bösecke, P.; Röber, S.; Bark, M.; Zachmann, H. G. *Polymer*, **1991**, *32*, 3097.

5. Koga, K.; Ohigashi, H. *J. Appl. Phys.*, **1986**, *59*, 2142.

6. Koga, K.; Nakano, N.; Hattori, T.; Ohigashi, H. *J. Appl. Phys.*, **1990**, *67*, 965.

7. Farmer, B. L.; Hopfinger, A. J.; Lando, J. B. *J. Appl. Phys.*, **1972**, *49*, 1232.

8. Moreira, R. L.; Saint-Gregoire, P.; Lopez, M.; Latour, M. *J. Polym. Sci., Polym. Phys. Ed.*, **1989**, *27*, 709.

9. Tanaka, H.; Yukawa, H.; Nishi, T. *Macromolecules*, **1988**, *21*, 2469.

10. Bourgaux-Leonard, C.; Legrand, J. F.; Renault, A.; Delzenne, P. *Polymer*, **1991**, *32*, 597.

11. Kobayashi, M.; Tashiro, K.; Tadokoro, H. *Macromolecules*, **1975**, *8*, 158.

12. Tashiro, K.; Itoh, Y.; Kobayashi, M.; Tadokoro, H. *Macromolecules*, **1985**, *18*, 2600.

13. Tashiro, K.; Kobayashi, M. *Polymer*, **1988**, *29*, 426.

14. Kim, K. J.; Reynolds, N. M.; Hsu, S. L. *Macromolecules*, **1989**, *22*, 4395.

15. Kim, K. J.; Reynolds, N. M.; Wang, Y. K.; Antolin, K.; Hsu, S. L.; Stidham, H. D. *submitted.*

16. Antoon, M. K.; D'Esposito, L.; Koenig, J. L. *Appl. Spectrosc.*, **1979**, *33*, 351.

17. Maliknowski, E. R.; Howery, D. G.; *Factor Analysis in Chemistry*; Wiley-Interscience: New York, 1980.

18. Shurvell, H. F.; Bulmer, J. T.; *Vibrational Spectra and Structure;* J. R. Durig, ed.; Elsevier Scientific: New York, 1977; p 91.

19. Burchell, D. J.; Hsu, S. L. *Polymer*, **1981**, *22*, 907.

20. Maliknowski, E. R. *Anal. Chim. Acta*, **1982**, *134*, 129.

21. Tashiro, K.; Takano, K.; Kobayashi, M.; Chatani, Y.; Tadokoro, H. *Polymer*, **1981**, *22*, 1312.

22. Li, G. R.; Kagami, N.; Ohigashi, H. *J. Appl. Phys.*, **1992**, *72*, 1056.

23. Ohigashi, H.; Kagami, N.; Li, G. R. *J. Appl. Phys.*, **1992**, *71*, 506.

CHAPTER III

STRUCTURAL CHANGES AND TRANSITIONS IN NONISOTHERMALLY CRYSTALLIZED P(VDF-TrFE)

Introduction

The piezoelectric and ferroelectric properties of PVDF and P(VDF-TrFE) copolymers arise from the orientation of molecular dipoles in the crystalline region of the polymers and therefore the crystal structure and molecular orientation are crucial in dictating the final properties (1-3). To influence the crystal structure of PVDF and other polymers it is possible to modify the crystallization conditions which will in turn result in different crystal phases, changes in sample crystallinity, defect content, lamellar thickness, and crystallite size (4-13). From studies of PVDF different temperature regions of crystallization have been defined. At high temperatures of crystallization (150-160°C) the α and γ polymorphs are formed, accompanied by a transformation from the α to the γ form when the crystallization is carried out for long periods of time. Only the α polymorph is formed at high degrees of supercooling, while crystallization under high pressure or at higher temperatures (175-185°C) results in the formation of the γ polymorph (5, 14, 15). The β polymorph occurs during crystallization at high temperatures and high pressures (5, 14, 16). Marand et al. (8) found that for PVDF the relative nucleation and growth rates of the α and γ phases differ as a function of the crystallization temperature. From these studies it has been shown that the crystal structure of PVDF varies with T_{cry}.

The defect content in terms of the head-to-head/tail-to-tail (HHTT) linkages in PVDF have been shown to have a large influence on the crystal structure, polymorphism and Curie transitions (17). Higher defect contents (13.5 - 15.5 mol %) allow for a clear Curie transition to be observed in PVDF. Due to the differences in defect content in PVDF

resins, equilibrium crystallization parameters needed to quantify the crystallization kinetics have been difficult to define. In several studies of PVDF crystallization, equilibrium melting points for the PVDF have been measured, but the values range from 175 - 210°C, with the differences believed to be due to varying purity of samples having different defect contents (13, 15, 18, 19).

Copolymer units, like HHTT linkages, act as defects in PVDF. As a result of the chemical defects in the chain, there is a decrease in the crystal packing efficiency that reduces the steric and electrostatic repulsions between neighboring sites. Due to the decrease in the interchain interactions the all trans conformation is favored at low temperatures, as opposed to the usually obtained TGTG' conformation of the α crystal phase of PVDF. An effect related to the chemical defects of copolymer units is the reduction in the Curie temperature below the melting transition of the ferroelectric phase in P(VDF-TrFE) copolymers, while it coincides with the melt in PVDF (20).

The crystal structure of PVDF-tetrafluoroethylene copolymers has been shown to be affected by the initial crystallization into the paraelectric phase which subsequently undergoes a crystal-crystal transition to the ferroelectric phase (9). Similar results has been found for P(VDF-TrFE) copolymers where crystallization in the paraelectric phase can be modified to allow for greater conformational defects which are then frozen into the crystal structure, preventing a complete conversion to the ferroelectric phase (21-23).

From studies made on the crystallization of P(VDF-TrFE) copolymers it has been shown that the crystallization temperature strongly effects the ferroelectric phase transition (21, 22). The changes in the ferroelectric phase transition are believed to arise from the changed crystalline structure formed under different crystallization conditions, but no conclusive structural characterization has been presented to support this hypothesis (22). WAXD measurements on samples prepared with different thermal treatments showed no significant differences (21). In cooling experiments on P(VDF-TrFE) copolymers, Stack and Ting (21) found that the effect of changing the rate of cooling these copolymers from

the melt through the crystallization temperature has a larger effect on subsequent transition temperatures than when the cooling rate is varied through the Curie transition.

It is our objective to study the structural changes in P(VDF-TrFE) copolymers that arise from changes in the crystallization conditions. The transition temperatures as a function of crystallization temperature have already been studied for several copolymer compositions (22), but the related structural differences coming from the crystallization into the paraelectric phase which transforms to the ferroelectric phase at the Curie transition have not been investigated. The transition temperatures and their enthalpies on heating and cooling measured by differential scanning calorimetry (DSC) will be presented for the nonisothermal crystallization of P(VDF-TrFE) copolymers and will be related to the crystal structure formed by cooling at different rates through the crystallization temperature. The chain conformation distribution, which is known to vary with the crystal phases, will be measured using Fourier transform Raman spectroscopy. The changes in the crystal phase content, interplanar spacing, and crystallite dimensions will be measured using WAXD.

The advent of FT-Raman spectroscopy has made the structural study of fluoropolymers much easier than with the dispersive instrument. The near infrared excitation of the Nd-YAG laser (1.06μm) precludes the problem of fluorescence that has limited the study of all but the most pure polymer samples by dispersive Raman. The Fourier transform system also has the advantages of higher throughput and multiplexing (24).

Nonisothermal crystallization experiments are useful to investigate because such experiments more closely resemble real processing conditions such as fiber spinning, extrusion, and molding than do isothermal experiments. This study entails the crystallization of P(VDF-TrFE) copolymers with 83/17 molar composition at cooling rates of 0.01-3°C/min from the melt through the crystallization temperature. There has been little work done to date on the kinetics of nonisothermal crystallization with one limitation being the lack of kinetic parameters to use in any model that has been presented (25). In an

extension of the Avrami equations, Ozawa did derive a kinetic analysis of nonisothermal crystallization which will be applied to the crystallization data presented here (26).

Experimental

The random copolymers of P(VDF-TrFE) were purified by reprecipitation into methanol from acetone solution, filtered and dried under vacuum. Films were then cast from a 1% acetone solution. Samples of 5-10 mg were used in a Dupont 2910 DSC for crystallization experiments. Samples were heated to 150°C, held for 10 minutes to melt them completely, then cooled at rates of 3, 1, 0.5, 0.1, 0.02, and 0.01°C/min from 150 - 125°C, and uniformly at 3°C/min from 125°C to room temperature. Film samples (~0.02mm) were crystallized under comparable conditions in a small oven designed in this lab and controlled by a program run on an AT computer (Appendix B). These samples were prepared to compare the effect of sample thickness on crystallization and to have samples thin enough to measure infrared spectra. Transition temperatures were measured during the cooling runs at varying rates in the DSC and on subsequent heating at 20°C/min. The FT-Raman spectra were measured on a Bruker IFS66 FT-Raman spectrometer equipped with a Nd-YAG laser operating at 200 mW power. Typically 512 scans were collected. Infrared spectra were measured on an IBM IR32 spectrometer using 128 scans at $2cm^{-1}$ resolution. The wide-angle X-ray diffraction studies were performed on a Rigaku-Denki instrument equipped with a sealed target, using nickel filtered CuKα radiation with a 1.5418Å wavelength. A Statton camera was used for detection. An Optron C-4100 microdensitometer was used to digitize WAXD patterns that were recorded on film. The diffracted intensity was corrected using the Lorentz factor for randomly oriented crystalline substances, and a geometric factor that accounts for the change in the distance the X-rays travel as they move radially from the center of the film, with the corrected intensity given by:

$$I_{corr} = I_{obs}(1+ \tan^2 2\theta)(\sin 2\theta \sin\theta) \qquad (3.1)$$

WAXD of the film samples was run on a a Rigaku D/MAX-2BX horizontal X-ray diffractometer operating in the reflection mode at a scan speed of 0.2 or 2°/min. The intensity was corrected with the Lorentz factor.

Results and Discussion

The change in the rate of cooling the copolymer samples through the crystallization temperature effectively changes both the crystallization time and the maximum crystallization temperature (Figure 3.1). At the slower cooling rates the crystallization occurs at a higher temperature, which can be measured from the DSC thermogram At the higher temperatures crystallization takes more time as is expected at lower degrees of supercooling (12). From crystallization studies of PVDF it is known that different polymorphs crystallize at different temperatures (4, 5). The final crystal structure can be readily identified in the homopolymer after the crystallization, as this is the structure that will remain when the sample has been cooled to room temperature. In P(VDF-TrFE) copolymers, the structure that is formed upon crystallization undergoes the paraelectric-to-ferroelectric transition above room temperature, so the effect of the crystallization conditions on the final structure involves also the influence that the crystallization has on the Curie transition. The longer crystallization times associated with the slower cooling rate may serve as annealing of the crystals, which allows a perfection of crystalline order (12). In this case of crystallization in the conformationally disordered paraelectric phase of P(VDF-TrFE), the annealing will give a more stable paraelectric phase with a high defect content in terms of gauche (G) conformers. Annealing or slow crystallization of the copolymer result in the perfection of a disordered crystalline phase.

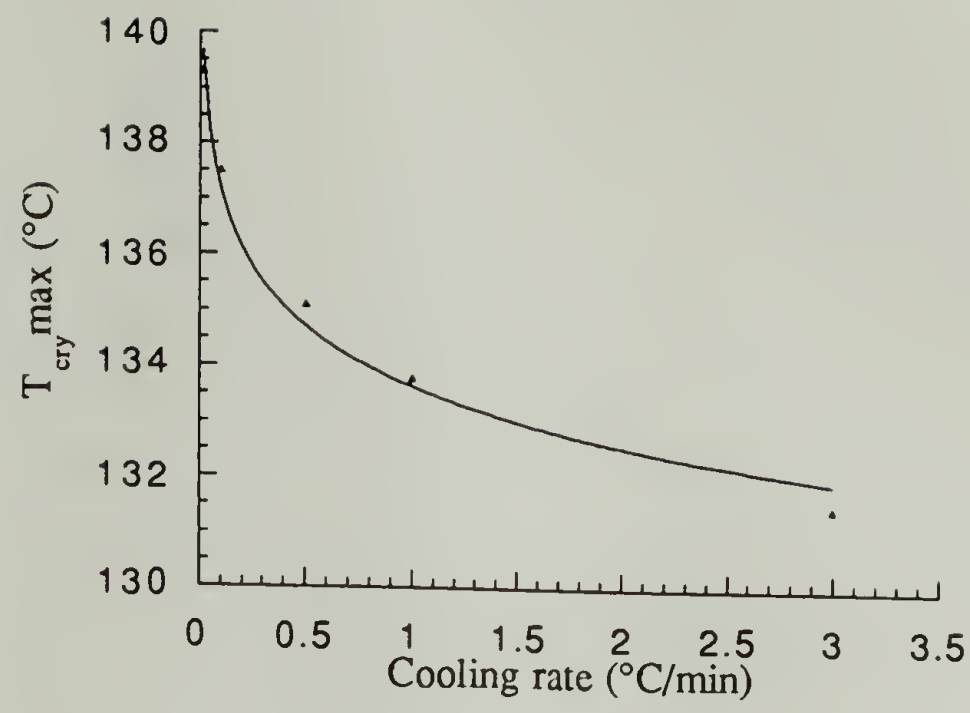

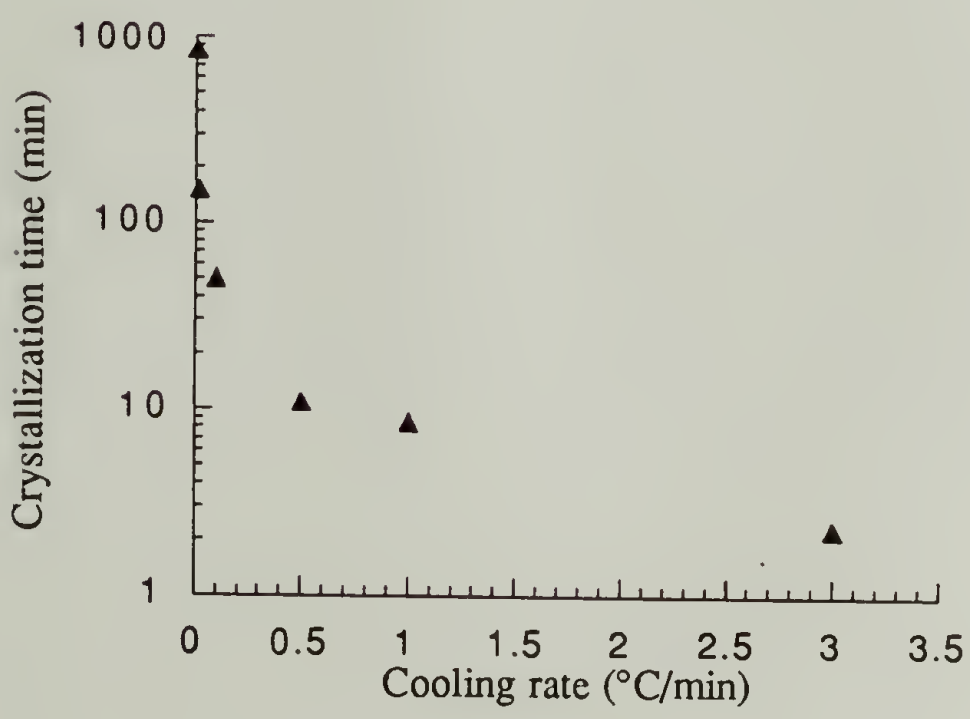

Figure 3.1 Crystallization temperature (top) and time (bottom) as a function of cooling

An analysis of the kinetics of nonisothermal crystallization from thermoanalytical data was developed by Ozawa (26) from an extension of the Avrami equation to accommodate the case of heating or cooling at a constant rate during the crystallization process. This has been applied to the crystallization data of these copolymers that have been prepared by cooling at constant rates through the crystallization temperature.

In the Ozawa analysis one measures the degree of conversion at temperature T, C(T), at cooling rate a. This value is related to the cooling function of the process by the following

$$\log[-\ln(1-C(T))] = \log \chi(T) - n\log a \qquad (3.2)$$

From a plot of log[-ln(1-C(T))] vs. log a at a given temperature the Avrami coefficient n and the cooling function can be determined (Figure 3.2).

The resulting plot shows that there is a linear dependence of log[-ln(1-C(T))] on the cooling rate, with the slopes giving information on the dimensionality of the growth. At the lower temperatures (131-136°C) the growth is one dimensional, becoming two dimensional above 137°C.

The cooling crystallization function of the copolymer obtained from the intercept of the Avrami-like curves is plotted in Figure 3.3. This shows that at lower temperatures the crystallization is faster and occurs to a greater extent, as is expected in polymer crystallization. Knowledge of the function $\chi(T)$ over a broad temperature range allows for the determination of the kinetic crystallizability that characterizes the degree of crystallinity reached on cooling a material from the melting temperature to the glass transition temperature (25).

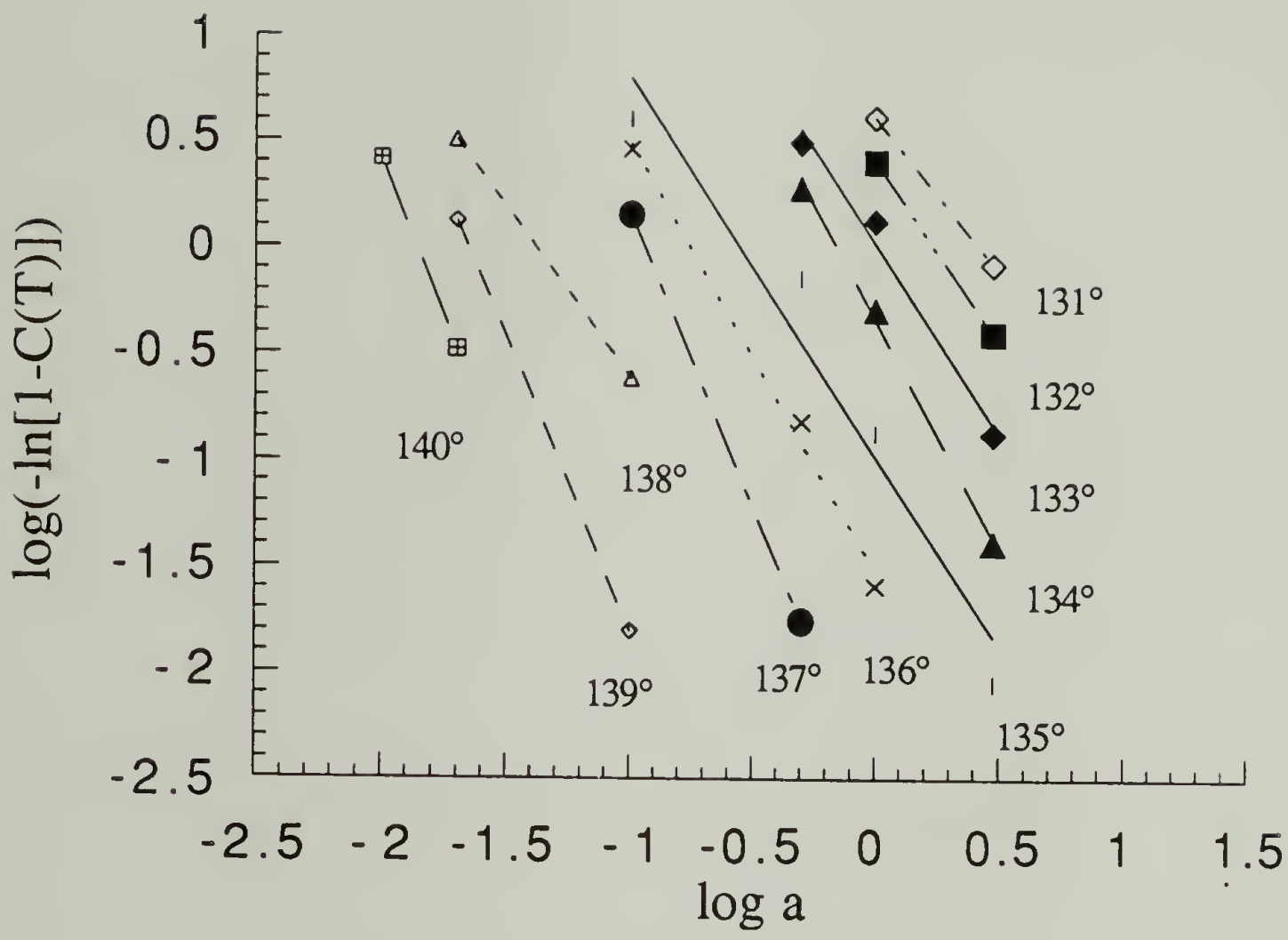

Figure 3.2 Dynamic cooling crystallization of 83/17 mol% P(VDF-TrFE) copolymer at different cooling rates (a).

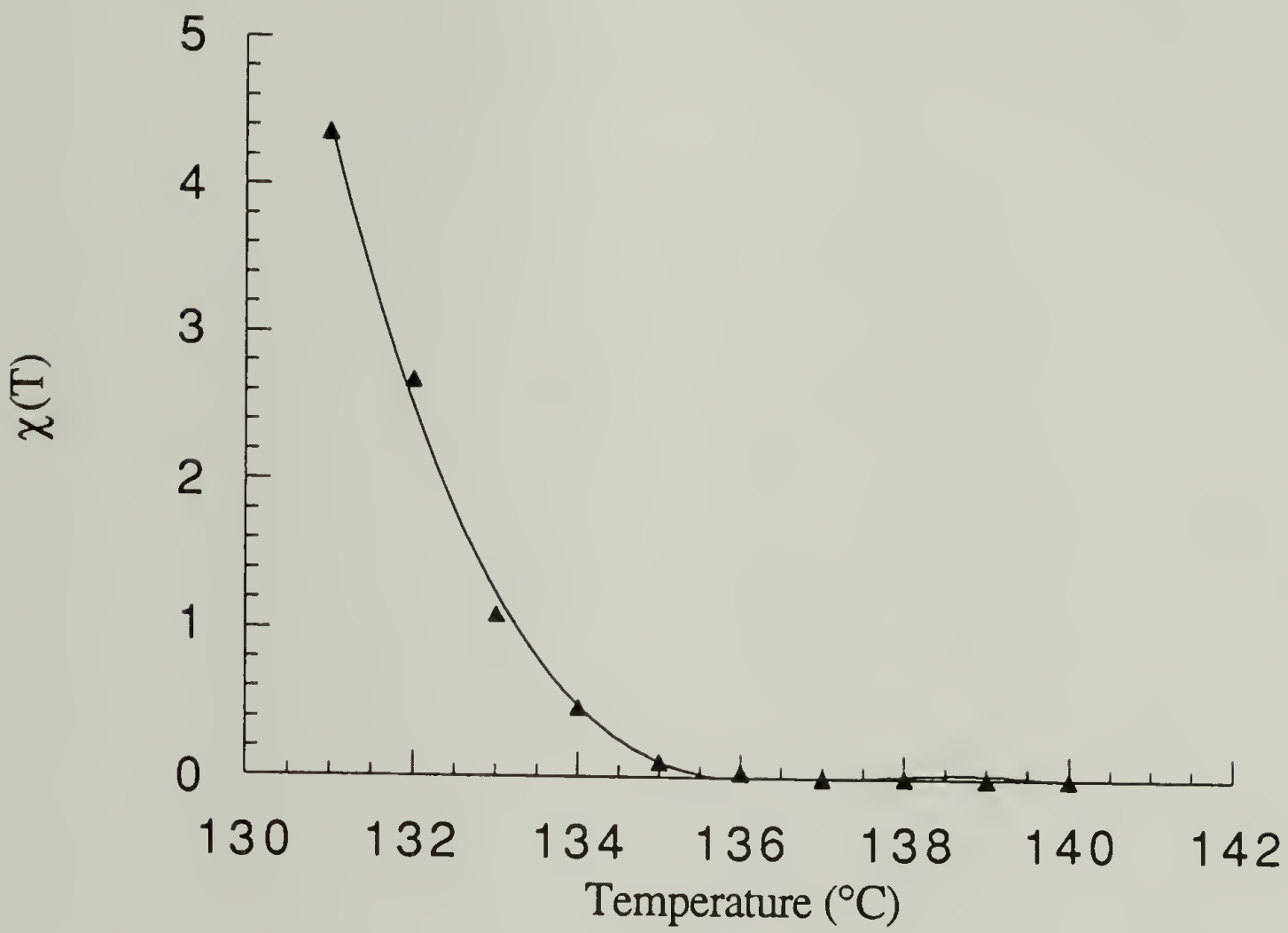

Figure 3.3 Cooling crystallization function of P(VDF-TrFE) copolymer from nonisothermal crystallization.

Crystallization and Transition Behavior Measured by DSC

The cooling thermograms associated with the different cooling rates exhibit different crystallization temperatures (Figure 3.1). The Curie transition in all cases is composed of two peaks whose temperatures and relative magnitude change with cooling rate (Figure 3.4). The presence of two Curie transitions suggests that there are two types of paraelectric crystals that have been formed and undergo a paraelectric-to-ferroelectric transition. In a polymorphic system such as P(VDF-TrFE) there is only one stable polymorph at any one temperature, but metastable structures may also be present and change by solid-solid transitions with thermal treatment (12). The two Curie transitions may arise from a solid-solid transition of the α and γ phases to the β phase. There may be a transformation of α to γ phase crystals during the cooling process, as the γ phase chain conformation is intermediate between that of the α and β phase. The first transition appears at about 84°C, and the second at ~77°C, with the temperatures continually decreasing as the cooling rate is decreased. The lowered transition temperatures with slower cooling rate suggest that the samples that have a longer crystallization time have formed a more perfected paraelectric phase that requires more energy to return to the ferroelectric phase. The smaller magnitude of the transitions suggests that the transformation to the ferroelectric phase does not occur to as great an extent in the more slowly cooled samples. The change in the relative magnitude of the transitions suggests that at longer times there is more material undergoing the transformation of α to γ phase during the cooling crystallization, so the α to β phase transition decreases and the γ to β transition then predominates.

On measuring the transition temperatures of these samples on subsequent heating it was found that the Curie transition, T_c, decreased for samples cooled more slowly, and T_m increased (Table 3.1), such that the sample cooled at 0.02°C/min has a nearly complete separation of the transitions that tend to overlap in the other cases. In a sample quenched into liquid nitrogen from 155°C, there is only one transition observed

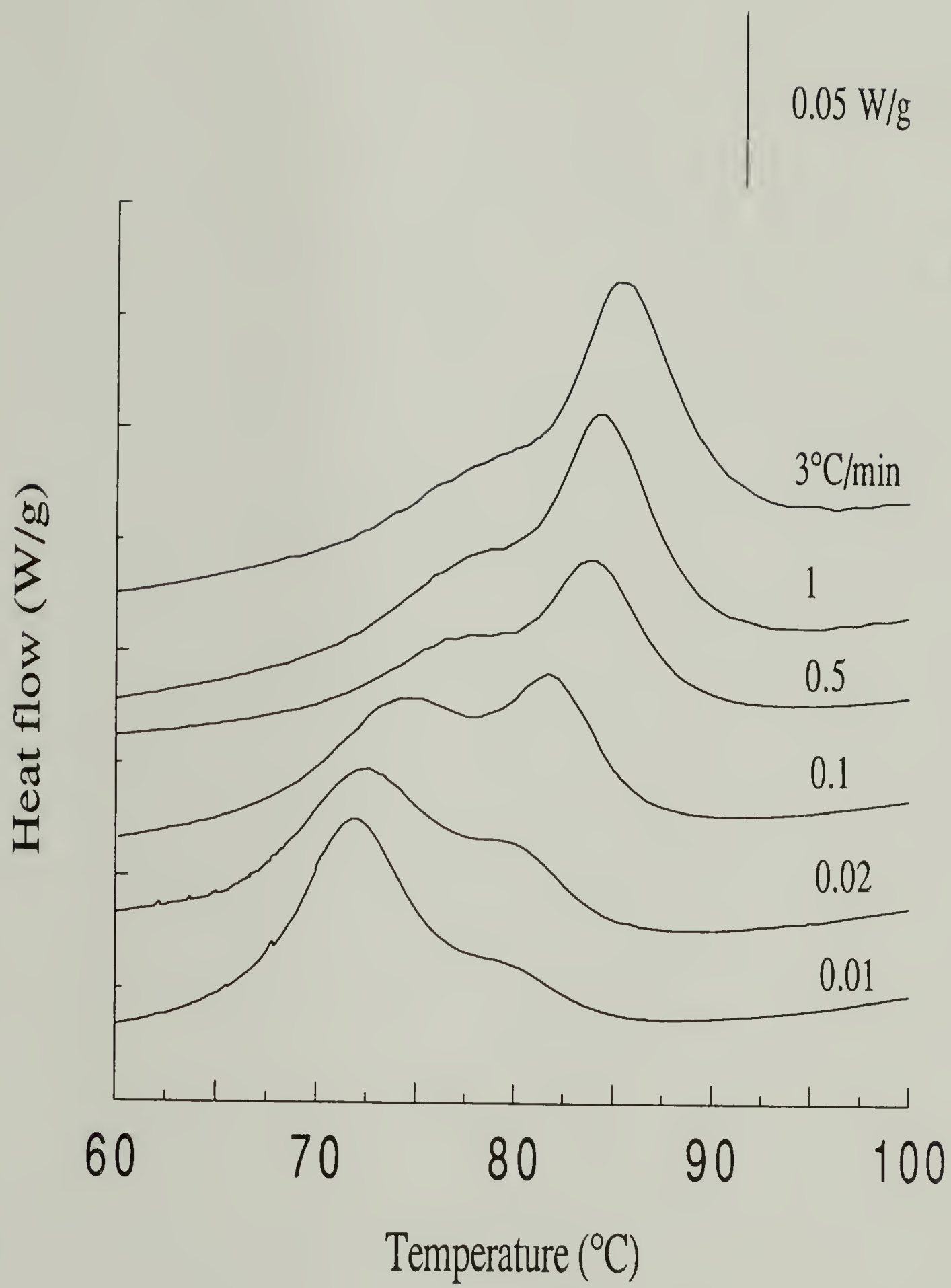

Figure 3.4 Curie transitions on cooling at different rates through the crystallization temperature.

due to the coalescence of the transitions (Figure 3.5). The decreased T_c in slowly cooled samples is indicative of the presence of disordered ferroelectric crystals that more easily undergo the Curie transition. The greater disorder is also seen in the breadth of the Curie transition that appears to include two solid-solid transitions involving materials with different degrees of order (Figure 3.6). The divergence of the transition temperatures as the cooling rate is decreased is shown in Figure 3.7. The melting temperature and the heat of fusion increase with the slower cooling rate as the sample crystallinity increases by 40% at the longer crystallization times. This increased crystallinity at the higher crystallization temperatures (slower cooling rates) is as generally observed for crystallization of most polymers (27).

Table 3.1 Summary of DSC measurements from nonisothermal crystallization

Cooling rate	T_{c1}(°C)	T_{c2}(°C)	T_c(°C)	T_m(°C)	ΔH_m(J/g)
quenched	-	-	148	148	53.9*
3.0(°C/min)	85	78	140	149	24.9
1.0	83	77	139	150	26.9
0.5	84	77	138	150	27.5
0.1	81	74	137	152	27.8
0.02	80	73	136	153	28.6
0.01	80	72	137	156	34.9

* enthalpy of overlapping transitions

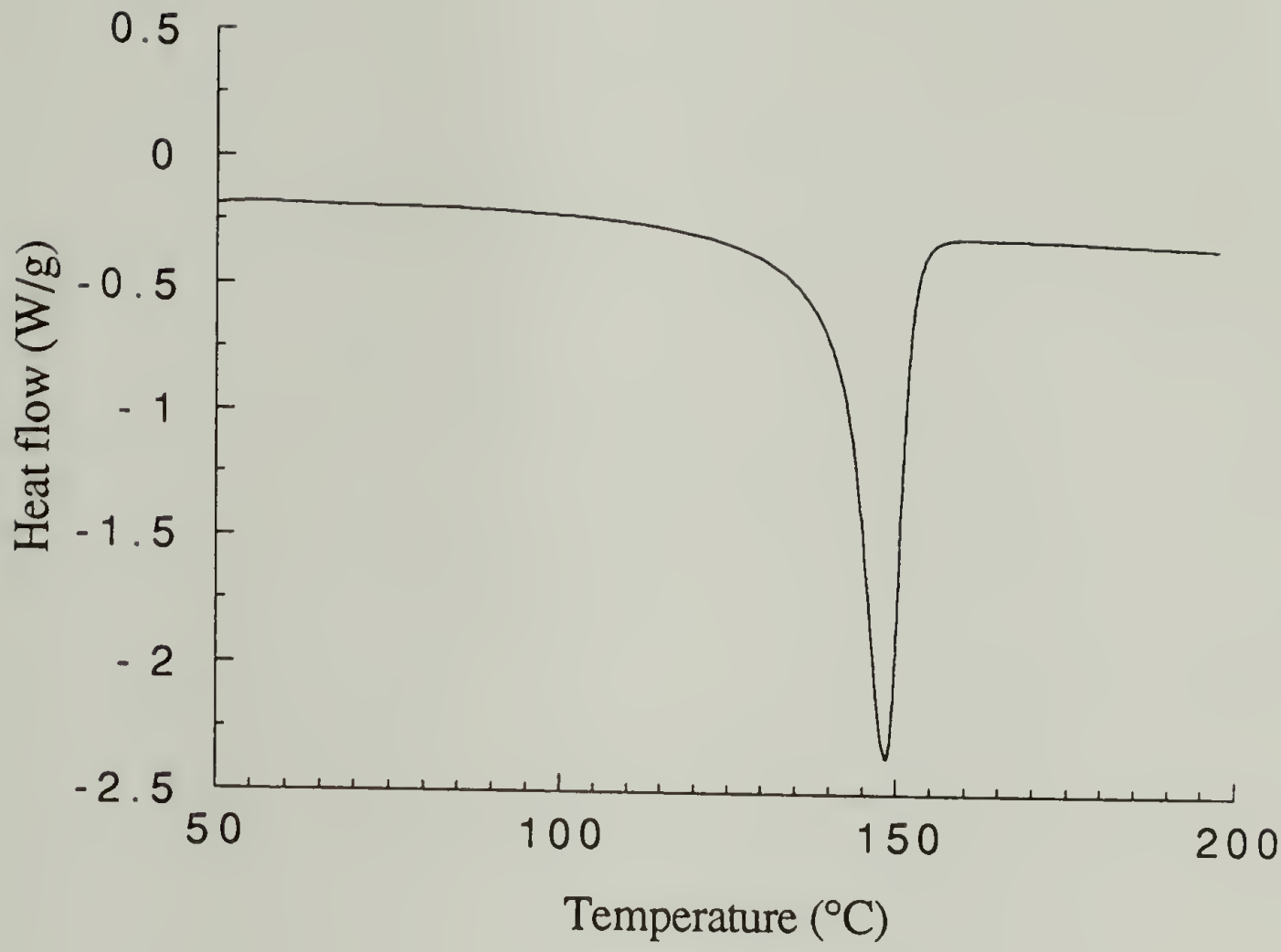

Figure 3.5 DSC thermogram of sample quenched from the melt into liquid nitrogen.

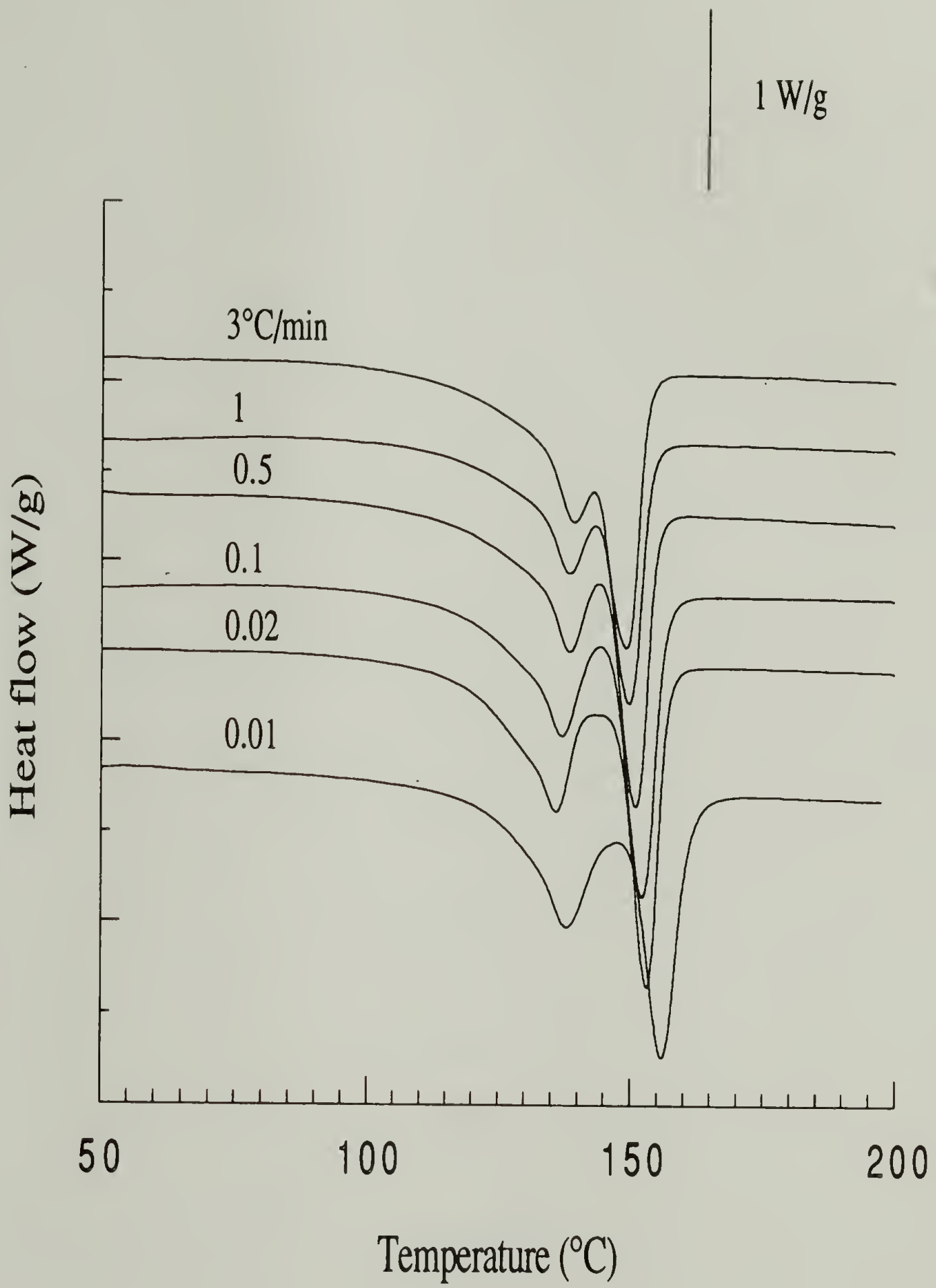

Figure 3.6 DSC thermograms on heating at 20°C/min of samples crystallized at different cooling rates.

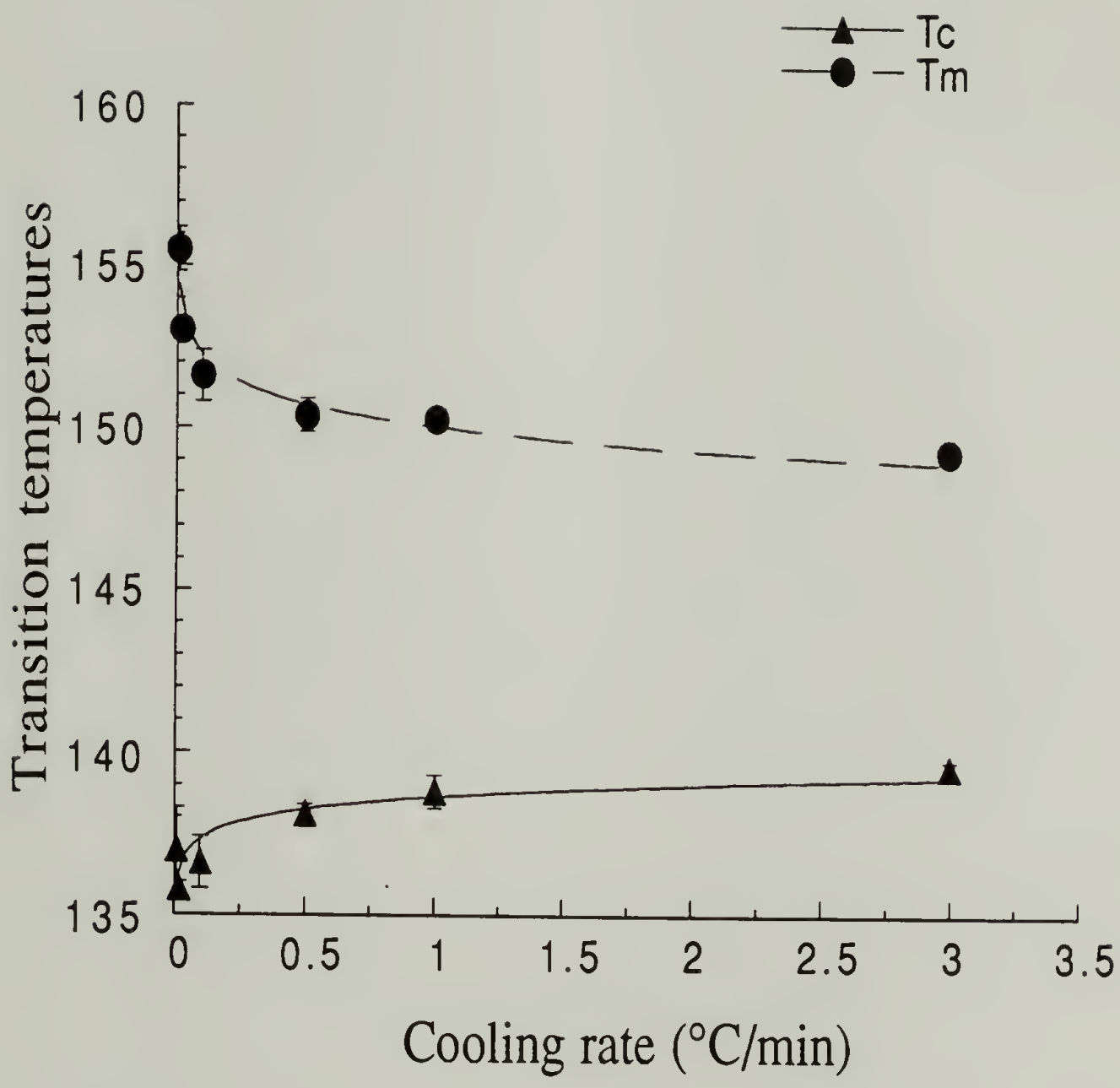

Figure 3.7 Transition temperatures as a function of cooling rate.

Spectroscopic Analysis of Chain Conformation Distribution

Vibrational spectroscopy is a technique sensitive to the measurement of local chain conformation and is therefore invaluable in the study of the crystal phases of PVDF and its copolymers which possess different chain conformations. The assignment of the various crystal phases of PVDF has been made based on normal coordinate analysis (28, 29). These assignments are applied in the study of P(VDF-TrFE) copolymers as better calculations are not available. Vibrations due to trans and gauche linkages are used to measure the relative conformational distribution in the copolymer chain. In P(VDF-TrFE) copolymers the symmetric CF_2 vibration for long trans sequences appears at 842 cm^{-1} and at 800 cm^{-1} for TGT conformations. The ratio of the peak intensities of these vibrations gives a measure of the β phase content relative to that of α and γ phases.

From the FT-Raman spectra of samples that have been cooled at different rates it is seen that the gauche conformation content increases with the slower cooling rates (Figure 3.8). The presence of gauche linkages in the slower cooled samples arises from the fact that these samples reside in the paraelectric phase for longer times, allowing for a perfection of the defect-ridden paraelectric state that then does not undergo a complete transformation to the ferroelectric state as it passes through the Curie transition. The smaller Curie transitions observed in the DSC are now accountable by the fact that the transformation to the ferroelectric phase is incomplete, as the final RT structure possesses many gauche defects that are frozen in during the slow cooling process.

Further spectroscopic evidence for the retention of α phase crystals is that with slower cooling rates the 442 cm^{-1} β phase band disappears as the α phase vibration at 410 cm^{-1} increases in intensity. The half-width of the 510 cm^{-1} β phase band increases as the α phase content increases because of an increasing contribution from the α phase vibration at 530 cm^{-1}. The $t(CF_2)$ vibration shifts from 268 cm^{-1} for the 3°C/min to 274 cm^{-1} for cooling at 0.02°C/min. The $t(CF_2)$ band in PVDF is centered at 287 cm^{-1} for the α phase and at 263 cm^{-1} for the β phase. With slower cooling rates the α and γ phase

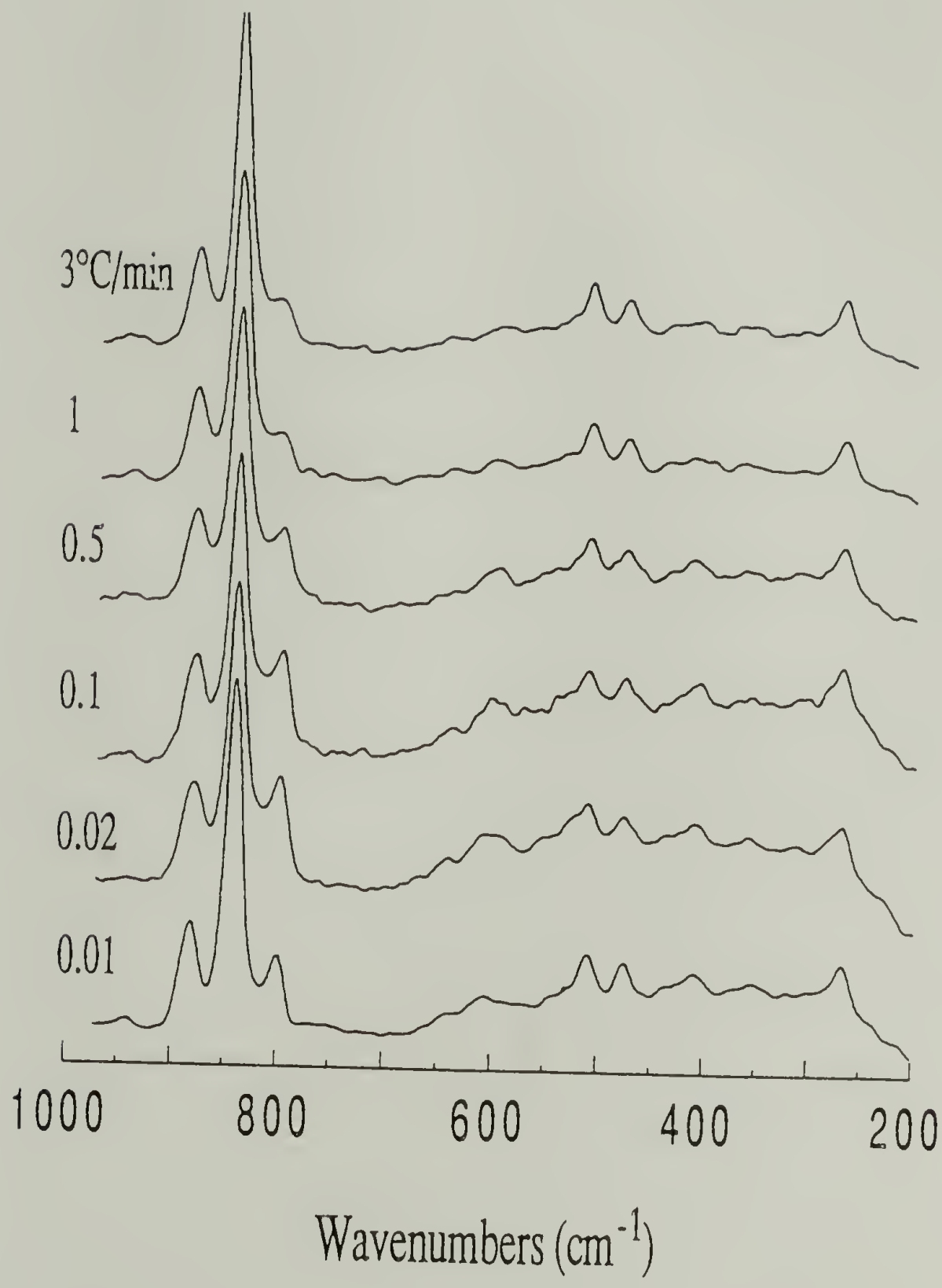

Figure 3.8 FT-Raman spectra of samples prepared using different cooling rates.

bands in the 300 cm^{-1} region begin to develop. Other observable spectral changes with the changed cooling rates are an increase in G vibrations at 610 and 410 cm^{-1}.

The FT-Raman data clearly show that the rate of cooling through the crystallization temperature affects the final chain conformation of the copolymers. The slower cooled samples that have longer crystallization times and higher crystallization temperatures form more stabilized paraelectric phases that suppress a complete paraelectric-to-ferroelectric transition on cooling. The stable, but more disordered, paraelectric phase formed during the crystallization results in a room temperature structure that retains some disorder of gauche conformers.

Crystal Morphology Determined by WAXD

Crystallization conditions can influence the final structure of polymers very markedly (12). So far we have seen how the chain conformation distribution and transition temperatures in the P(VDF-TrFE) copolymers are modified by varying the cooling rate through the crystallization temperature. Changes in the crystal structure are also expected with the different cooling rates used in the crystallization. WAXD gives information on the crystal structure, interplanar spacing, crystallinity and crystallite size in crystalline polymers (30). Extensive work has been done on the measurement of the crystal parameters of the crystal phases of PVDF and the identification of the crystal phases in the P(VDF-TrFE) copolymers crystallized under different conditions will be based on those values (14, 31, 32).

Crystal Phase Identification from Bragg Reflections. The P(VDF-TrFE) copolymers cooled at different rates exhibit different reflections in their X-ray diffraction patterns. The X-ray diffraction patterns of samples cooled at 3 and 1°C/min have β phase reflections, while all other samples also have α(201) and (002) reflections with their intensity increasing as the cooling rate is decreased (Figure 3.9). The presence of

A

B

C

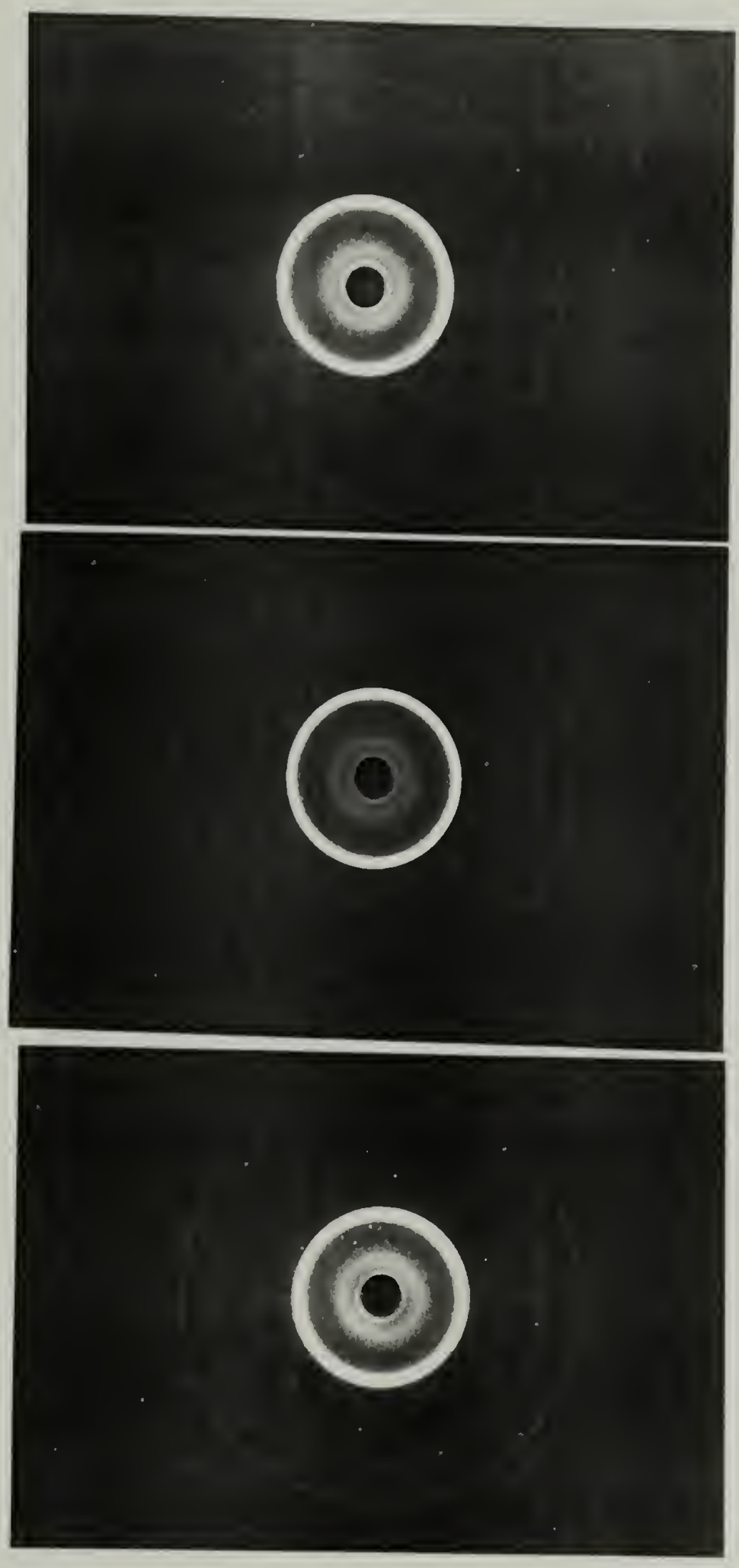

Figure 3.9 Wide-angle X-ray diffraction patterns of samples cooled at different rates. A: 3°C/min; B: 0.5°C/min; C: 0.02°C/min.

distinct reflections for the α and β phases is clear evidence for the coexistence of the crystalline phases at room temperature when samples have been cooled more slowly, and not just a ferroelectric phase with increased G defects. The presence of the paraelectric γ phase cannot be determined by WAXD because the structure factor of the γ phase (111) reflection expected at 22.8° is too low to detect it accurately by WAXD (20).

The interplanar spacing of the P(VDF-TrFE) crystalline state can be measured from the position of the WAXD reflections. The α(200) and β(200)(110) reflections overlap, but the interplanar spacing perpendicular to the chain axis can be measured from the β(200)(110) reflection. This interchain distance is seen to increase as the cooling rate is decreased (Table 3.2) as the chains that possess more G conformers are not able to pack as tightly, causing an expansion in the interplanar distance. Hence from the change in the interplanar spacing it is seen that there are G conformers present within the β phase. The presence of separate α phase reflections shows that the coherence of TGTG' conformations is great enough to form a separate crystal phase. The increased G content measured by FT-Raman can be associated with the retention of α phase crystals and also the presence of G defects within the β phase. Real-time WAXD studies of P(VDF-TrFE) copolymers with a 60/40 molar composition have also shown that there is a coexistence of crystalline phases at room temperature on cooling from the melt (33). In annealing experiments of P(VDF-TrFE) copolymers with 52-75 mol % VDF it was found that the interchain spacing increases with annealing temperature. This indicates that at annealing temperatures near T_c there is a growth of the α phase (34).

A relative measure of the α and β phase crystal content in the different samples was measured from the intensity corrected WAXD curves. A curve fitting program was used to deconvolute the α(110) and β(200)(110) reflections and determine the contribution of each to the overall area. It was found that the α phase content increased from 15% at 3°C/min

Table 3.2 WAXD measurements for different cooling rates

3°C/min	1°	0.5°	0.1°	0.02°	0.01°	assignment
d(Å) i	d(Å) i	d(Å) i	d(Å) i	d(Å) i	d(Å) i	
4.40 vs	4.41 vs	4.41 vs	4.43 vs	4.43 vs	4.50 vs	β(200)(110)α(110)
		3.34 vvw	3.36 w	3.36 m	3.38 m	α(201)
2.56 m	2.56 m	2.55 m	2.55 m	2.56 s	2.60 m	β(001)(310)
			2.29 vvw	2.32 w	2.29 w	α(002)
2.21 s	2.21 s	2.20 s	2.20 s	2.21 s	2.21 s	β(111)(201)(400)

cooling to 50% at 0.01°C/min cooling rate (Figure 3.10). This substantial increase in α phase content agrees with the spectroscopic data that show a higher G content under slower crystallization conditions. The increase in the α phase content is seen in the decrease in the Curie transitions on cooling indicative of an incomplete transition to the ferroelectric phase. The greater disorder in the structure causes a lowering in the Curie transition on subsequent heating as well.

Estimated Crystallite Size from HWHH of β(001) Reflection. WAXD can be used to measure the mean crystallite size from the half width of a meridional reflection according to the Scherrer equation:

$$L_{hkl}=\frac{K\lambda}{\beta\cos\theta} \qquad (3.3)$$

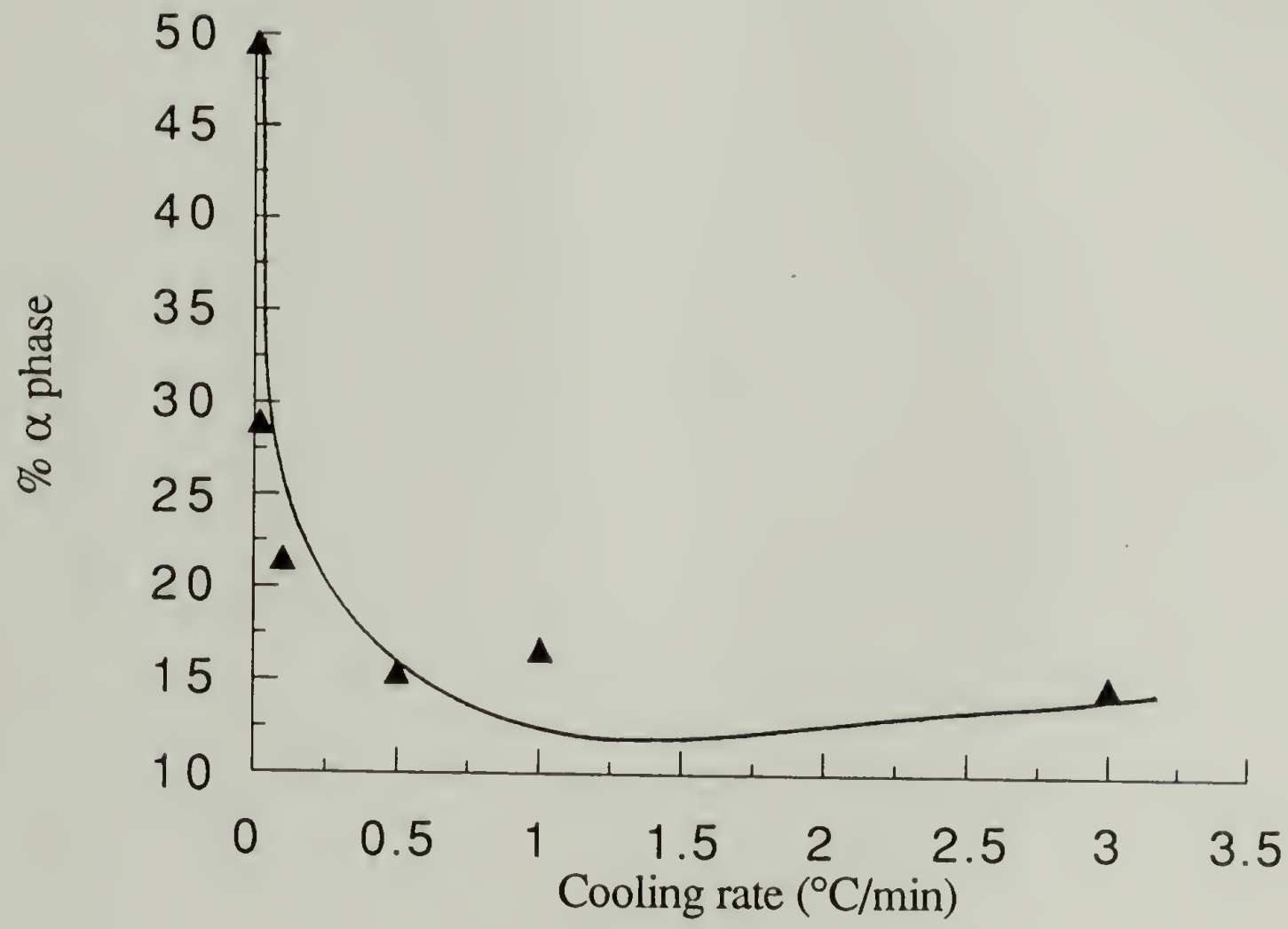

Figure 3.10 α phase content as a function of cooling rate.

where L_{hkl} is the mean crystallite dimension perpendicular to the planes (hkl), β is the half width at half height (HWHH) of the meridional reflection in radians, K is a constant taken equal to one, and λ is the wavelength of the radiation used. Since this equation does not account for the lattice distortions that prevail in polymer crystals, it can give only an estimate of crystallite size (30). From the HWHH of the $\beta(001)$ reflection of samples cooled at different rates through the crystallization temperature it is found that in general β phase crystals with a smaller lamellar thickness are formed at the slower cooling rate (Figure 3.11). This is probably due to the increased presence of α phase crystals that hinder the formation of large β phase crystals. At the slowest cooling rate (0.01°C/min) a larger crystallite size is measured which may account for the higher Curie transition temperature also measured in this case. Larger β phase crystals in this case may arise from the transformation of large α phase crystals grown during the slow cooling process that then transform to the β phase at the Curie transition. With the approximate nature of the Scherrer equation, and the fact that the defect content in these copolymers changes with their thermal history, no conclusions about their crystallite size as measured by this relation are possible. A measure of α phase crystal dimensions is not possible due to the absence of a meridional reflection in the WAXD, but the increased T_m suggests that larger α phase crystals are grown at the slower cooling rates.

Film Samples Crystallized at Different Cooling Rates

Film samples with thickness of ~0.02mm were crystallized in a small oven by cooling through the crystallization temperature at similar rates as used for DSC prepared samples to enable the preparation of films that could be characterized by FTIR. The cast films were placed between aluminum foil that was then put between two copper plates that make up the sample cell of the heater. One disadvantage of the use of this oven is the inability to measure the transition temperatures during thermal treatment as is possible when samples are prepared in the DSC.

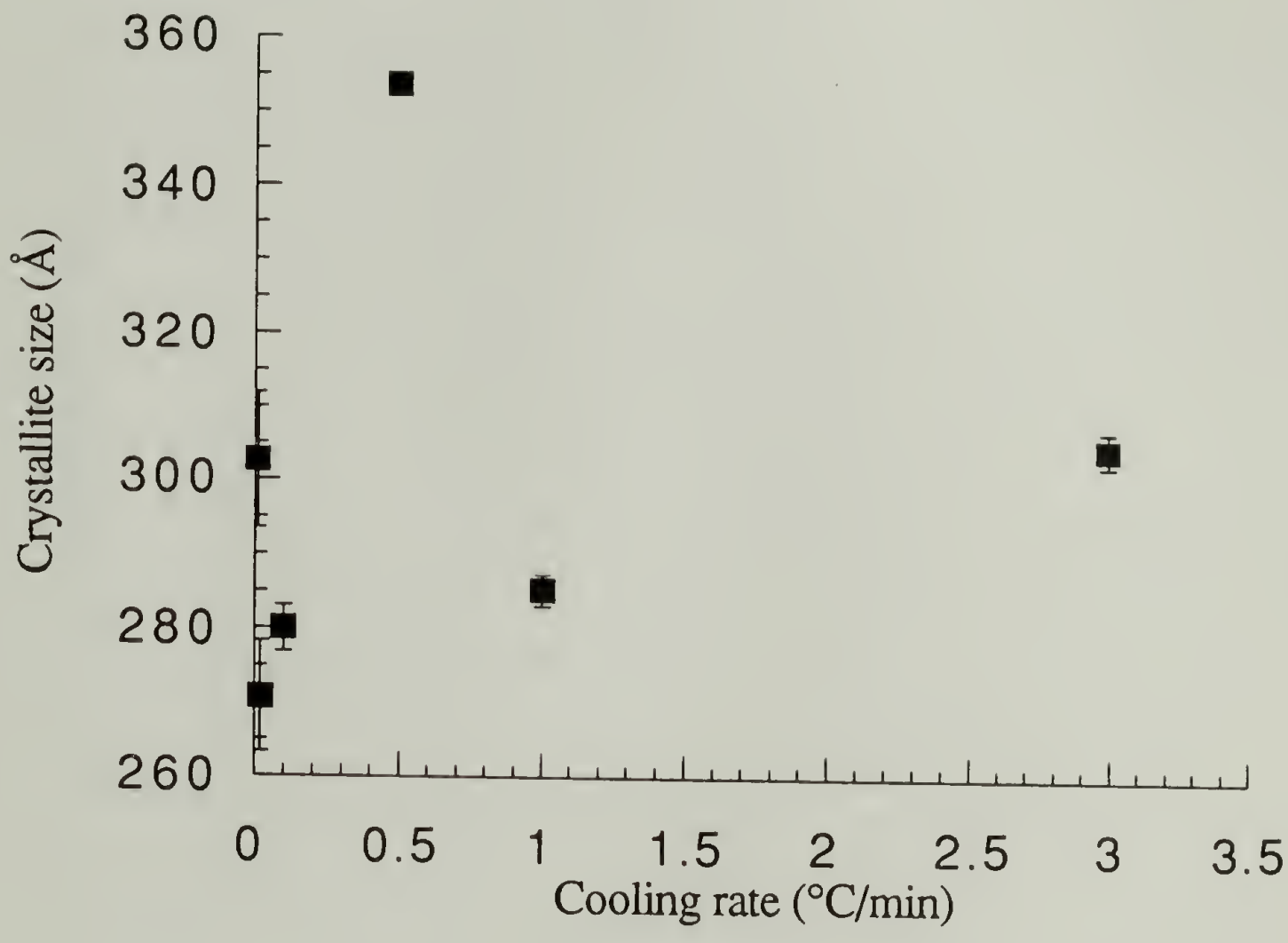

Figure 3.11 Apparent crystallite size as a function of cooling rate.

The transition temperatures subsequent to the thermal treatment were measured by heating the films in the DSC. Transition temperatures show the same trend as found for the thick samples, but with a less marked difference between T_c and T_m as the cooling rate is decreased (Figure 3.12). The difference between the thin films and larger samples may be due to the effect of the substrate on the crystal formation in thin films. In recent studies of thin film P(VDF-TrFE) crystallization and annealing it was suggested that the substrate acts as a nucleation site for crystal formation and imposes a strain on the crystals as they grow (23).

Conformational distribution changes were measured from the FT-Raman spectra (Figure 3.13) and again show that the more slowly cooled samples have higher intensity for G vibrations at 800 cm^{-1} and 610 cm^{-1}. As for the transition temperatures, the conformational changes measured by FT-Raman are not as great in the thin films. For FT-Raman, this could be due to the insensitivity with such thin film samples which have poor scattering.

The films are thin enough to enable the measurement of FTIR spectra by transmission which can then be analyzed by factor analysis. The spectra show that in the slowly cooled films there are α phase vibrations at 610 cm^{-1} and at a vibration attributed to the T_3G conformational sequence at 776 cm^{-1} of the elusive γ phase (Figure 3.14). The factor analysis results for six samples with different cooling rates (Table 3.3) display a minimum in the Maliknowski indicator function, IND, for three factors. The first three eigenspectra all show significant intensity meaning that they contribute to the data set needed to describe the data for the samples. From these factor analysis results it is clear that the samples prepared by crystallizing at different rates through the crystallization temperature form three crystal structures which result in differences in their transition temperatures that arise from chain conformational differences.

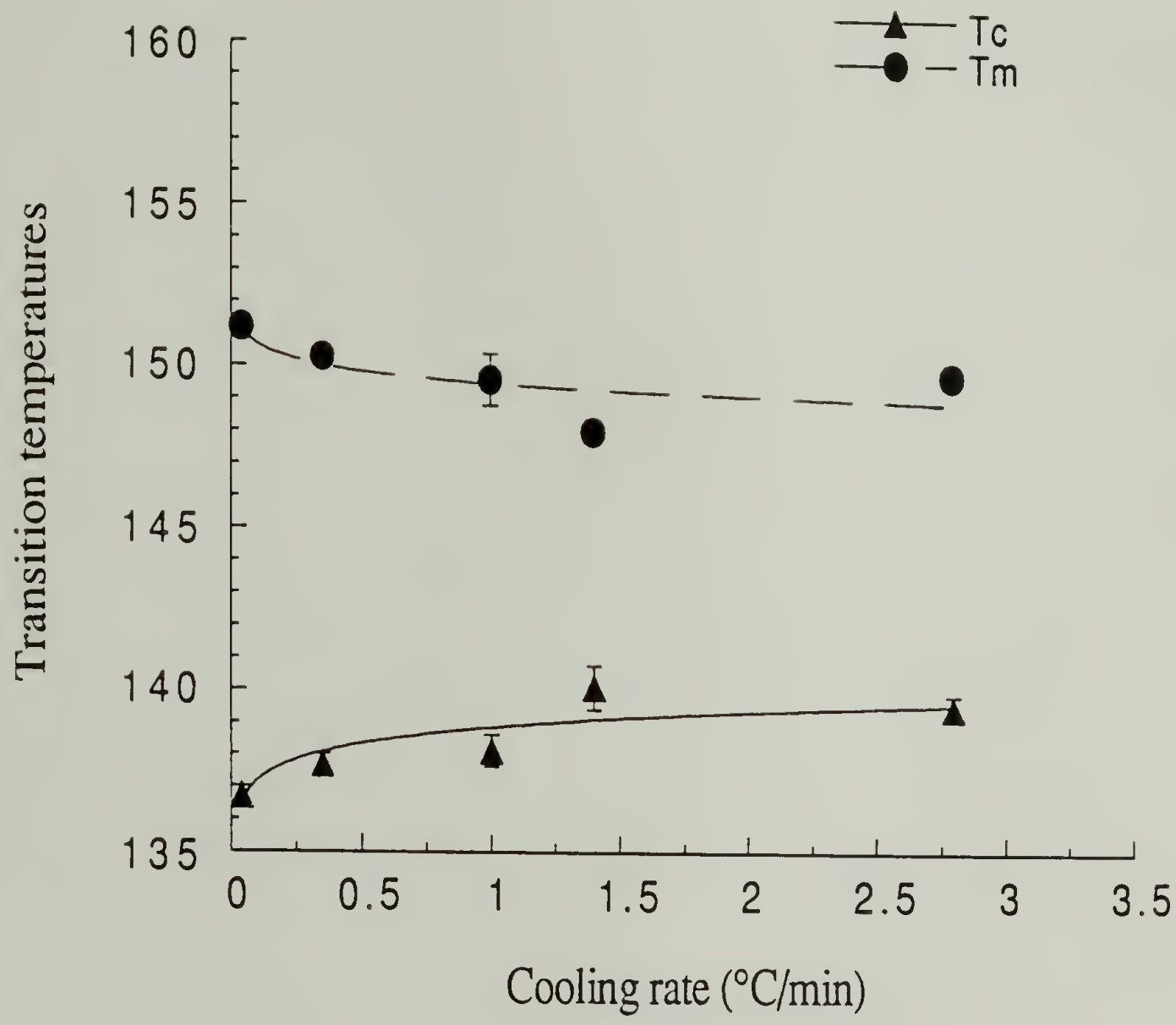

Figure 3.12 Transition temperatures as a function of cooling rate for film samples.

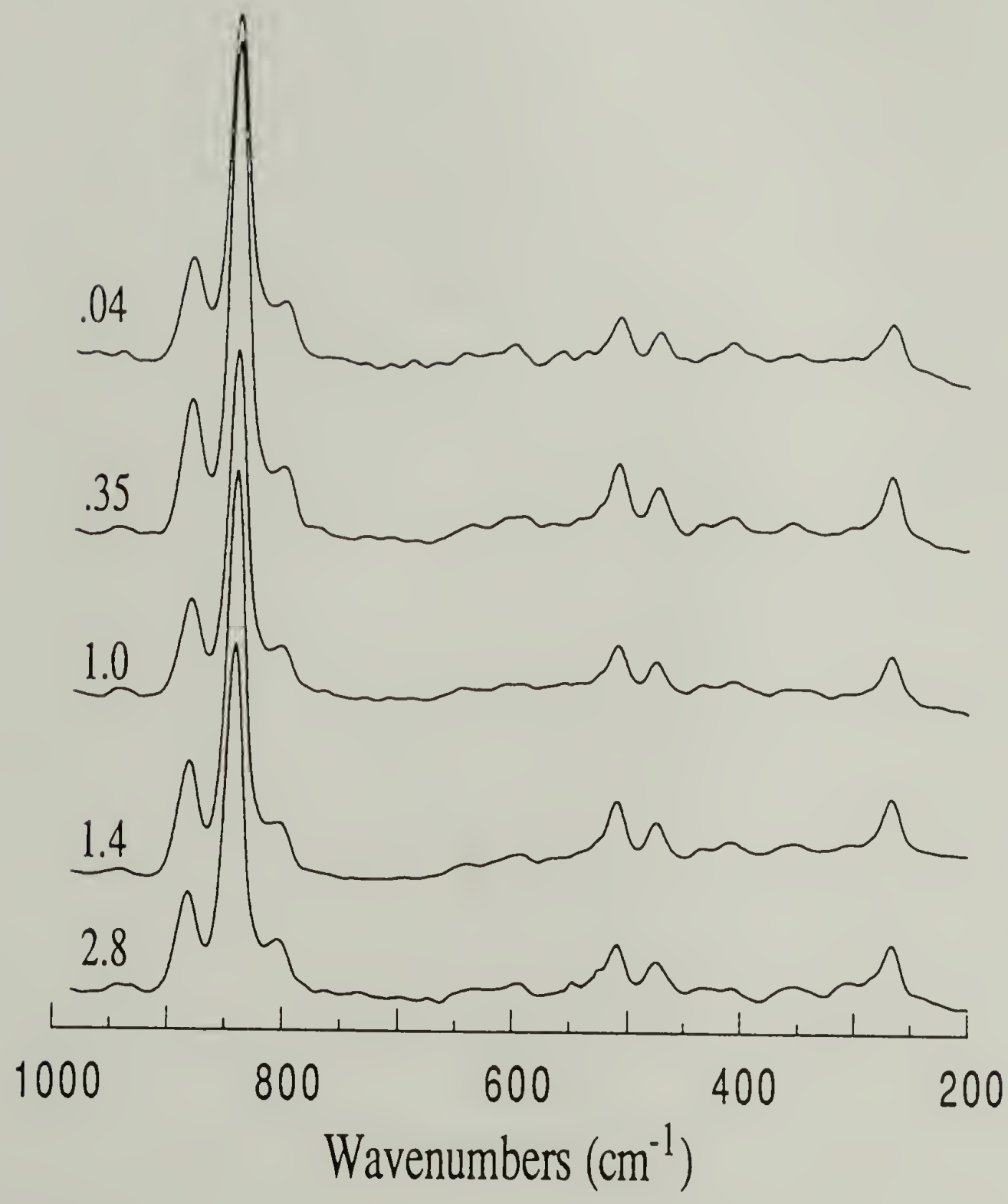

Figure 3.13 FT-Raman spectra of film samples prepared using different cooling rates.

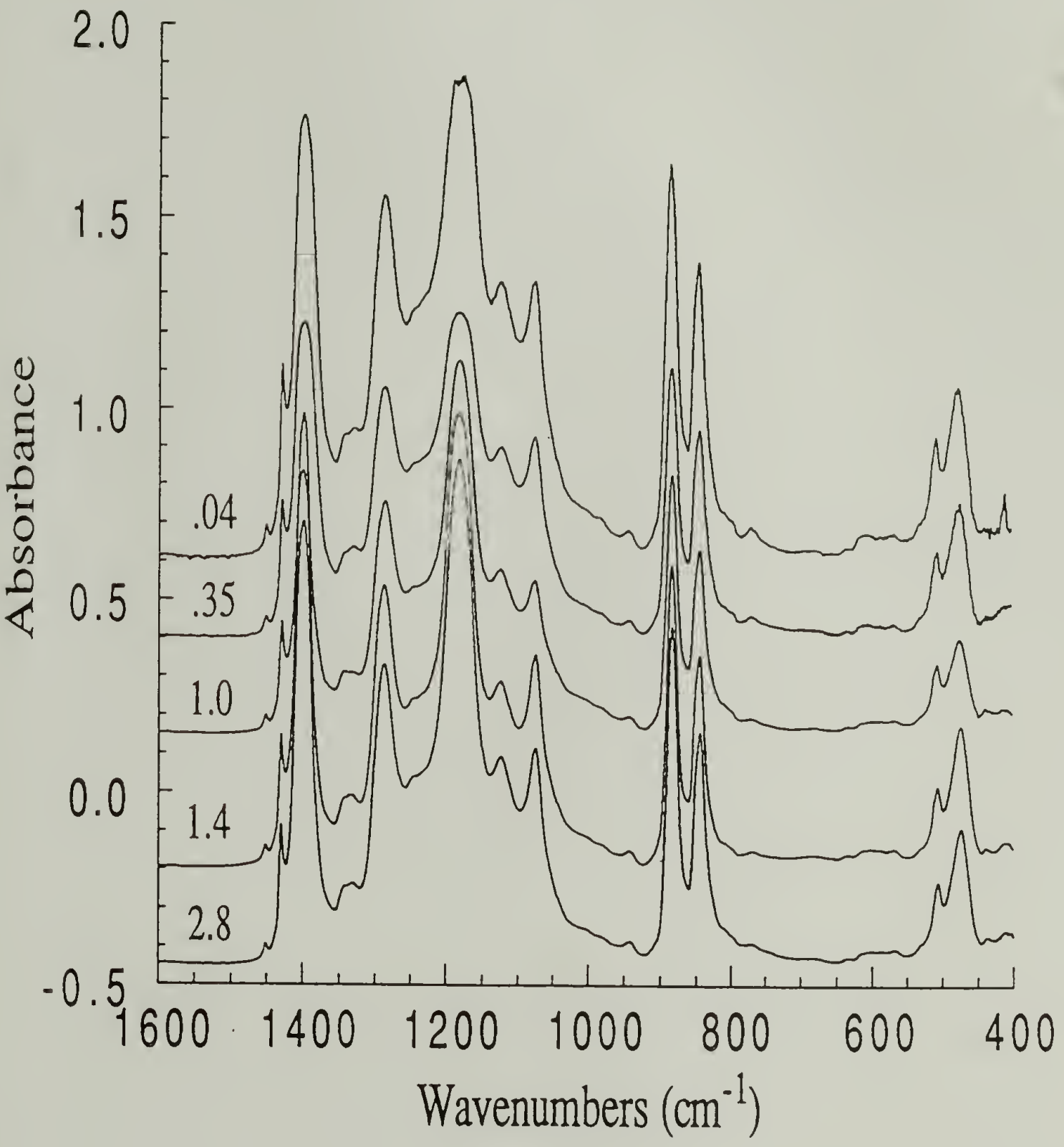

Figure 3.14 FTIR spectra of film samples crystallized at different cooling rates.

The WAXD data again show the presence of α and β phase reflections for more slowly cooled samples. Diffraction data show that the α(200) peak has a stronger intensity in the slower cooling regime as seen in the WAXD diffraction scans for these films (Figure 3.15). Due to differences in the experimental conditions of the diffraction scans, quantitative analysis of this data is not possible.

Table 3.3 Factor analysis results for films cooled at different rates

component	eigenvalue	RE	IND	RSD
1	711.492	.0482	.001928	.017974
2	5.77727	.034177	.002136	.011406
3	3.33495	.014878	.001653	.004302
4	.39463	.009740	.002435	.002301
5	.11087	.007515	.007515	.001256

Conclusions

Nonisothermal crystallization by cooling at different rates through the crystallization temperature of P(VDF-TrFE) 83/17 copolymers has effectively been used to modify their crystal structure. Slow cooling rates enable a perfection of the paraelectric α phase that has a TGTG' chain conformation, such that upon returning to room temperature many gauche defects are retained within the structure. The Curie transition is suppressed for samples crystallized most slowly, so that the two Curie transitions on cooling occur at lower temperatures and with lower enthalpies than in the more rapidly cooled samples.

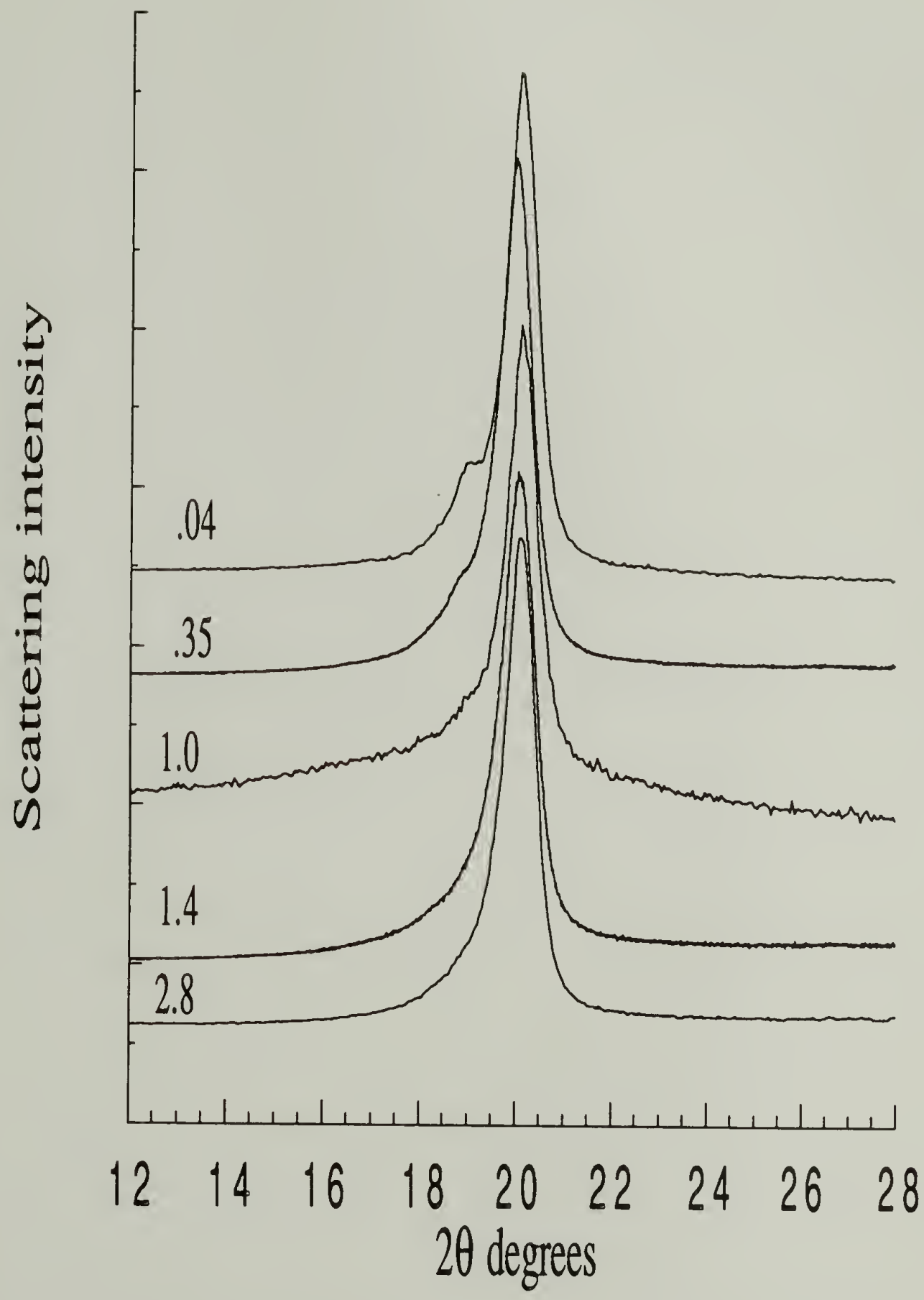

Figure 3.15 Wide-angle X-ray diffractograms of films crystallized at different cooling rates.

Spectroscopic data show that there is a higher content of gauche conformers in more slowly cooled samples. WAXD identifies the gauche defects to be attributable to the retention of α phase crystals in the slower crystallization as both α and β phase reflections are observed. The change in interplanar spacing shows that there is also disorder of G conformers in the β phase crystals that are formed under these conditions of cooling at 0.5°C/min and slower. The crystallite size for these copolymers with a high defect content in terms of conformational irregularities cannot be accurately described by the Scherrer equation.

The crystallinity of the copolymers is increased in the slower cooling case, as seen by the increase in the heat of fusion, accompanied by a 6°C increase in the melting temperature. The Curie transition temperature decreases by 4°C, as the transition becomes more diffuse, reflecting the increasing disorder in the more slowly cooled samples.

The ability to increase the sample crystallinity and change the crystal phase composition allows one to have a greater control over the piezoelectric properties of the copolymer which are dependent on these variables as well as the dipolar orientation (23). The crystal structure formed by crystallizing at slower cooling rates results in samples of higher crystallinity and α phase content. The mobility of the crystalline structure is greater with the presence of α phase, containing conformational defects, which consequently leads to higher piezoelectric activity because of an increased ability to get orientation in a poling field.

Using Ozawa's analysis for nonisothermal crystallization (26), it is found that the growth of P(VDF-TrFE) copolymers with 83/17 composition is two dimensional above 137°C, and one dimensional from 131-136°C. The cooling crystallization function indicates that the crystallization is faster and occurs to a greater extent at lower temperatures. The analysis makes no provisions for solid-solid transformations that may occur during the crystallization process.

Film samples were also prepared by cooling at differnt rates through the crystallization temperature. Structural analysis indicates that they follow similar trends as

do the larger samples prepared in the DSC, though the differences in transition temperatures and chain conformation distribution ase not as marked. Factor analysis of FTIR spectra of thin film samples indicates that there are three crystalline phases that contribute to the data from samples cooled through the crystallization temperature at different rates. This is in agreement with the presence of two Curie transitions in the cooling thermograms, and with suggestions made by other groups from thermal data that three phases exist in copolymers with a high VDF content (35-37).

References

1. Davis, G. T.; *The Applications of Ferroelectric Polymers;* T. T. Wang, J. M. Herbert and A. M. Glass, ed.; Chapman and Hall: New York, 1988; p 37.

2. Furukawa, T.; Wang, T. T.; *The Applications of Ferroelectric Polymers;* T. T. Wang, J. M. Herbert and A. M. Glass, ed.; Chapman and Hall: New York, 1988; p 64.

3. Furukawa, T. *IEEE Trans. El. Ins.*, **1989**, *24*, 375.

4. Lovinger, A. J. *J. Polym. Sci., Polym. Phys. Ed.*, **1980**, *18*, 793.

5. Lovinger, A. J.; *Developments in Crystalline Polymers-1;* D. C. Bassett, ed.; Applied Science: London, 1982; p 195.

6. Lovinger, A. J.; Davis, G. T.; Furukawa, T.; Broadhurst, M. G. *Macromolecules*, **1982**, *15*, 323.

7. Lovinger, A. J.; Furukawa, T.; Davis, G. T.; Broadhurst, M. G. *Polymer*, **1983**, *24*, 1225.

8. Marand, H. L.; Stein, R. S.; Stack, G. M. *J. Polym. Sci., Polym. Phys. Ed.*, **1988**, *26*, 1361.

9. Marand, H.; Stein, R. S. *Macromolecules*, **1989**, *22*, 444.

10. Marand, H.; Stein, R. S. *J. Poly. Sci., Polym. Phys. Ed.*, **1989**, *27*, 1089.

11. Wunderlich, B.; *Macromolecular Physics Vol.1*; Academic Press: New York, 1973.

12. Wunderlich, B.; *Macromolecular Physics Vol. 2*; Academic Press: New York, 1976.

13. Yadav, Y. S.; Jain, P. C. *J. Macromol. Sci.-Phys.*, **1986**, *B25*, 335.

14. Doll, W. W.; Lando, J. B. *J. Macromol. Sci.- Phys.*, **1968**, *B2*, 219.

15. Osaki, S.; Ishida, Y. *J. Polym. Sci., Polym. Phys. Ed.*, **1975**, *13*, 1071.

16. Hasegawa, R.; Takahashi, Y.; Chatani, Y.; Tadokoro, H. *Polymer J.*, **1972**, *3*, 600.

17. Lovinger, A. J.; Davis, D. D.; Cais, R. E.; Kometani, J. M. *Polymer*, **1987**, *28*, 617

18. Welch, G. J.; Miller, R. L. *J. Polym. Sci., Polym. Phys. Ed.*, **1976**, *14*, 1683.

19. Mancarella, C.; Martuscelli, E. *Polymer*, **1977**, *18*, 1240.

20. Marand, H. L., Ph.D. Dissertation, University of Massachusetts, **1988**.

21. Stack, G. M.; Ting, R. Y. *J. Polym. Sci., Polym. Phys. Ed.*, **1988**, *26*, 55.

22. Tanaka, H.; Yukawa, H.; Nishi, T. *Macromolecules*, **1988**, *21*, 2469.

23. Bongianni, W. *Ferroelectrics*, **1990**, *103*, 57.

24. Hendra, P.; Jones, C.; Warnes, G.; *Fourier Transform Raman Spectroscopy: Instrumental and Chemical Applications*; Ellis Horwood: New York, 1991.

25. Walsiak, A. *Chemtracts-Macro. Chem.*, **1991**, *2*, 211.

26. Ozawa, T. *Polymer*, **1971**, *12*, 150.

27. Mandelkern, L.; *Crystallization of Polymers*; McGraw-Hill: New York, 1964.

28. Kobayashi, M.; Tashiro, K.; Tadokoro, H. *Macromolecules*, **1975**, *8*, 158.

29. Tashiro, K.; Itoh, Y.; Kobayashi, M.; Tadokoro, H. *Macromolecules*, **1985**, *18*, 2600.

30. Alexander, L. E.; *X-Ray Diffraction Methods in Polymer Science*; Robert E. Krieger: Malabar, FL, 1969.

31. Lando, J. B.; Doll, W. W. *J. Macromol. Sci.-Phys.*, **1968**, *B2*, 205.

32. Weinhold, S.; Litt, M. H.; Lando, J. B. *Macromolecules*, **1980**, *13*, 1178.

33. Lopez Cabarcos, E.; Gonzalez Arche, A.; Baltá Calleja, F. J.; Bösecke, P.; Röber, S.; Bark, M.; Zachmann, H. G. *Polymer*, **1991**, *32*, 3097.

34. Fernandez, M. V.; Suzuki, A.; Chiba, A. *Macromolecules*, **1987**, *20*, 1806.

35. Moreira, R. L.; Saint-Gregoire, P.; Lopez, M.; Latour, M. *J. Polym. Sci., Polym. Phys. Ed.*, **1989**, *27*, 709.

36. Moreira, R. L.; Saint-Gregoire, P.; Latour, M. *Phase Transitions*, **1989**, *14*, 243.

37. Koga, K.; Nakano, N.; Hattori, T.; Ohigashi, H. *J. Appl. Phys.*, **1990**, *67*, 965.

CHAPTER IV

STRUCTURAL CHANGES AND TRANSITIONS IN ISOTHERMALLY CRYSTALLIZED P(VDF-TrFE)

Introduction

From the nonisothermal crystallization experiments on 83/17 P(VDF-TrFE) copolymers it was found that slower cooling rates, which correspond to longer crystallization times and higher crystallization temperatures, result in a more disordered structure at RT. This is shown by the increased intensity for gauche conformations in vibrational spectra, higher contribution from α phase reflections in the WAXD, and the decrease in the Curie transition temperatures on cooling and heating. The sample crystallinity was also increased as evidenced by a higher heat of fusion. The effect of the crystallization time and temperature on structure cannot be separated from the nonisothermal experiments so isothermal crystallization experiments will be carried out on the copolymers for different periods of time at 135°C. In this way, only the crystallization time will be varied to see its effect on the structure and transition behavior of the copolymers.

Previous studies have been made on the isothermal crystallization of PVDF (1-5) as well as of copolymers of PVDF with tetrafluoroethylene (P(VDF-TFE)) with different copolymer compositions (6, 7). Different temperature regions have been defined for PVDF crystallization in which there is a growth of α and γ phase crystals, with a transformation of α to γ phase crystals occurring at isothermal crystallizations above 154°C (2, 3). For the P(VDF-TFE) copolymers with 81/19 molar composition it was found that they crystallize predominantly into the paraelectric phase that subsequently undergoes the Curie transition at a rate strongly dependent on the isothermal temperature (7).

Studies have been made of the variation of structure of P(VDF-TrFE) copolymers of different composition for samples that have been uniaxially oriented or poled in a high electric field, but isothermal crystallization studies have been limited (8-13).

In a study of the crystallization of P(VDF-TrFE) copolymers with a 65/35 molar composition Tanaka et al. (14), using DSC, found that the crystalline structure of the ferroelectric phase depends on the crystallization temperature. When crystallization is performed below the Curie temperature there is only an ordered ferroelectric phase formed, while when the crystallization temperature is above T_c there is also a more disordered ferroelectric phase present due to incomplete transformation from the paraelectric to the ferroelectric phase.

It is expected from the related work on crystallization of ferroelectric polymers and copolymers (1-14) that the crystallization time will result in structural changes due to the possibility of transformation between crystalline forms at temperatures near the melting point. The Curie temperature is close to the melting temperature and the structural changes of the crystallization may be associated with the chain conformational changes occurring at the Curie transition. It is the objective of this work to determine the effect of crystallization time at 135°C on the structure and phase transition temperatures for P(VDF-TrFE) copolymer with an 83/17 molar composition. The crystallization at 140°C for different times and the subsequent Curie transition of the copolymers will be measured by WAXD at elevated temperatures.

Experimental

Isothermal crystallization experiments were performed in a DuPont DSC 2910 by melting the copolymer sample (~10mg) at 155°C for 10 minutes before cooling down at 5°C/min to 135°C where it was held isothermally for 8 - 1250 minutes, then cooled to RT at 3°C/min. Curie transition temperatures were measured during the cooling down step. T_c

and T_m were measured on subsequent heating in the DSC at 20°C/min. Conformational distributions in the RT structure were measured by FT-Raman spectroscopy. Crystal phases were identified from WAXD reflections. The relative phase content and crystallite size were measured from digitized WAXD data.

WAXD diffractograms were recorded on a Rigaku AU-200 diffractometer for cast film samples held at 140°C for five minutes and for four hours, then at decreasing temperatures through the Curie transition. The samples were scanned over the range 2θ = 5-50° at a speed of 2 or 3°/min.

Results and Discussion

P(VDF-TrFE) copolymers crystallize rapidly at high undercoolings. The crystallization of P(VDF-TrFE) 83/17 copolymer at 135°C is complete in 8 minutes (Figure 4.1), so the crystallization of the isothermally crystallized samples is always complete. The additional time of the isothermal step is not part of the primary crystallization of the copolymer. Because the crystallization temperature is held constant, the only parameter that will effect the transition temperatures and the structure is the isothermal time at the crystallization temperature following the crystallization. There is mobility within the copolymer at 135°C so during the isothermal period structural changes may occur, leading to changes in the Curie transition and in the final morphology of the copolymer.

Crystallization at 135°C and Transition Behavior Measured by DSC

The Curie transitions on cooling show the same type of behavior as observed in nonisothermal crystallizations, with the temperatures decreasing and magnitude of the transitions changing with longer times (Figure 4.2, Table 4.1). This indicates that the longer isothermal times allow for a stabilization of the paraelectric α phase, thus thwarting a complete transformation to the ferroelectric phase on cooling through the Curie transition.

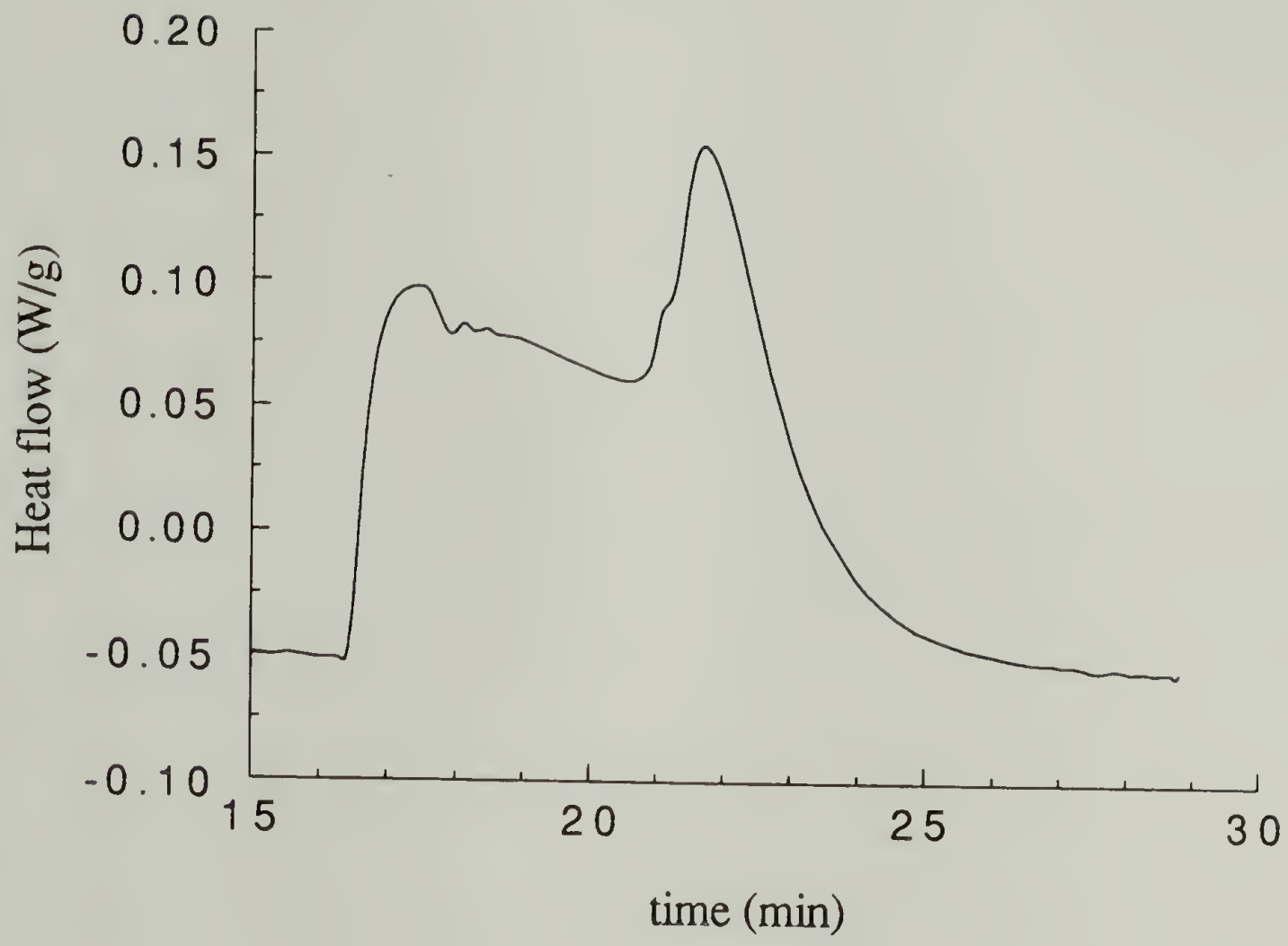

Figure 4.1 Crystallization curve at 135°C for P(VDF-TrFE) copolymer.

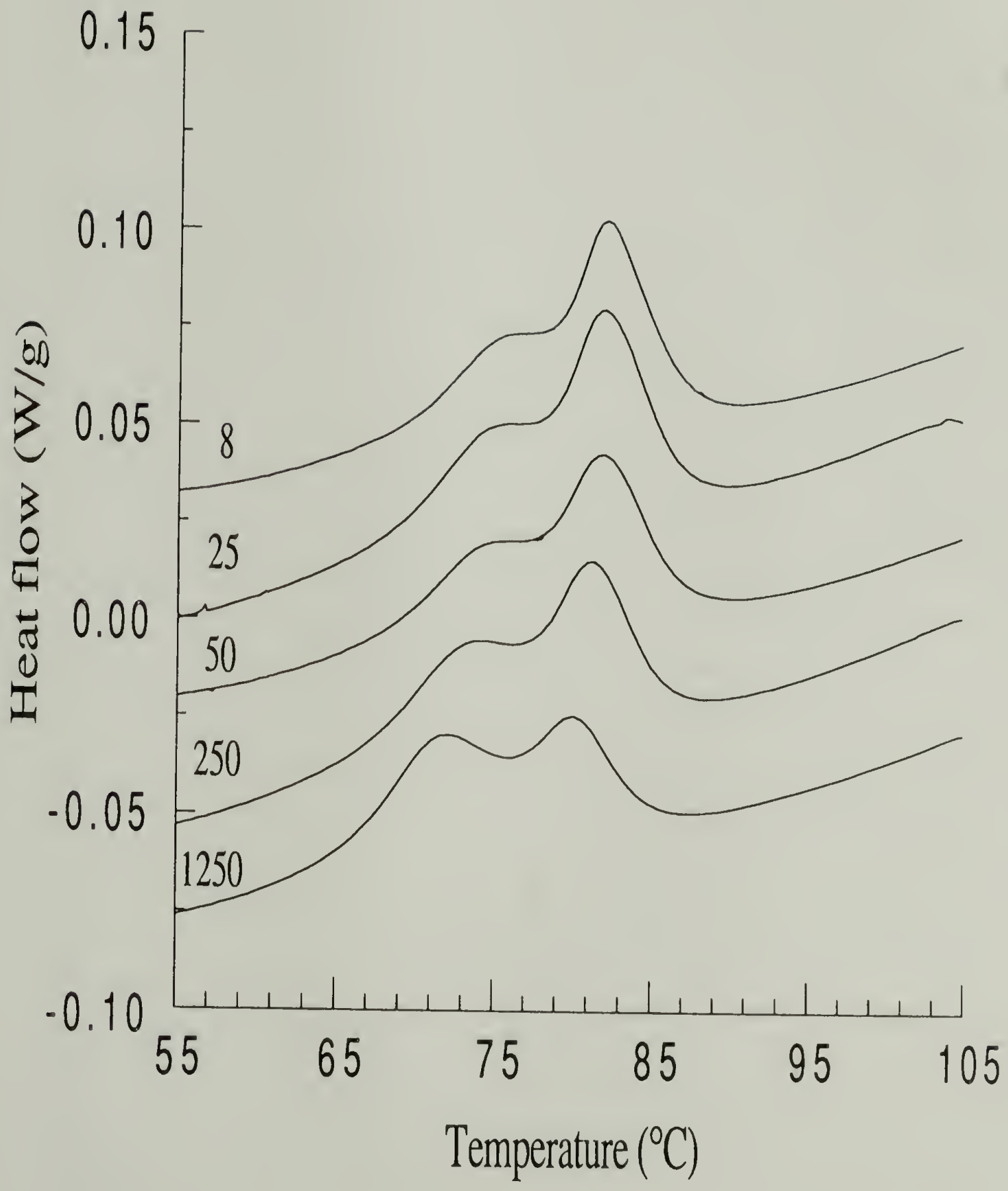

Figure 4.2 Curie transitions on cooling for samples crystallized at 135°C for different times.

The decreased transition temperatures arise from the greater stability of the crystallized phases, requiring a lower temperature for the transition to the ferroelectric phase. The change in the Curie transition temperatures is due to structural changes from a solid-solid transformation during the isothermal treatment during which there is still mobility in the copolymers. It is possible to get reorganization of the material to a more stable state and to have secondary crystallization that involves crystallization of amorphous regions and crystal perfection of the already crystallized regions (15). In PVDF crystallization there is a transformation of α to γ phase crystals during extended periods of crystallization at temperatures where both the α and γ phase crystals are formed from the melt (3). A similar transformation may also be occurring in the copolymer samples during the prolonged isothermal time, thus causing changes in the Curie transitions measured on cooling back to RT.

Table 4.1 Summary of DSC measurements for isothermally crystallized P(VDF-TrFE)

Isothermal time	T_{c1}(°C)	T_{c2}(°C)	T_c(°C)	T_m(°C)	ΔH_m(J/g)
8 (min)	83	77	140	152	31.5
25	83	76	139	152	33.1
50	82	75	139	152	35.0
250	82	74	139	153	33.5
1250	81	72	140	155	30.8

On subsequent heating of the isothermally crystallized copolymers the Curie and transition temperatures are measured and show an increase in the T_m with an almost constant value for T_c (Figure 4.3). The unchanged T_c suggests that the crystal phases formed with different crystallization times are not very different. The higher T_m could be due to an increase in the degree of crystallinity, defect content, or crystallite size with

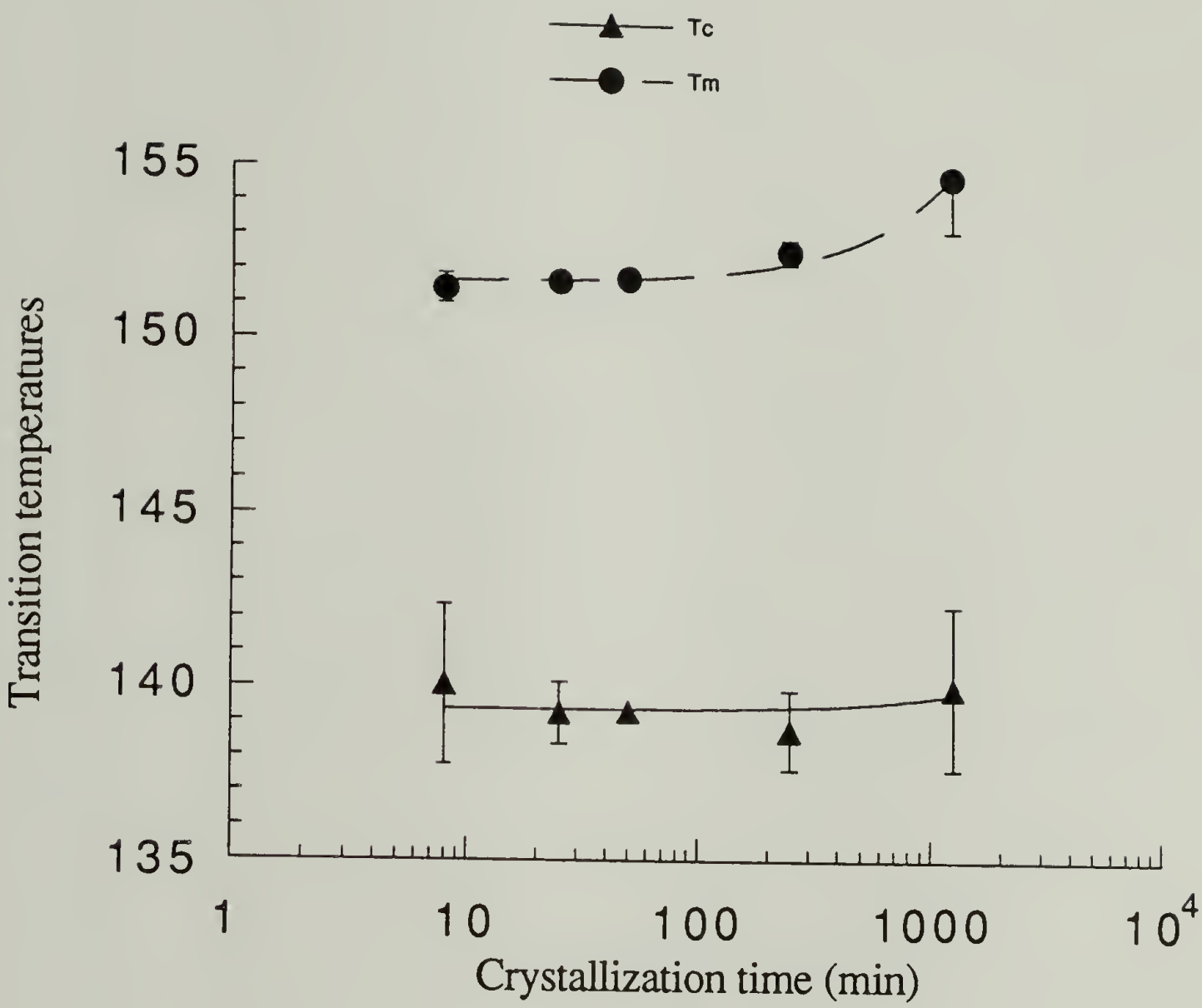

Figure 4.3 Transition temperatures as a function of crystallization time.

longer crystallization times. In fact the relative crystallinity as measured from the heat of fusion does not increase with crystallization time, but has a maximum value for the 50 minute isothermal time (Table 4.1). The heat of fusion is about 20% greater than for samples cooled at different rates, but does not increase with longer isothermal times indicating that the crystallization is not continuing during this time at 135°C. The structural changes must then arise from transformation of the crystalline material into different crystalline forms during the isothermal treatment.

Spectroscopic Analysis of Chain Conformation Distribution

The different crystal phases of PVDF and its copolymers have differences in their chain conformation that are measurable by vibrational spectroscopy. The FT-Raman spectra indicate that at longer crystallization times the RT structure has more G content as evidenced by an increase in the intensity of G vibrations at 800 and 610 cm^{-1} (Figure 4.4). It is important to note that there are G vibrations present even when the sample has been crystallized for only 8 minutes at 135°C, with the intensity of the G conformer bands gradually increasing with the longer isothermal times. This suggests that at 135°C the paraelectric α phase that is formed is of sufficient stability to be retained partially on returning to RT. The longer crystallization times serve as a period of perfection of the paraelectric phase such that more of its G conformers are retained on undergoing the Curie transition on cooling. It is seen therefore that the longer crystallization time allows for a perfection of α phase. The crystallization temperature of 135°C is one at which a relatively stable α phase is formed (compared with the fast cooling rates with lower crystallization temperatures). The increase in the G content with longer crystallization time is the same behavior as observed in the cooling rate experiments, where slower cooling rates resulted in room temperature structures with a higher G chain conformational distribution.

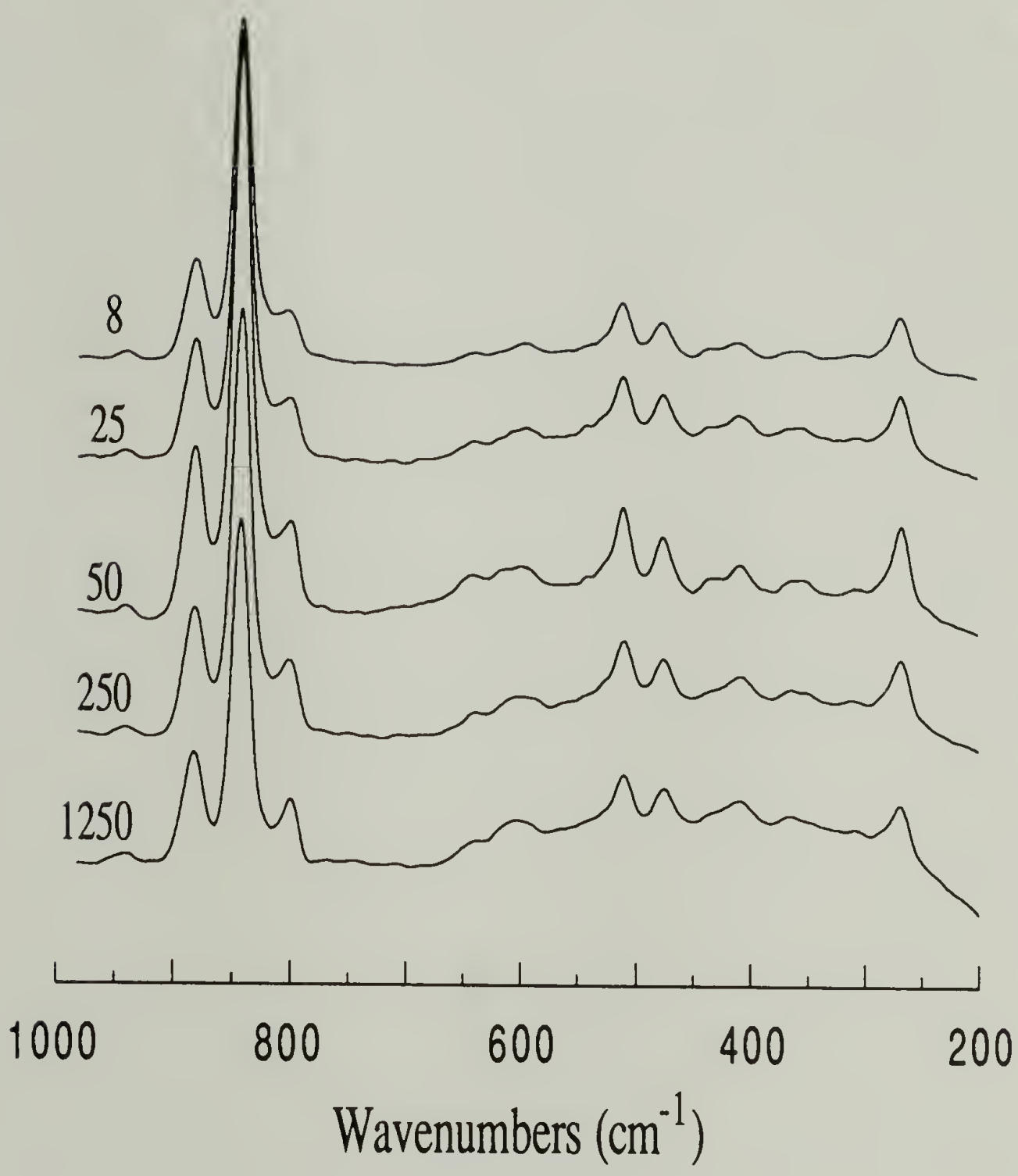

Figure 4.4 FT-Raman spectra of samples crystallized at 135°C for different times.

Crystal Morphology Determined by WAXD

The molecular structures of P(VDF-TrFE) can be identified from the WAXD patterns which have been identified for the different crystal phases (16). WAXD can also be used to determine interchain spacing and crystallite size in crystalline polymers. In this study it will be utilized in identifying the crystal phases and the relative content of them, and in estimating the size of β phase crystallites.

Crystal Phase Identification from Bragg Reflections. WAXD data show that for all the crystallization times there are α and β phase reflections present (Table 4.1). This is in agreement with the spectroscopic data that indicates that the α phase crystallized at 135°C is stable enough to inhibit a complete Curie transition to the ferroelectric phase, such that there is a coexistence of the α and β phases at RT regardless of the crystallization time. The relative amount of the α and β phase was measured from curve fitting of the WAXD microdensitometer intensity data and indicates that there is an increase from 23 to 44% α phase present at RT when the isothermal time is increased from 8 to 1250 minutes (Figure 4.5). The increase is indicative of the stabilization of the α phase at longer isothermal times. The microdensitometer traces of the WAXD data show that the α phase reflection becomes stronger with longer crystallization time (Figure 4.6). WAXD does not give any information about the transformation of α phase crystals to an intermediary crystal phase during longer isothermal periods, as the Curie transitions on cooling imply. This would best be measured by real-time experiments of the crystallization process.

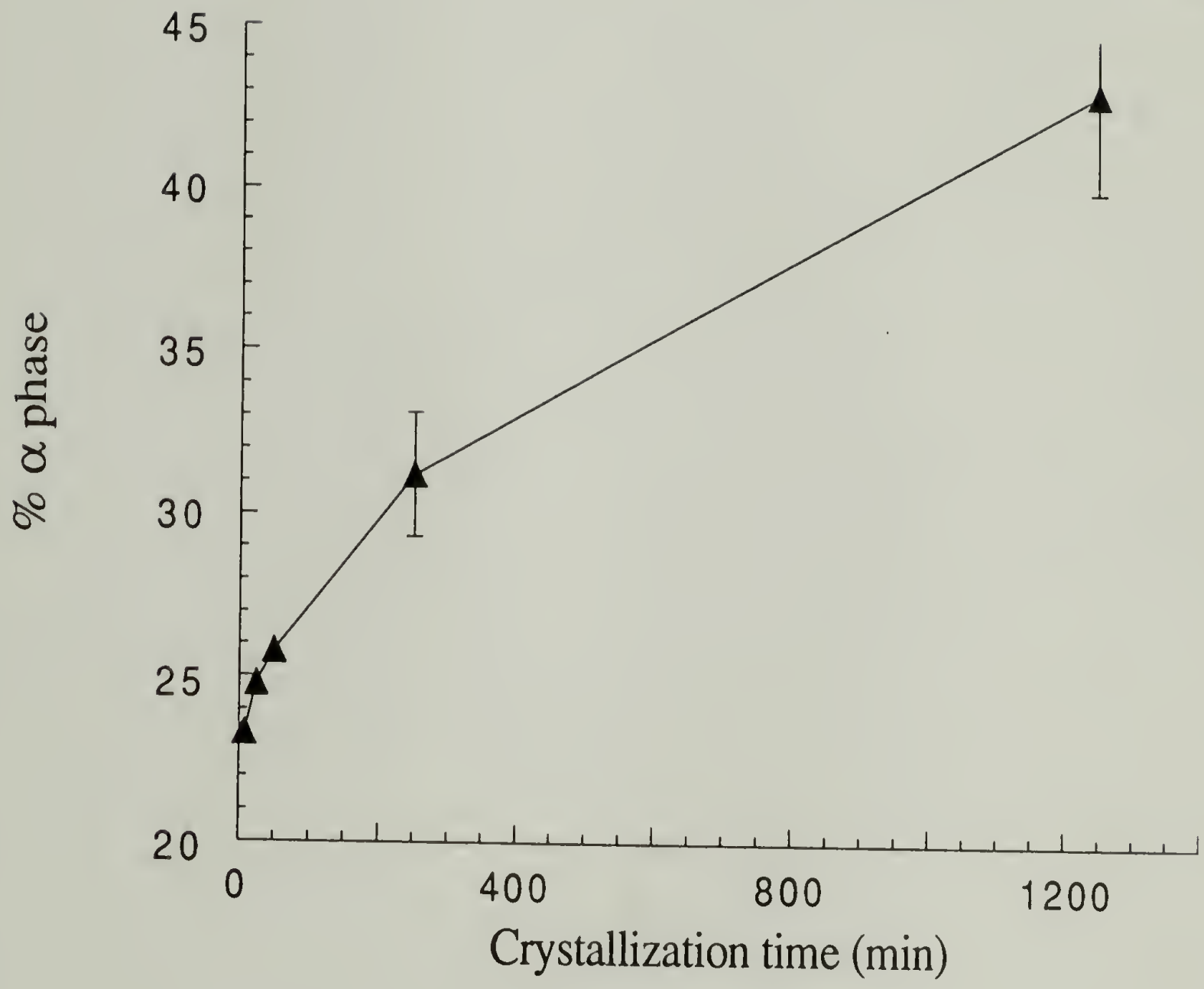

Figure 4.5 α phase content as a function of crystallization time from WAXD data.

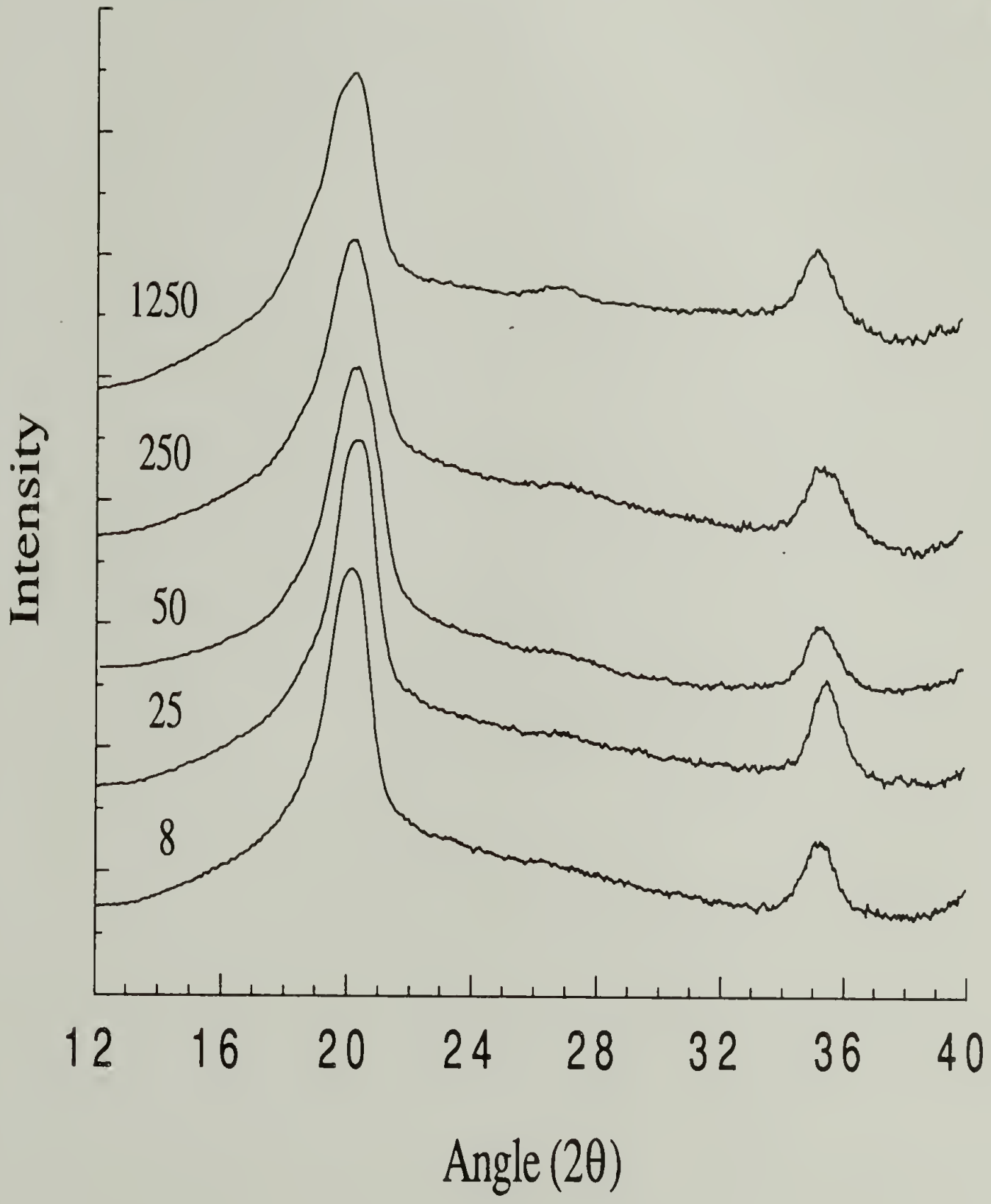

Figure 4.6 Microdensitometer traces of WAXD patterns of different crystallization times.

Table 4.2 WAXD measurements for isothermally crystallized samples

8min		25min		50min		250min		1250min		assignment
d(Å)	i	d(Å)	i	d(Å)	i	d(Å)	i	d(Å)	i	
4.83	vs	4.68	vs	4.82	vs	4.74	vs	4.89	vs	α(200)
4.38	vs	4.34	vs	4.45	vs	4.38	vs	4.33	vs	β(200)(110)α(110)
3.35	m	3.34	w	3.33	m	3.36	m	3.38	m	α(201)
2.56	s	2.54	s	2.54	s	2.56	s	2.57	s	β(001)(310)
2.21	vs	2.20	vs	2.23	vs	2.20	vs	2.22	vs	β(111)(201)

Estimated Crystallite Size from HWHH of β(001) Reflection. The crystallite dimensions can be measured from the half width of meridional reflections as previously mentioned. The lamellar thickness is most strongly affected by the crystallization temperature, but time allowed for crystal growth also influences the crystallite dimensions (15). If there are constraints on the volume available for a crystallizing sample, there may be a decrease in dimensions with crystallization time (17). The crystallite size as measured for the isothermally crystallized samples shows that there is a trend of decreasing size of β phase crystals with longer isothermal times (Figure 4.7). This is as expected, since at longer times there is a perfection of the α phase crystals, the presence of which hinders formation of large β phase crystals. The longer time also allows for the transformation of α phase to γ phase as is seen in PVDF, but this intermediary phase is not detectable in the RT samples. Due to the overlap of α phase reflections in WAXD with those of the β phase, α crystal dimensions cannot be measured. Since T_m is higher crystals with longer isothermal times, we can assume that larger α phase crystals are grown over time.

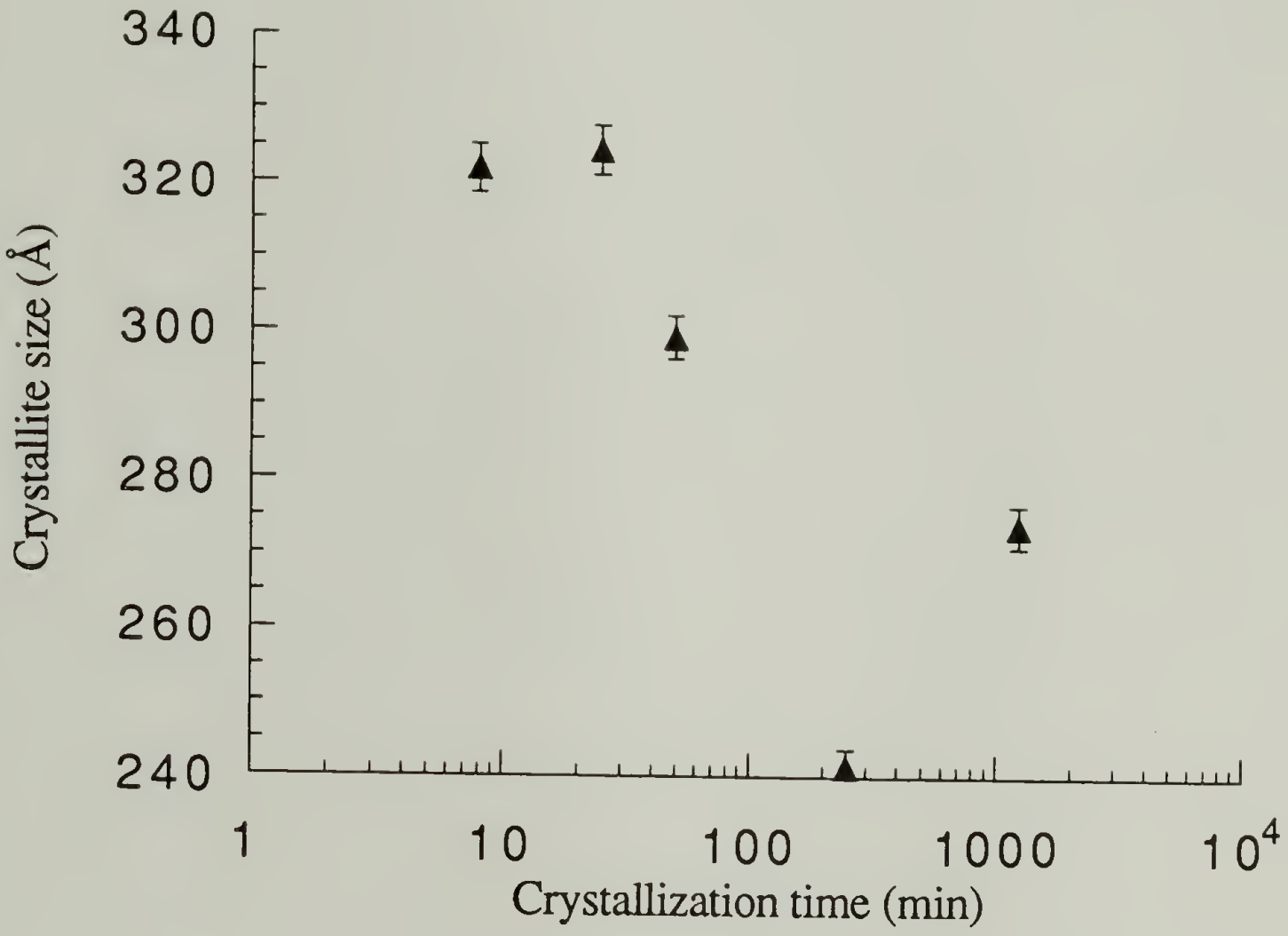

Figure 4.7 Apparent crystallite size as a function of crystallization time.

Crystallization and the Curie Transition Measured by Variable Temperature WAXD

In order to better understand the crystallization behavior of the P(VDF-TrFE) copolymer, variable temperature WAXD experiments were made after two different crystallization times at 140°C using a diffractometer with a position sensitive proportional counter. This allows us to see the crystallization of the copolymer at 140°C and the subsequent phase transition on cooling to RT. In the first experiment, the copolymer was quenched from 160°C to 140°C, and the WAXD scanned during a 30 minute exposure at different temperatures down to 70°C. The diffraction pattern shows that only an amorphous peak at 140°C, with the α phase crystalline peak appearing as the temperature is decreased. At 85°C, the β phase also appears, as the copolymer begins to undergo the Curie transition. The intensity of the β phase scattering increases as the α phase decreases down to 70°C (Figure 4.8B). In the second case, the copolymer was quenched from 160°C to 140°C where it was held for four hours. With the longer crystallization time, the α phase has crystallized at 140°C as evidenced by the α phase peak in the WAXD (Figure 4.8A). The Curie transition begins at 85°C but the β phase does not grow as rapidly in the sample that was held for an extended time at 140°C. This supports the fact that the slower crystallization processes result in a stabilization of the paraelectric α phase, causing a delay in the Curie transition. The room temperature diffraction pattern also possesses α phase reflections in the case of the four hour crystallization at 140°C. The α phase content was measured directly from the ratio of α and β phase peak intensities in the diffractometer data and is shown in figure 4.9. There is a larger α phase content at comparable temperatures for the sample held at 140°C because of the stability of this phase which suppresses the Curie transition and the development of the β phase.

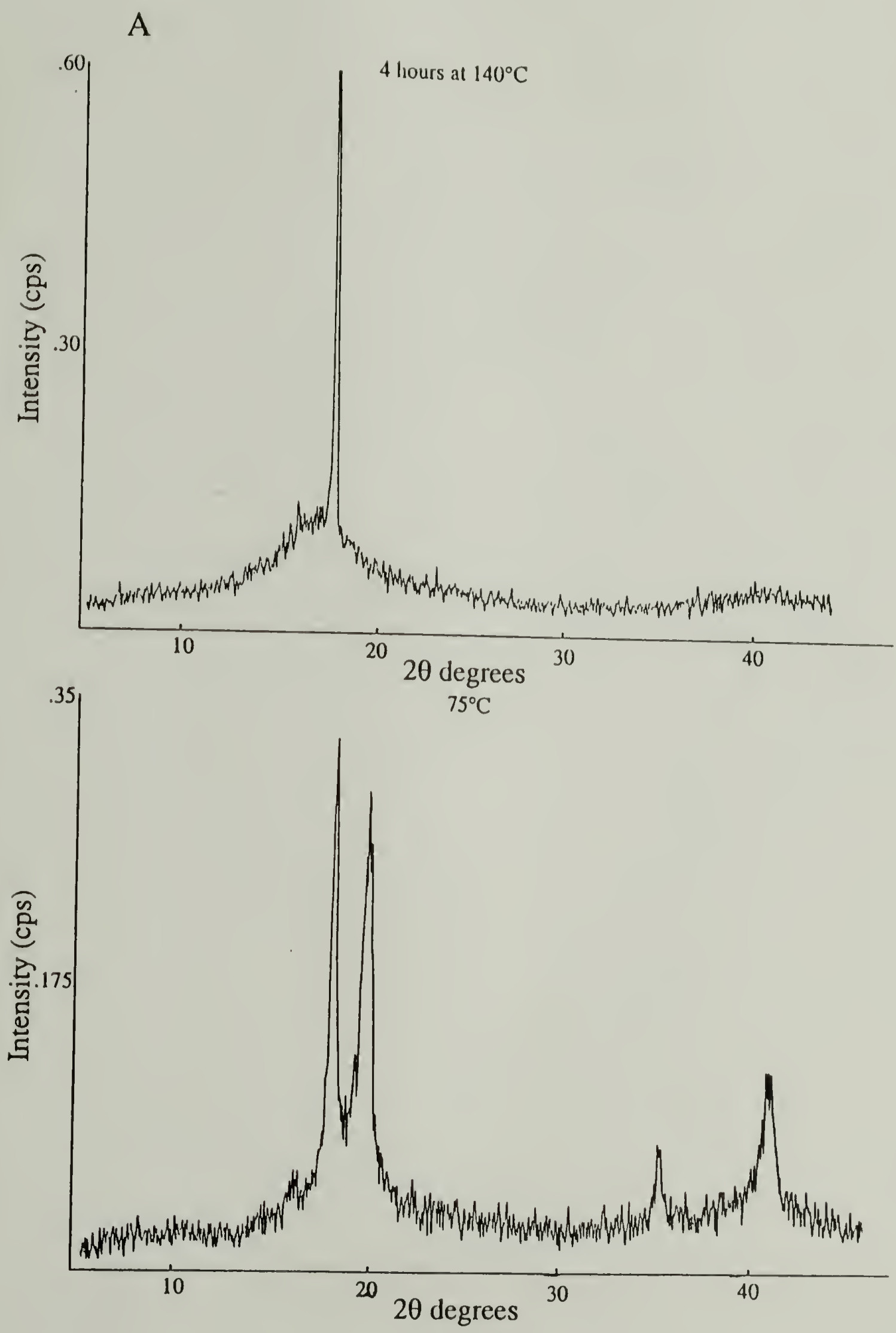

Figure 4.8 Wide-angle X-ray diffractograms measured at different temperatures.
A: Held at 140°C; B: Cooled directly.

(continued next page)

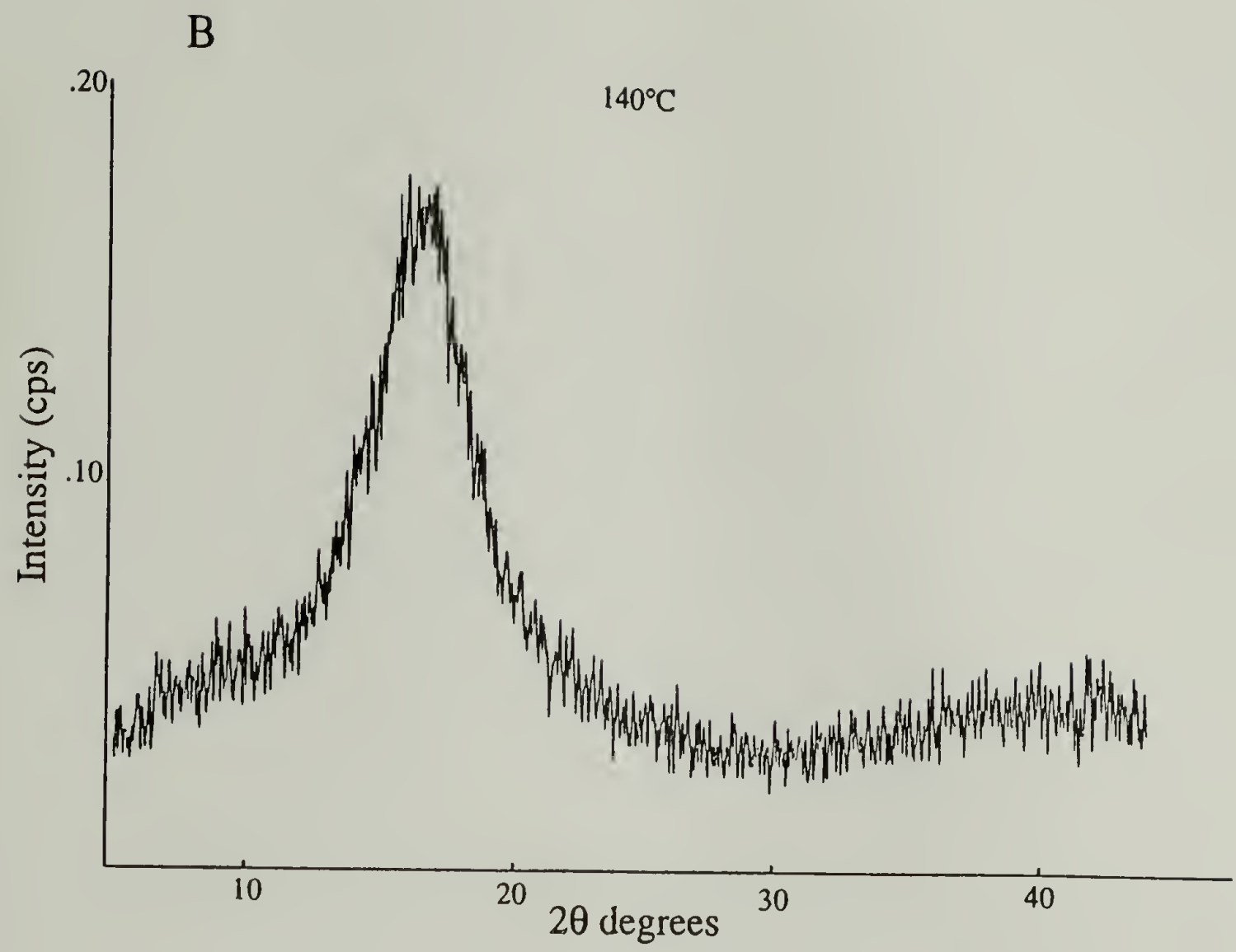

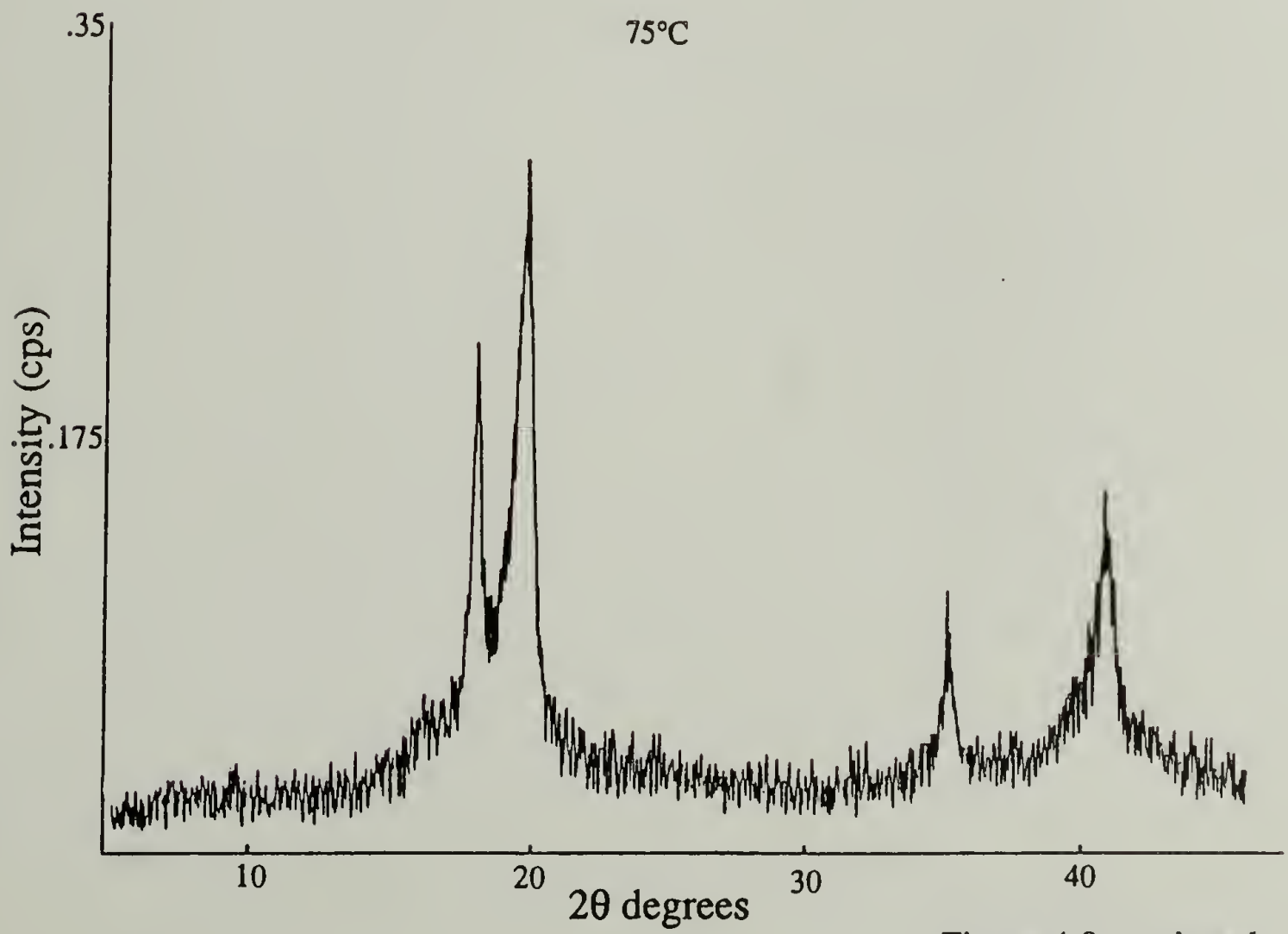

Figure 4.8 continued

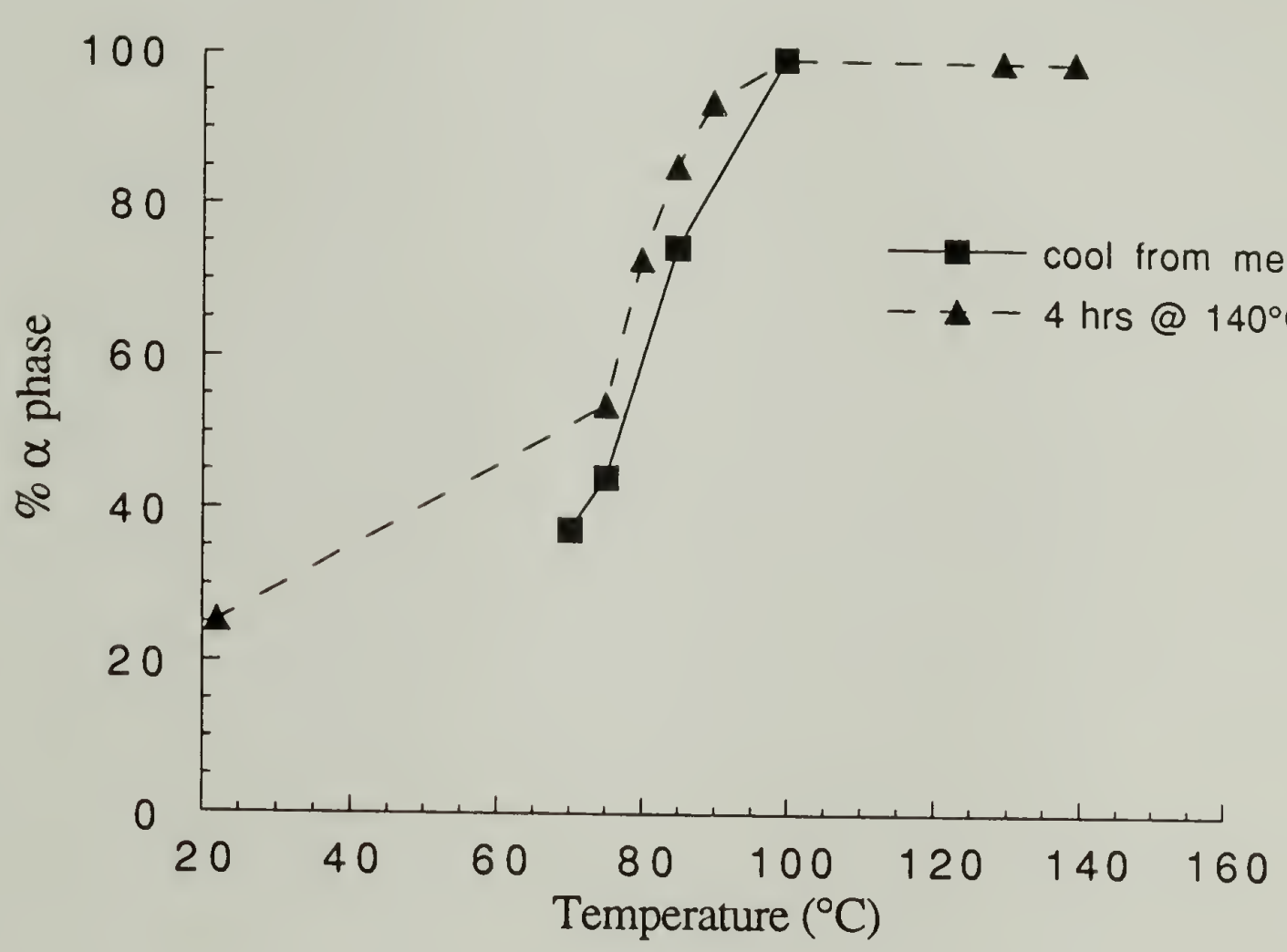

Figure 4.9 α phase content as a function of temperature.

Conclusions

The longer crystallization times at 135°C do not cause significant changes in the crystallinity of the room temperature samples, but do affect the microstructure of the polymer and its Curie transitions on cooling. The transition temperatures on cooling are decreased and their relative intensities are inverted on longer crystallization, as there is an increased stabilization of the paraelectric crystalline phase. The melting temperature is increased, though not accompanied by an increase in the heat of fusion. The chain conformation as measured by FT-Raman indicates that longer isothermal periods result in a more disordered structure possessing many gauche conformers. The WAXD data show that regardless of the crystallization time at 135°C, there are α and β phase crystals in the RT structure. Variable temperature WAXD confirms that longer crystallization times at elevated temperatures (140°C) enable a perfection of the paraelectric α phase, which is then retained to lower temperatures on returning to RT as seen by the persistence of the α phase WAXD peaks.

References

1. Lovinger, A. J. *Polymer*, **1981**, *22*, 412.

2. Lovinger, A. J. *J. Polym. Sci., Polym. Phys. Ed.*, **1980**, *18*, 793.

3. Lovinger, A. J. *Polymer*, **1980**, *21*, 1317.

4. Osaki, S.; Ishida, Y. *J. Polym. Sci., Polym. Phys. Ed.*, **1975**, *13*, 1071.

5. Nakamura, S.; Sasaki, T.; Funamoto, J.; Matsuzuki, K. *Die Makromol. Chemie*, **1975**, *176*, 3471.

6. Marand, H.; Stein, R. S. *Macromolecules*, **1989**, *22*, 444.

7. Marand, H. L. Ph.D. Dissertation, University of Massachusetts, **1988**.

8. Tashiro, K.; Takano, K.; Kobayashi, M.; Chatani, Y.; Tadokoro, H. *Polymer*, **1981**, *22*, 1312.

9. Tashiro, K.; Takano, K.; Kobayashi, M.; Chatani, Y.; Tadokoro, H. *Polymer*, **1984**, *25*, 195.

10. Tashiro, K.; Kobayashi, M. *Polymer*, **1986**, *27*, 667.

11. Tashiro, K.; Kobayashi, M. *Phase Transitions*, **1989**, *18*, 213.

12. Lovinger, A. J.; Furukawa, T.; Davis, G. T.; Broadhurst, M. G. *Polymer*, **1983**, *24*, 1233.

13. Lovinger, A. J.; Furukawa, T.; Davis, G. T.; Broadhurst, M. G. *Polymer*, **1983**, *24*, 1225.

14. Tanaka, H.; Yukawa, H.; Nishi, T. *Macromolecules*, **1988**, *21*, 2469.

15. Wunderlich, B.; *Macromolecular Physics Vol. 2*; Academic Press: New York, 1976.

16. Lando, J. B.; Doll, W. W. *J. Macromol. Sci.-Phys.*, **1968**, *B2*, 205.

17. Bassett, D. C.; *Principles of Polymer Morphology*; Cambridge University: London, 1981.

CHAPTER V

ORIENTATION

Introduction

To better understand the vibrational assignments of the different phases of PVDF and P(VDF-TrFE), polarized infrared spectra of a highly oriented copolymer film have been measured. Due to the lack of an appropriate force field for fluoropolymers, the geometry of the crystal structures has not been well defined. Using a highly oriented sample will enable the measurement of the transition moment angles for the CF_2 vibrations that are highly coupled.

Piezoelectric and pyroelectric activities of a material are dependent on the orientation of dipoles in the material and on the orientation of crystals, therefore by mechanical drawing or electrical poling of PVDF and P(VDF-TrFE), the piezoelectric activity can be enhanced (1). Mechanical deformation such as stretching or drawing causes a preferential alignment of molecular chains in the amorphous and crystalline phases. Poling in an electric field causes a rotation of molecular dipoles in the crystalline phase in the field direction. Both of these processes also induce a transformation to the all trans chain conformation of the β phase of PVDF (2-4).

Poling of PVDF induces the conversion of the nonpolar α phase to the polar β phase under proper poling conditions (field strength, time, temperature), while allowing the alignment of the dipole moments of PVDF in the direction of the external electric field. IR measurements have been used to show the conformational changes and the orientation of CF_2 dipoles upon poling (4). The poling of β phase PVDF films results in a simultaneous increase in crystallinity and orientation (5). The polar analog of the α phase, α_p, may also be obtained on poling the α phase. One mechanism that has been proposed for this

transformation involves 90° rotations around every G and G' bond on alternating chains with all the rotations being in the direction of the applied field (6).

In spectroscopic studies of the effect of an electric field on a P(VDF-TrFE) copolymer with 75 mol % VDF, intensity changes of FTIR absorbances were used to show that molecular chains are rotated by the application of the field, as in PVDF. Electric fields are effective in both dipolar and crystal orientation. Poling an oriented film at room temperature had virtually no effect on the microstructure, while at temperatures close to the Curie point the orientation was improved with poling. The application of a poling field resulted in an increase in the trans sequences in the copolymer, accompanied by an increase in the degree of crystallinity, and an improvement in the packing density of the copolymer (7, 8).

Orientation of the crystal on the molecular level can be achieved by mechanical deformation of PVDF and its copolymers. Mechanical deformation of PVDF at 50 - 100°C causes a rotation of the bonds to give the $\alpha \rightarrow \beta$ phase transformation, so that the β phase of PVDF can be obtained by deformation of the α phase that is formed on melt crystallization (2, 3). Stretching of the γ phase of PVDF to draw ratios of four times at 150°C results in a crystal-crystal transition to a highly oriented β phase (9).

Applying mechanical stress to P(VDF-TrFE) copolymers with 50 - 65 mol % VDF causes an irreversible transformation to the β phase analog. The application of tensile force therefore induces the chain conformational transition from gauche to trans linkages as it does in the PVDF homopolymer. Stretched copolymer samples exhibit a higher T_C than their unoriented counterparts due to the ordering in the crystal structure caused by orientation (10). Lovinger et al. (11) claim that drawing does not markedly modify the structure of P(VDF-TrFE) copolymers with 65 - 78 mol % VDF, though there is a slight improvement in their molecular packing on drawing. Mechanical drawing has been used to obtain the β-phase from P(VDF-TrFE) copolymers with greater than 82 mol % VDF, which are believed to crystallize from the melt or solution into a mixture of α, β, and γ

phases. The β phase thus formed has lower piezo- and ferroelectric properties than one formed by poling (12).

Solid state extrusion techniques (Figure 5.1) have been used to obtain the oriented β phase of PVDF, but at high temperatures the α→β phase transformation only occurs to a low extent. It has been found that the solid state coextrusion of PVDF in a split billet of polyethylene is an efficient process of orienting PVDF at temperatures of ~125°C. At this temperature high degrees of uniaxial orientation are achieved, accompanied by a complete transformation of the α phase to the β phase. With coextrusion the crystallinity in PVDF increases by ~7% (13).

Highly oriented P(VDF-TrFE) copolymers have not been extensively studied, though several studies have been made on their electric field induced dipolar orientation (7, 8). In this study we are interested in the microstructural changes brought about by highly orienting P(VDF-TrFE) copolymers with 83 mol % VDF. Such a study may give a better understanding of the improvement in piezoelectric properties that are expected with orientation. The preparation of a highly oriented sample will enable a more accurate assignment of vibrational bands. Vibrational spectroscopy is used to indicate the structural and orientation changes that are produced by the coextrusion of the copolymers. The degree of orientation will also be measured, since previous measurements have not been made on these copolymers.

Orientation Measurements

A quantitative measure of the orientation of the crystalline and amorphous regions within the mechanically deformed sample is needed. This requires the measurement of the fraction of the crystalline and amorphous phase present and the orientation function of each phase. A relative measure of the fraction of each phase can be measured by WAXD, whereas absolute values are measurable from DSC enthalpy values. Infrared spectroscopy

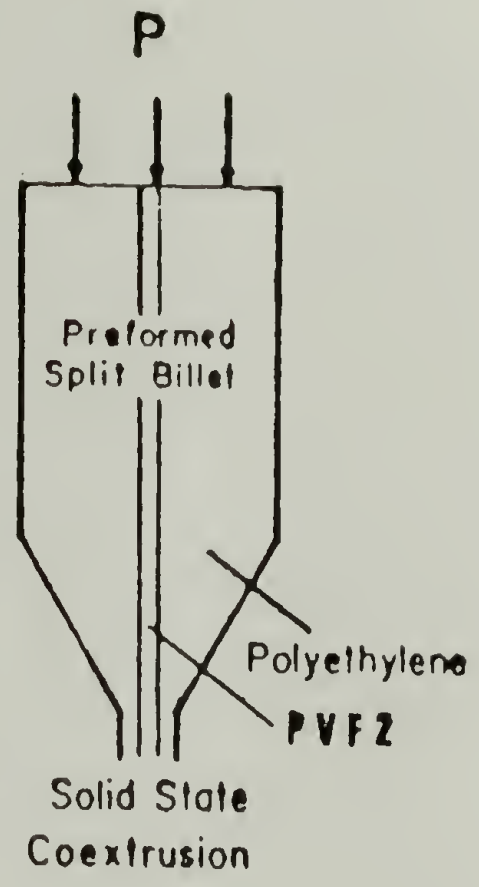

Figure 5.1 Schematic diagram illustrating the split-billet coextrusion technique. (from ref. 13)

can give an absolute measure of crystallinity if separate IR absorption bands due only to the crystalline and amorphous regions can be identified. Since this is not the case for P(VDF-TrFE), WAXD and DSC are used to measure the relative percentage crystallinity. It is also necessary to identify which crystal phases are present in the oriented samples, which can be done from WAXD data and FTIR spectra.

WAXD Orientation Studies

The crystalline orientation can be measured from an analysis of the intensity of the reflection arcs of the wide-angle diffraction patterns. The average crystalline orientation is quantified by Hermans' orientation function that describes the orientation of the crystallite axis relative to some reference direction in the sample (14):

$$f_x = \frac{3\cos^2 x - 1}{2} \qquad (5.1)$$

The orientation angle, x, is the angle between the chain axis and the draw direction. The Hermans' orientation function implies that all the crystallographic axes are cylindrically symmetric about the reference direction. The orientation function f has a value from 1 to -1/2 with 1 corresponding to a sample with complete parallel orientation to the stretch direction, 0 for random orientation and -1/2 for orientation perpendicular to the stretch direction.

The model for uniaxial orientation proposed by Stein (Figure 5.2) indicates that there are three orientation functions that define the degree of orientation of the three crystallographic axes with respect to the stretching direction (15). This model was developed for an orthorhombic system and is therefore applicable to PVDF in the β phase.

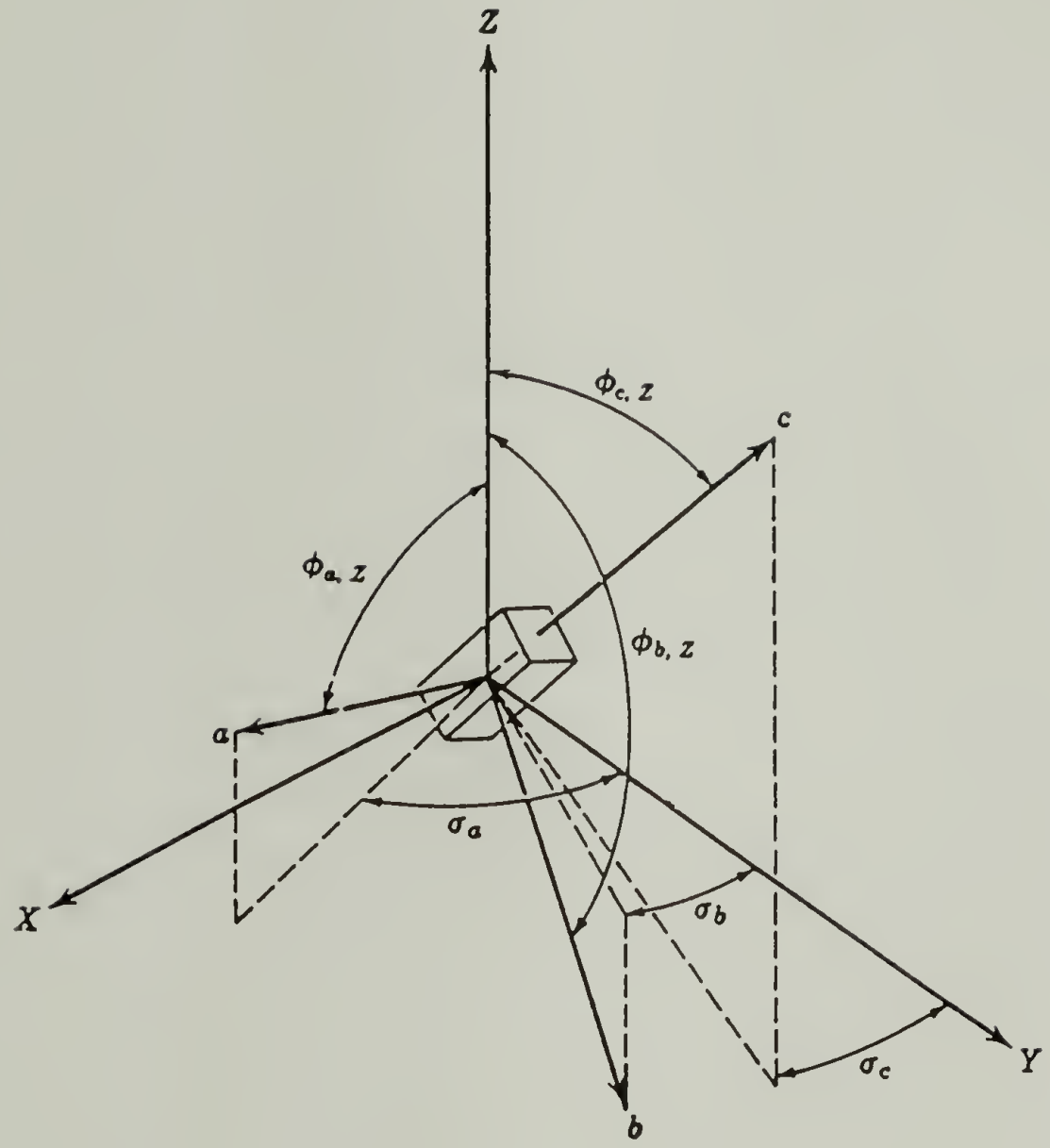

Figure 5.2 Model for the orientation modes in orthorhombic polymers. (from ref. 15)

The orientation functions are defined as

$$f_\alpha=\frac{3\cos^2\alpha-1}{2} \qquad (5.2)$$

$$f_\beta=\frac{3\cos^2\beta-1}{2} \qquad (5.3)$$

$$f_\varepsilon=\frac{3\cos^2\varepsilon-1}{2} \qquad (5.4)$$

Due to the orthogonality of the three mutually perpendicular planes,

$$f\alpha + f\beta + f\varepsilon = 0. \qquad (5.5)$$

For this model the three orientation functions are not independent and therefore only two are needed to characterize fully the orientation.

The determination of $\cos^2 x_{hkl}$ requires a measurement of the azimuthal intensity distribution of reflections for the different crystal axes. For a uniaxially oriented sample:

$$\cos^2 x_{hkl}=\frac{\int_0^{\frac{\pi}{2}} I(\rho)\cos^2\rho\sin\rho d\rho}{\int_0^{\frac{\pi}{2}} I(\rho)\sin\rho d\rho} \qquad (5.6)$$

From $\cos^2 x_{hkl}$ then the orientation function for the different axes can be determined (16, 17).

For comparison of the relative axial orientation between a series of related polymers the azimuthal breadth of the intensity in a diffraction arc can be used. There is a relation between the intensity at a given angle in a diffraction arc and the number of crystallites oriented at that angle to the fiber axis, hence the integral breadth may be used as an orientation index (16).

Infrared Dichroism

Another powerful method of quantifying orientation of deformed polymer systems is that of infrared dichroism that can be used to measure the orientation functions of the crystalline and the amorphous regions (Figure 5.3). With IR dichroism one measures the transition moment angle, α_v, which is the angle of the dipole moment vector of a certain chemical group with respect to the chain axis. The dichroic ratio, R, is calculated from the ratio of absorption intensities from spectra that have been measured with radiation polarized parallel and perpendicular to the draw direction:

$$R = A_{\parallel}/A_{\perp} \qquad (5.7)$$

The transition moment angle can be measured from a sample in which the molecules are perfectly aligned parallel to the chain axis giving:

$$R_o = 2\cot^2\alpha_v. \qquad (5.8)$$

The dichroic ratio is a measure of the degree of orientation of molecules relative to the orientation function. The second moment of the orientation function is defined:

$$f = \frac{(R-1)(R_o+2)}{(R+2)(R_o-1)} \qquad (5.9)$$

When this is evaluated in terms of the average orientation of polymer molecules it is equivalent to Hermans' orientation function.

If a sample is known to be perfectly oriented in the axial direction then the transition moment angles for all the absorbance bands can be calculated from their observed dichroic ratios. It is therefore possible to get information about the geometric structure of a polymer chain from dichroic ratio measurements (18).

In order to make an accurate comparison of the microstructure of samples with different draw ratios, it is necessary to ensure that the sample crystallinity and conformational distribution are the same. This can be done by comparing the IR spectra that are exclusive of contributions of the sample orientation, A_o, which can be calculated

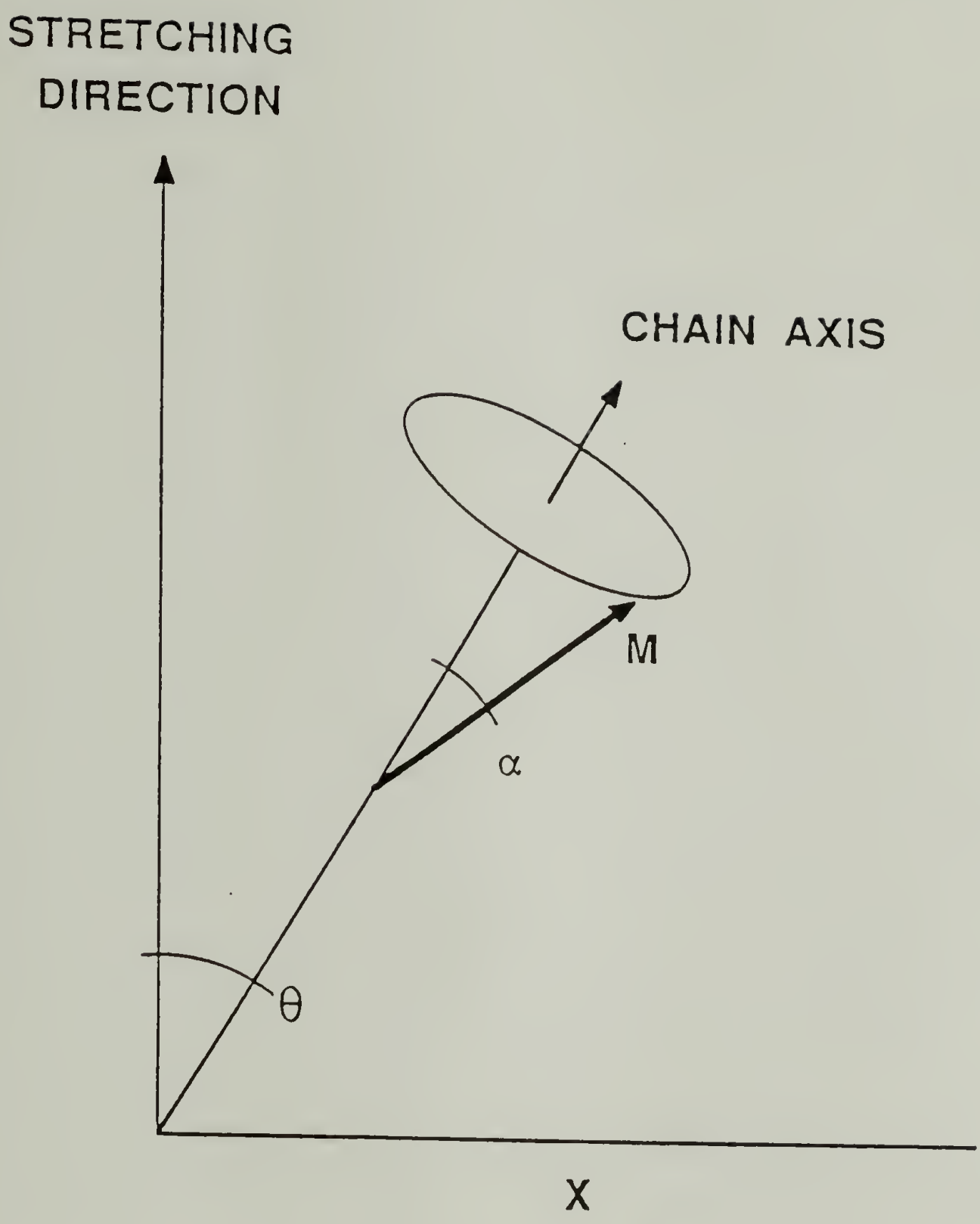

Figure 5.3 Schematic representation of the relationship between the transition moment (M), chain axis, and the stretching direction. (from ref. 18)

from the polarized spectra.

$$A_0=\frac{A_{\parallel}+2A_{\perp}}{3} \qquad (5.10)$$

Experimentally determining the orientation function by an independent method such as WAXD and combining this f value with the experimentally determined dichroic ratio allows an explicit solution of the transition moment angle with no need for approximations or model assumptions (17).

Experimental

The split billet coextrusion technique was used to prepare highly oriented films of P(VDF-TrFE) copolymers. Cast films of P(VDF-TrFE) were embedded in a split billet of polyethylene. The billet was coextruded at 100°C in an Instron Capillary Rheometer, extruding through a conical brass die. An extrusion rate of 0.05 cm/min was used to achieve draw ratios of 4.4 and 6.5 times. The draw ratio was measured from the extension of ink marks that were made on the P(VDF-TrFE) film before coextrusion.

The oriented films thus obtained were characterized by WAXD, DSC, and FTIR. Infrared spectra were measured on an IBM IR32 spectrometer, using a wire-grid polarizer to obtain polarized spectra. The degree of orientation was measured from dichroic ratios measured from the polarized FTIR. For the crystalline regions, orientation was measured from intensity distribution of WAXD obtained from microdensitometer traces around the azimuthal angle of different reflections recorded on photographic film.

Results and Discussion

The oriented samples were predominantly in the all trans β phase as evidenced by the presence of only β phase reflections in the WAXD data. The WAXD has oriented arcs

for the (200), (002), and (111) reflections with equatorial maxima indicating c-axis orientation along the extrusion direction (Figure 5.4). The Curie transition temperature was increased by 5°C from the cast film to 130°C, and was much less diffuse, indicating that the coextrusion process gives a more ordered ferroelectric phase (Figure 5.5). Tm is unchanged from the cast film to the oriented films while the heat of fusion increases by ~25% by drawing 4.4x indicating an increase in the sample crystallinity for coextruded samples. Higher crystallinity is also evidenced by the intensification of WAXD reflections.

To assess the spectroscopic changes in the sample conformation induced by orientation the A_o spectra, which do not include orientation contributions, are calculated and compared (Figure 5.6). In comparing these spectra with that of an unoriented sample it is seen that there is an increase in intensity of β phase vibrations at 1284 and 842 cm^{-1} accompanied by a shift of 4 cm^{-1} of the long trans vibration seen at 1280 cm^{-1} in the cast film. The frequency shift toward higher wavenumbers for this vibration is due to an increase in the crystallinity of the sample and ordering of the β phase upon coextrusion as this vibration has also been determined to be due to the pure crystalline phase in a P(VDF-TrFE) copolymer with 75 mol % VDF (19). The sharpening of vibrations at 1076 and 842 cm^{-1} is further proof of increased crystallinity and a decrease in the conformational distribution in coextruded samples as compared with the cast film. There is also a large decrease in the intensity of the shoulder at 1238 cm^{-1} that is assigned to the amorphous phase (19).

The dichroic ratios for various vibrations were measured from polarized FTIR spectra (Figure 5.7). The orientation was measured from the vibrational band at 844 cm^{-1} for which the transition moment angle has been measured in oriented PVDF to be 74° (20). This band was chosen over the 3012 cm^{-1} CH_2 asymmetric stretching vibration with a 90° transition moment angle because of its higher intensity. Using this band the orientation was found to be 0.88 for the sample extended 4.4x and 0.94 for the sample with an extension ratio of 6.5. These are lower limits for the degree of chain orientation because

A

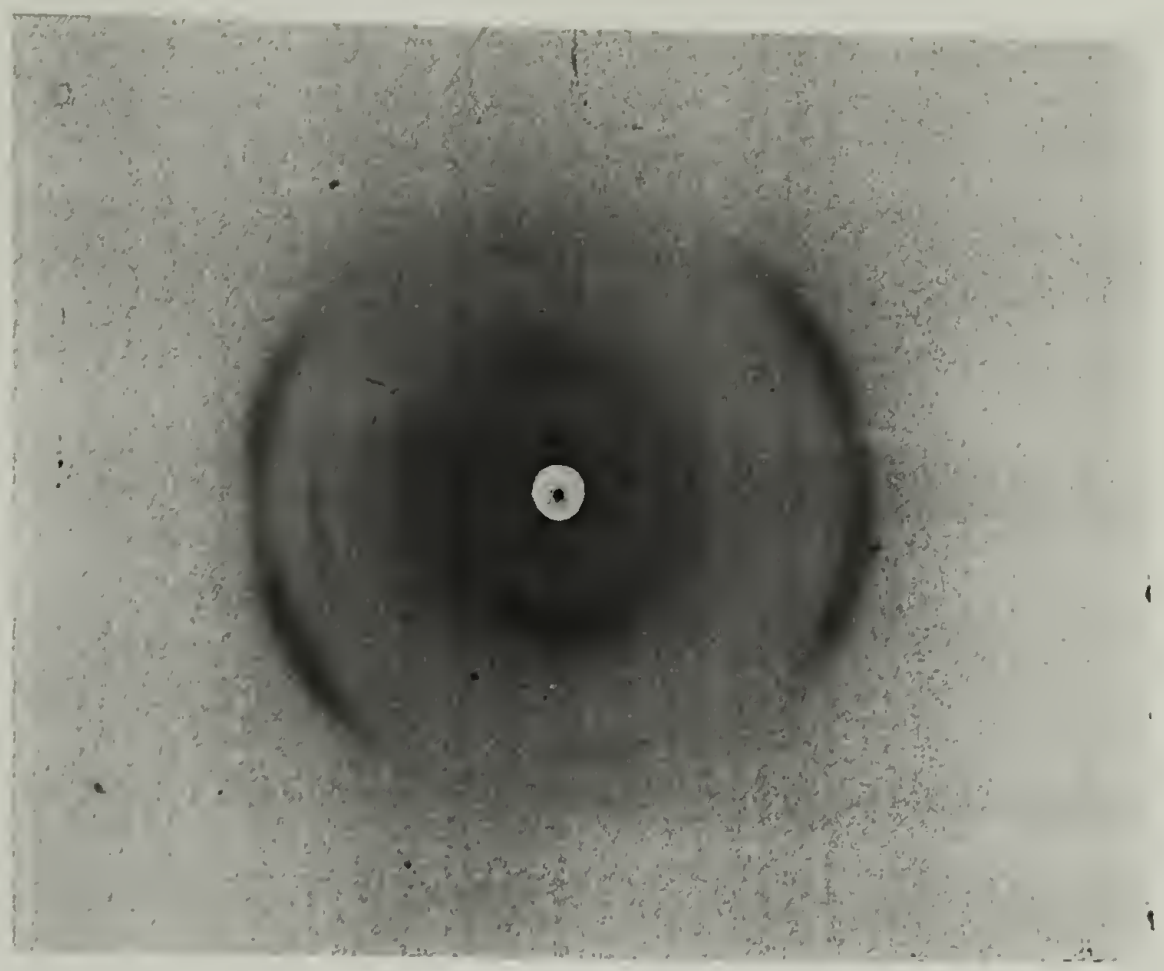

B

Figure 5.4 Wide-angle X-ray diffraction patterns of coextruded P(VDF-TrFE) copolymer. A: draw ratio = 4.4; B: draw ratio = 6.5.

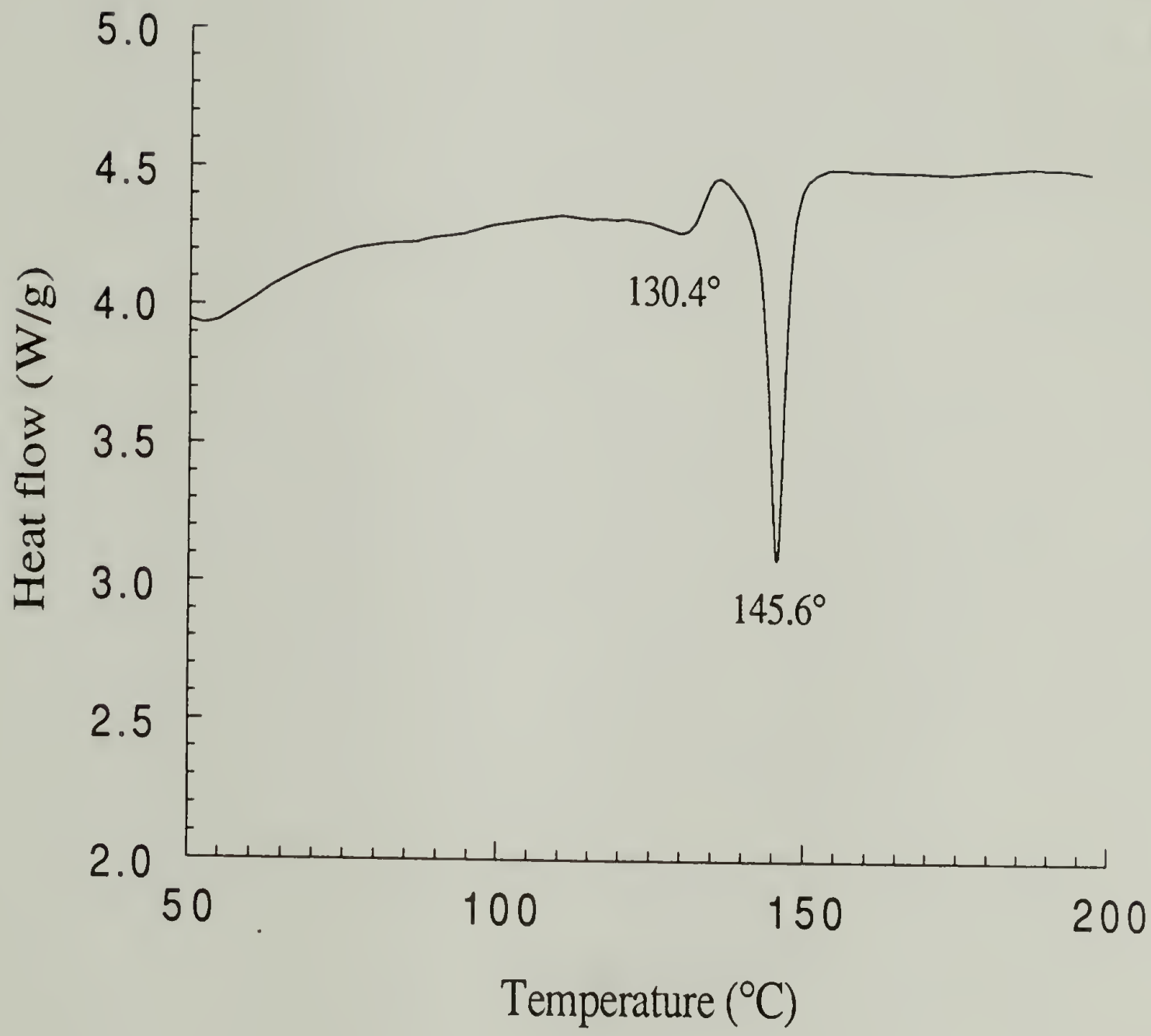

Figure 5.5 DSC thermogram of P(VDF-TrFE) copolymer coextruded to a draw ratio of 4.4.

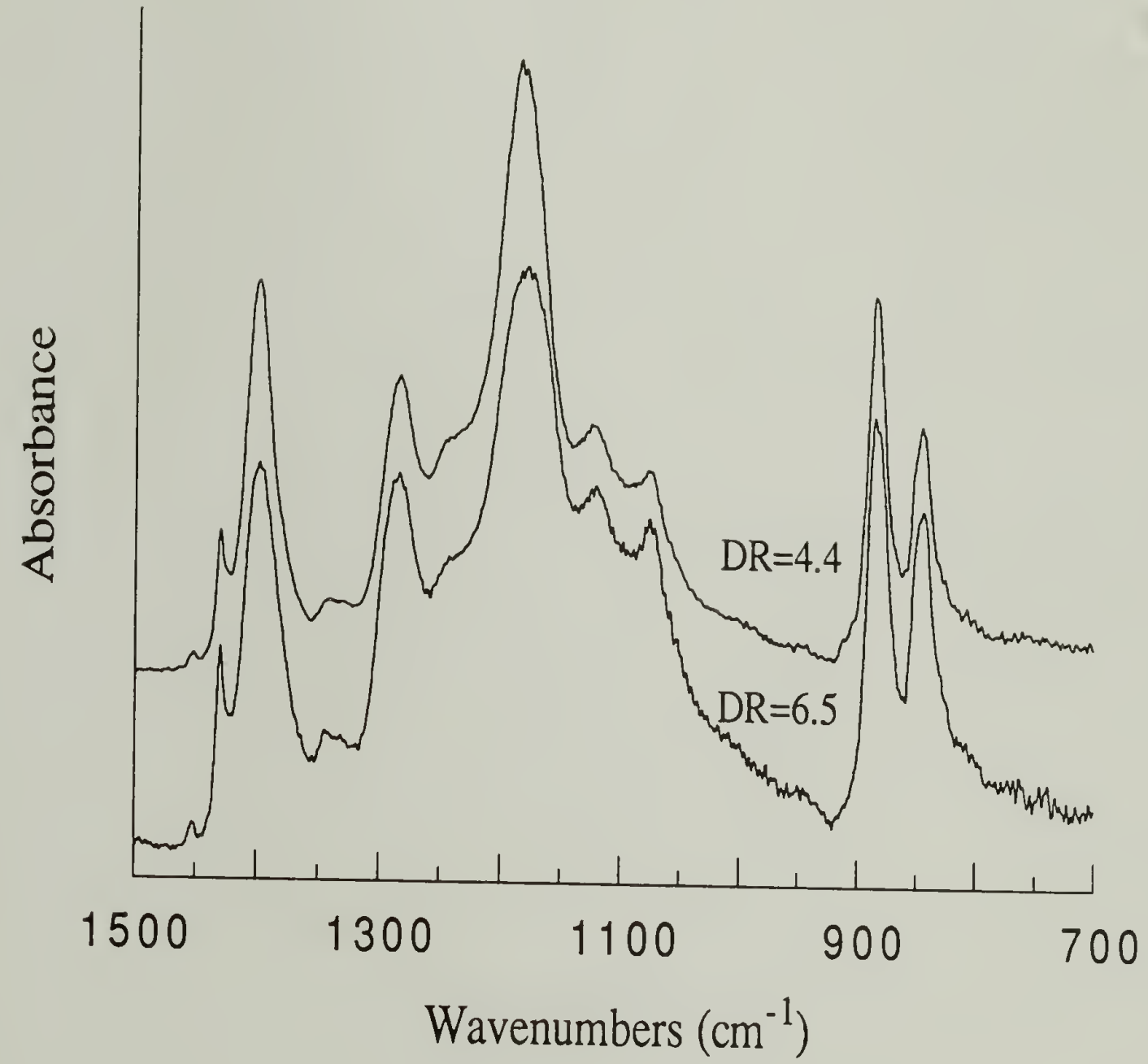

Figure 5.6 A_O infrared spectra of coextruded P(VDF-TrFE) copolymer with draw ratio of 4.4 (top) and 6.5 (bottom).

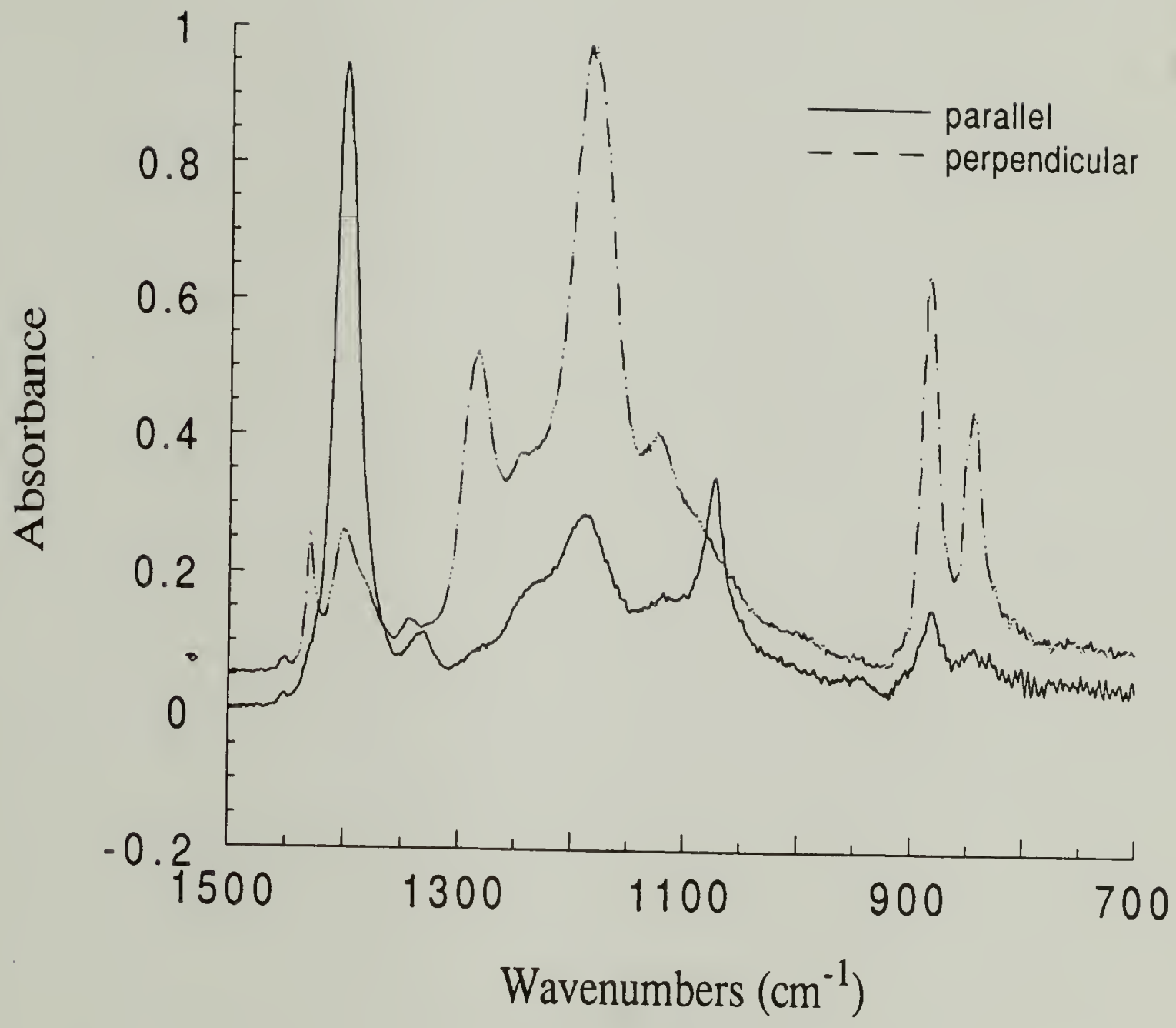

Figure 5.7 Polarized infrared spectra of coextruded P(VDF-TrFE) copolymer with draw ratio of 4.4.

influences such as infrared beam divergence and sample misalignment can only decrease the observed dichroic ratios (18). A list of the analyzed bands, their assignments and the measured dichroic ratios is given in Table 5.1.

Table 5.1 Measured dichroic ratios for coextruded P(VDF-TrFE) copolymer.

wavenumber(cm^{-1})	Polarization	dichroic ratio		assignment(21)
		DR=4.4	DR=6.5	
1400	∥	3.63	3.00	$w(CH_2)\nu_a(CC)$
1285	⊥	.261	.278	$\nu_a(CF_2)r(CF_2)r(CH_2)$
1075	∥	1.83	1.57	$\nu_a(CC)w(CF_2)w(CH_2)$
882	⊥	.262	.254	$\nu_a(CF_2)r(CH_2)r(CH_2)$
844	⊥	.234	.204	$\nu_s(CC)\nu_s(CF_2)$

The transition dipole moment angle for the different bands can be approximated by assuming that the samples have perfect uniaxial orientation (22). This calculation will give information that is useful in determining vibrational band assignments by normal coordinate analysis, which to this time have not been made for P(VDF-TrFE) copolymers. The only previously reported transition moment angles are those for a melt drawn PVDF homopolymer (20) so the transition moments measured in this study cannot be assessed for their validity. These are the first reported transition moment angles and orientation values for this P(VDF-TrFE) copolymer and are listed in Table 5.2.

The orientation of the crystalline phase was independently measured from the azimuthal intensity distribution of microdensitometer traces of WAXD reflection arcs. This should give a larger value of orientation since it is only a measure of crystalline orientation, which is presumed to be higher than for amorphous regions. The orientation values measured from WAXD techniques were 0.76 for the sample extended 6.5x and 0.43 for

Table 5.2 Calculated transition moment angles assuming perfect orientation

wavenumber(cm^{-1})	Transition moment angle
1401	37.9°±1.8
1286	69.8°±0.4
1075	47.4°±1.5
882	70.2°±0.2
842	71.7°±0.8

the one extended 4.4x, and have a large margin of error due to the noise in the intensity signal. For this reason these values were not coupled with FTIR dichroic ratio measurements to measure the transition moment angle of the chain. Orientation measurements from WAXD are based on the integrated intensity of the scattering pattern, which is not directly measured using a microdensitometer. True intensity measurements are made from a diffractometer with a positional sensitive proportional counter, as opposed to the relative intensity from microdensitometer traces. Better accuracy in orientation measurements from WAXD requires the construction of a pole figure from diffraction intensity measured from tilting a sample with respect to the X-ray beam.

On comparing the azimuthal scans of the X-ray diffraction patterns for the two coextruded samples it is clear that the higher draw ratio results in greater number of crystallites oriented to the fiber axis, giving a much narrower azimuthal curve (Figure 5.8).

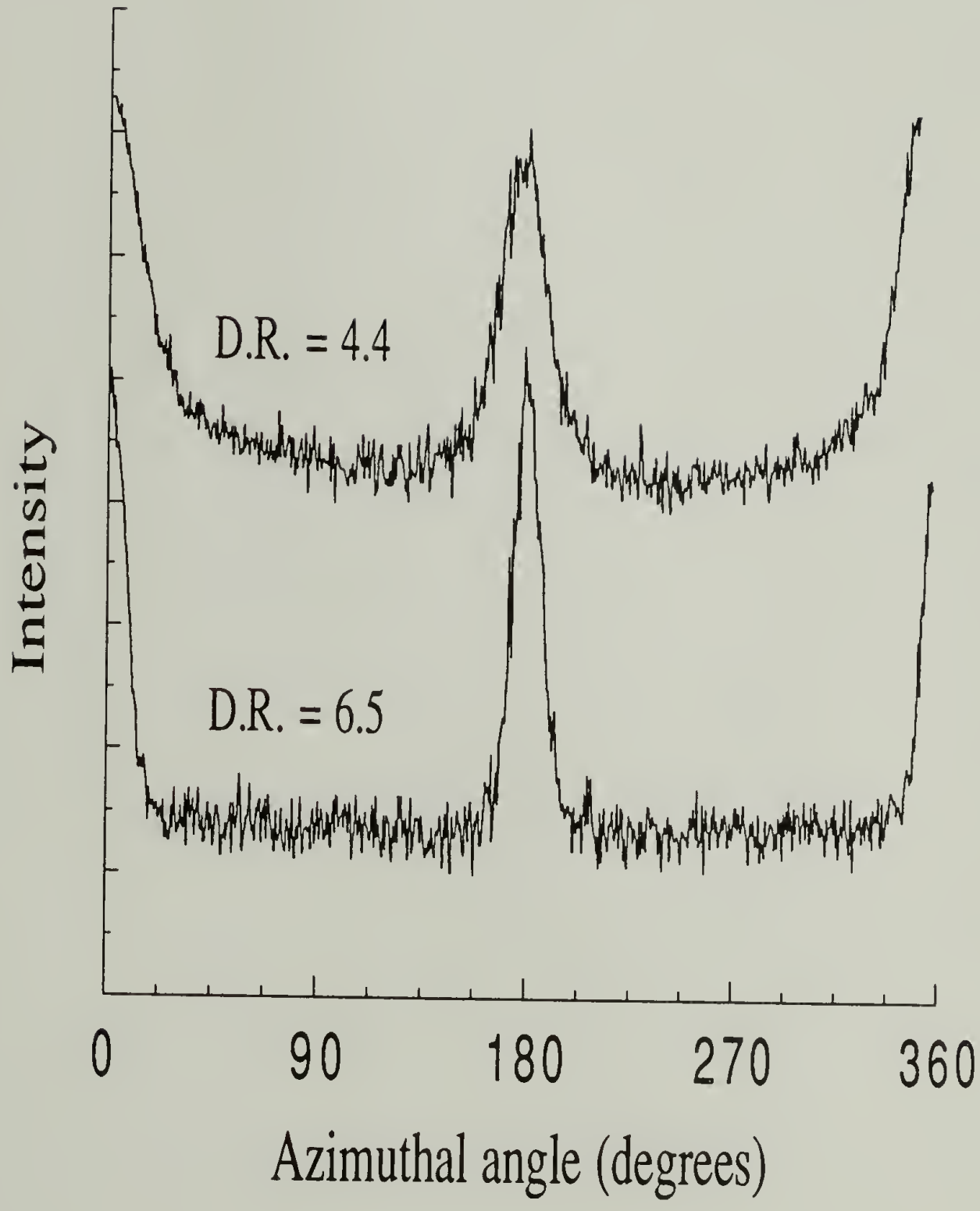

Figure 5.8 Azimuthal scan of the β(200) reflection of coextruded P(VDF-TrFE) copolymer with draw ratio of 4.4 (top) and 6.5 (bottom).

Conclusions

In this study of the orientation of P(VDF-TrFE) copolymers by the split-billet coextrusion technique, the microstructure of the copolymer is predominantly in the ferroelectric β phase as measured by infrared spectroscopy and WAXD. Coextrusion results in highly oriented samples with orientation values of 0.88-0.93 measured from polarized infrared. The orientation of these 83/17 copolymers are higher than any previously reported orientation values for any composition of P(VDF-TrFE) copolymers. The preparation of such well oriented samples enables a measurement of the transition dipole moments from infrared dichroism data.

The sample crystallinity increases with coextrusion as seen by the sharpening of the vibrational bands and increase in the heat of fusion measured by DSC. The WAXD patterns also exhibit high degrees of orientation, but a complete description of the orientation requires the construction of pole figures from diffractometric measurements. The orientation increases as the extension ratio is increased, as does the Curie transition temperature signifying more order upon drawing. The increased orientation of these copolymers and high β phase content shows the effectiveness of the coextrusion technique in obtaining P(VDF-TrFE) copolymers with improved piezoelectric activity.

References

1. Bongianni, W. *Ferroelectrics*, **1990**, *103*, 57.

2. Lovinger, A. J.; *Developments in Crystalline Polymers-1;* D. C. Bassett, ed.; Applied Science: London, 1982; p 195.

3. Hasegawa, R.; Takahashi, Y.; Chatani, Y.; Tadokoro, H. *Polymer J.*, **1972**, *3*, 600.

4. Danz, R. *Polym. Bull.*, **1982**, *7*, 497.

5. Janke, A.; Künstler, W.; Geiss, D.; Danz, R.; Stark, W.; *Morphology of Polymers;* B. Sedlacek, ed.; Walter de Gruyter & Co.: New York, 1986; p 673.

6. Lovinger, A. J. *Macromolecules*, **1981**, *14*, 225.

7. Reynolds, N. M.; Kim, K. J.; Chang, C.; Hsu, S. L. *Macromolecules*, **1989**, *22*, 1092.

8. Kim, K. J.; Reynolds, N. M.; Wang, Y. K.; Antolin, K.; Hsu, S. L.; Stidham, H. D. *submitted.*

9. Servet, B.; Broussoux, D.; Micheron, F. *J. Appl. Phys.*, **1981**, *52*, 5926.

10. Tashiro, K.; Kobayashi, M. *Phase Transitions*, **1989**, *18*, 213.

11. Lovinger, A. J.; Furukawa, T.; Davis, G. T.; Broadhurst, M. G. *Polymer*, **1983**, *24*, 1233.

12. Koga, K.; Nakano, N.; Hattori, T.; Ohigashi, H. *J. Appl. Phys.*, **1990**, *67*, 965.

13. Shimada, T.; Zachariades, A. E.; Mead, W. T.; Porter, R. S. *J. Crystal Growth*, **1980**, *48*, 334.

14. Hermans, J. J.; Hermans, P. H.; Vermaas, D.; Weidinger, A. *Rec. Trav. Chim.*, **1946**, *65*, 427.

15. Stein, R. S. *J. Polym. Sci.*, **1958**, *31*, 327.

16. Alexander, L. E.; *X-Ray Diffraction Methods in Polymer Science*; Robert E. Krieger: Malabar, FL, 1969.

17. Samuels, R. J.; *Structured Polymer Properties*; Wiley-Interscience: New York, 1974.

18. Zbinden, R.; *Infrared Spectroscopy of High Polymers*; Academic Press: New York, 1964.

19. Kim, K. J.; Reynolds, N. M.; Hsu, S. L. *Macromolecules*, **1989**, *22*, 4395.

20. Reynolds, N. M., Ph.D. Dissertation, University of Massachusetts, **1990**.

21. Kobayashi, M.; Tashiro, K.; Tadokoro, H. *Macromolecules*, **1975**, *8*, 158.

22. Jasse, B.; Koenig, J. L. *J. Macromol. Sci.-Rev. Macromol. Chem.*, **1979**, *C17*, 61.

CHAPTER VI

RECOMMENDATIONS FOR FUTURE WORK

Results

The structure and phase transition behavior of P(VDF-TrFE) copolymers with an 83/17 molar composition have been studied by vibrational spectroscopy, wide-angle X-ray diffraction, and differential scanning calorimetry. Variable temperature FTIR studies with factor analysis have shown that there are three crystalline phases present in these copolymers over the temperature range of 25-135°C, which is above the Curie transition.

Melt crystallization of the copolymers has been used to enhance the sample crystallinity and to increase the paraelectric phase content in the room temperature structure. Longer crystallization processes in the nonisothermal and isothermal experiments permit a perfection of the gauche-containing α phase which is retained somewhat on undergoing the Curie transition on cooling. The Curie transition temperatures on cooing and heating are decreased, reflecting the presence of the stabilized α phase with the β phase. The melting temperature increases in the samples crystallized for longer times due to the increased crystallinity. Vibrational spectroscopy and WAXD have proven to be useful techniques in characterizing the final structure of the copolymers formed under different crystallization conditions. Both techniques show an increase in the α phase content with longer crystallization times.

Highly oriented P(VDF-TrFE) copolymers have been prepared by solid-state coextrusion. These samples have been used to measure the transition moment angles for some of the vibrations of P(VDF-TrFE) which previously had not been reported.

Recommendations

The structure of P(VDF-TrFE) copolymers is highly composition dependent and has been shown to be strongly influenced by the crystallization conditions (1-5). To date it has been difficult to fully understand the structure of P(VDF-TrFE) because of differences in the sample preparation techniques and in composition. It is important that samples be purified, especially to remove PVDF homopolymer which may be present and could affect the crystal structure. It is also known that the structure of PVDF depends on the head-to-tail content in the chain (6). In order to better understand the crystal structure of the copolymers and the composition dependence, it would be best to measure accurately the composition as well as the head-to-tail content in the polymer chain. This can be done using fluorine NMR spectroscopy, which has been used to determine the reactivity ratios of vinylidene fluoride and trifluoroethylene as 0.7 and 0.5 respectively (7). The influence of the defect content on the microstructure of P(VDF-TrFE) would be better understood if it were measured in the copolymers.

The structure of P(VDF-TrFE) copolymers of different compositions and the molecular changes associated with their phase transition is important in assessing their utility as ferroelectric materials. Molecular modeling studies would provide a means of studying the stability and properties of the different observed and proposed crystalline structures of the copolymers. Such studies have been limited due to poor definition of force fields for halogenated molecules, but new force fields have recently been reported (8) for PVDF which may make such molecular dynamics simulations possible.

In a further study of the paraelectric to ferroelectric phase transition in P(VDF-TrFE), the copolymer could be quenched from the high temperature paraelectric phase to a low temperature where the formation of the ferroelectric phase could be monitored. This would give information on the crystallization of the ferroelectric phase. Similarly, the isothermal crystallization of the paraelectric phase can be studied by quenching from the

melt to a set crystallization temperature (i.e. 135°C) and following the development of the paraelectric phase. With proper temperature control these experiments can be done in a spectrophotometer where microstructural changes are detectable from the vibrations of the crystalline phases. The crystallization of the paraelectric α and γ phases can also be studied by optical microscopy as has been done for PVDF and P(VDF-TFE) (9-13).

The crystallization of P(VDF-TrFE) can be studied in real time X-ray experiments using synchrotron radiation. By this technique the cooling crystallization can be measured as can isothermal crystallization. This allows for the determination of the structures crystallized and of the structural changes which occur at the Curie transition, rather than just the room temperature structures which were characterized in this study. Using a simultaneous DSC and X-ray scattering method (14) would give direct information on the structures and phase transitions of the copolymers during different thermal treatments.

The behavior of PVDF and its copolymers in an electric field has been studied, as poling provides a means of transforming from the α to the β phase (1, 5, 15-23). It is interesting to see how the behavior of the copolymers in an electric field is affected by thermal treatment which modifies its crystalline structure. It is believed that copolymers with high crystallinity and a large portion of α phase will transform readily to an all trans ferroelectric state with strong piezoelectric activity.

References

1. Koga, K.; Nakano, N.; Hattori, T.; Ohigashi, H. *J. Appl. Phys.*, **1990**, *67*, 965.

2. Ohigashi, H.; Kagami, N.; Li, G. R. *J. Appl. Phys.*, **1992**, *71*, 506.

3. Stack, G. M.; Ting, R. Y. *J. Polym. Sci., Polym. Phys. Ed.*, **1988**, *26*, 55.

4. Tanaka, H.; Yukawa, H.; Nishi, T. *Macromolecules*, **1988**, *21*, 2469.

5. Tashiro, K.; Kobayashi, M. *Phase Transitions*, **1989**, *18*, 213.

6. Lovinger, A. J.; Davis, D. D.; Cais, R. E.; Kometani, J. M. *Polymer*, **1987**, *28*, 617.

7. Yagi, T.; Tatemoto, M. *Polymer J.*, **1979**, *11*, 429.

8. Karasawa, N.; Goddard, W. A., III. *Macromolecules*, **1992**, *25*, 7268.

9. Marand, H.; Stein, R. S. *Macromolecules*, **1989**, *22*, 444.

10. Marand, H. L., Ph.D. Dissertation, University of Massachusetts, **1988**.

11. Lovinger, A. J. *Polymer*, **1981**, *22*, 412.

12. Lovinger, A. J. *Polymer*, **1980**, *21*, 1317.

13. Lovinger, A. J. *J. Polym. Sci., Polym. Phys. Ed.*, **1980**, *18*, 793.

14. Russell, T. P.; Koberstein, J. T. *J . Poly. Sci., Polym. Phys. Ed.*, **1985**, *23*, 1109.

15. Tashiro, K.; Takano, K.; Kobayashi, M.; Chatani, Y.; Tadokoro, H. *Ferroelectrics*, **1984**, *57*, 297.

16. Reynolds, N. M.; Kim, K. J.; Chang, C.; Hsu, S. L. *Macromolecules*, **1989**, *22*, 1092.

17. Marand, H.; Stein, R. S. *J. Poly. Sci., Polym. Phys. Ed.*, **1989**, *27*, 1089.

18. Marand, H. L.; Stein, R. S.; Stack, G. M. *J. Polym. Sci., Polym. Phys. Ed.*, **1988**, *26*, 1361.

19. Lu, F. J.; Hsu, S. L. *Macromolecules*, **1986**, *19*, 326.

20. Lovinger, A. J.; Furukawa, T.; Davis, G. T.; Broadhurst, M. G. *Polymer*, **1983**, *24*, 1225.

21. Lovinger, A. J.; *Developments in Crystalline Polymers-1;* D. C. Bassett, ed.; Applied Science: London, 1982; p 195.

22. Davis, G. T.; McKinney, J. E.; Broadhurst, M. G.; Roth, S. C. *J. Appl. Phys.*, **1978**, *49*, 4998.

23. Danz, R. *Polym. Bull.*, **1982**, *7*, 497.

APPENDIX A

ARRAY BASIC PROGRAM FOR FACTOR ANALYSIS

```
'Core AB code of PCA decomposition - (Both SVD of Covar & NIPALS)
'(c) Galactic Industries Corp.


'Note: This program is the core code to perform a PCA on a series of spectra.
'Both the decomposition of the Spectral Covariance matrix and NIPALS methods
'are enclosed.  The first method is much faster, but can suffer some loss in
'precision in the covariance.  Please see the notes below the first routine
'for information on this.

'This is expanded to work on spectra that are loaded into the memory
'and to recreate a abstact eigenspectra from the factor analysis eigenvectors.
'Modifications by K. Antolin, April 1992
' further modified July 31,1992

'Description of variables used and dimensionality
        'n=# of spectra, p=# of spectral data points
        'a=max # of PCA factors calculated, here changed to n-1
        'err, laster = keeps track of error in scores in each iteration


10      free
20      dim filename(80,100)                    'max of 100 files
30      dim sname(20)                                   'data file to be created
40      input " Enter number of spectra to be used:    ",n
50      input "Enter output filename :",$sname
60      input " Enter x-axis range " sw,ew
70      a=n
TO ESTABLISH P VALUE SO THAT CAN DIMENSION MATRICES, LOAD A
SPECTRUM INTO MEMORY

80      printline 24:print "select first file"; 1
90      menufile $filename,"File:"
100     loadspc $filename
110     openspc $filename,G
120     p=npts(#s(sw,ew))                       'number of data points to use
125     print "# points in spectrum is:";p
130     dim temp1(p)                            ' data array of single file
140     dim X(n,p)                                      'data matrix
150     temp1=G(sw,ew)
160     X(0)= temp1
170     closespc G

'read in files used in FA
200     for i=1 to n-1
210             printline 24: print "Select file "; i+1
220             menufile $filename, "File: "    'get spectrum filename
230     '       loadspc $filename       'load SPC into memory(optional)
240     '       see     'display on screen
```

```
250             openspc $filename,G                     ' opens disk-based trace
270             temp1=G(sw,ew)                          ' and puts into temp1
280     '       print "Data: ", freq #s(ew), #s(ew)
290             X(i)=temp1                              'move array into data matrix
300             closespc G
310     next i

'to check that memory & read files are the same
'output values of the two to the screen
'       for i=0 to p-1
'       printline 24: print " Data from read file : ", temp1(i)
'       next i
' print data matrix
        for i=0 to n-1
         printline 24: print " Data matrix row: ", i,X(i);i+1
        next i

'Dimensionality of matrices used for calculation
' arbitrarily set a=10 for max. # of factors in analysis for large n
'       a=10
400     dim Z(n,n)              'spectra data covariance for SVD
410     dim Z1(n,n)             ' regenerated covariance matrix
420     dim L(a,n)              'eigenvector matrix
430     dim F(a,p)              'abstract eigenspectra matrix
440     dim lambda(a,a)         'diagonal matrix of Eigenvalues
450     dim Llast(1,n)                  'temporary row vector
460     dim Ltemp(n,1)                  'temporary column vector
470     dim D(a,p)              'regenerated data matrix


        portout -30,6                           'sets output to 10 columns

'*************************************************************************
**********
'Perform the PCA by decomposition of Covariance matrix

500     open "c", #1, $sname  'open output file
510     print #1, "filename", $sname, n,sw,ew
'520    print #1, "Covariance Matrix"

600     printline 24 : print "Calculating covariance matrix...."
610     Z = X [#] trans(X)                      'calc covar matrix (NxN)
 'Print out covariance matrix
620     for i=0 to a-1
         printline 24: print " Row # :", i+1, Z(i)
'630    print #1, Z(i)   'writes Z matrix to file
         TRZ = TRZ + Z(i,i)                     'calculates trace of Z
         printline 24: print "trace Z: ", TRZ
640     next i
650      print #1,"       "
660      print #1,"row","eigenvector", " "," ","lambda"        'file header
670     L = 0.1                                         'initialize L to arbitrary value
```

```
680     for i = 0 to a-1
                printline 24 :print "Calculating vector #";i+1
690             mc=0 : err = 99999                      'Do the PCA to get eigenvectors
700             mc = mc+1 : laster = err                'and eigenvalues
710             Llast = L(i)
720             Ltemp = Z [#] trans(Llast)
730             L(i) = trans(Ltemp)
740             lambda(i,i) = sqrt(sumd2(L(i),0))
750             L(i) = L(i)/lambda(i,i)
760             err = sqrt(sumd2(L(i),Llast))
770             if err<=sqrt(sumd2(Llast,0))*1e-6 goto 800
780             if abs(err-laster)>abs(err*1e-6) and mc<100 goto 700
800     Llast = L(i)
810             onerror 3000
820             print #1,i,Llast,lambda(i,i)
830             Z = Z - (trans(Llast) [#] Llast)*lambda(i,i)      'calc resids
                printline 24:print "Vector # "; i+1,Llast
840     next i
850     if n < 6 goto 910
860     print #1,"          "
870     print #1, "eigenvalues"
880     for i= 0 to a-1
890      print #1, lambda(i,i)
900     next i

910     printline 24 : print "Calculating Factors....."
920     print
930      F =L [#] X             'Calculate abstract eigenspectra

'Calculate errors according to Maliknowski's analysis
'use this to find IND, etc
1000    dim RE(n)
1010    dim SRE(n)

1030    dim IE(n)
1040    dim SIE(n)
1050    dim XE(n)
1060    dim SXE(n)
1070    dim IND(n)

1080    print #1, " "
1090    print #1, "n", "RE"," ", "IE"," ", "XE"," ","IND"," ", "RSD"        ' header

        printline 24:print        "Calculating Errors....."
        print
1100    for i=1 to a-1
1110            REsum =0
                for j= i+1 to a
                Resum= Resum + lambda (j-1,j-1)
1119            next j
1120            SRE(i) =REsum/(p*(a-i))
1130            RE(i) = sqrt(SRE(i))
1140            SIE(i) = (i/a)*SRE(i)
1150            IE(i) = sqrt(SIE(i))
```

```
1160            SXE(i) = REsum/(p*a)
1170            XE(i) = sqrt(SXE(i))
1180            IND(i) = RE(i)/(squared(a-i))
1190            EIGSUM= EIGSUM + lambda(i-1,i-1)
1200            RSD = TRZ - EIGSUM                          'calculate residual
1210            if ABS(RSD) > 0.0000001 then 1230           'square deviation
1220            GOTO 1270
1230            IF RSD > 0 then 1250
1240            RSD = -1*RSD
1250            RSDi = (RSD/(p-i))
1260            RSD = (1/n)*SQRT(RSDi)
1270            print #1,i,RE(i),IE(i),XE(i),IND(i),RSD     'output errors to file
1280    next i
1290    close #1


'output eigenspectra

1300    for i=0 to a-1
                printline 24: print " Eigenspectra row :", i+1, F(i)
        next i


'calculate regenerated data matrix from eigenvector matrix
'1400   printline 24: print "Calculating regenerated data matrix..."
'1410   D =trans(L)[#] F
```

```
'print it out
 '      input "Enter regenerated datafile name ", $sname
 '      string sname = $sname
'1420   for i=0 to a-1
'1430   string sname,0

'1440   open "C", #1, $sname
'1450   for j= 0 to p-1
'1460   pt= sw -j*((sw-ew)/p)
'1470   SD = D(i,j)
'1480   print #1,pt,SD,
'1490   next j
'1500   printline 24: print "Writing data file #:", i+1
'1510   close #1
'1520   next i

1530    Input "Do you want to write abs eigenspec to file?(y=1,n=0)",reply
1540    if reply= 0 then 2000
1550    Input "filename for abs          eigenspectra", $sname
1560     string sname = $sname
1570     for i= 0 to a-1
1580             string sname,0
1590             open "C",#1,$sname
1600             for j= 0 to p-1
1610             pt= sw- j*((sw-ew)/p)
1620             AE= F(i,j)
```

```
1630            print #1, pt, AE
1640            next j
1650            close #1
1660    next i


'Now correct for effects of round off of 32 bit # in covar matrix approach
'which makes the vectors not perfectly orthogonal.  So need to regenerate
'Eigenvalues and vector scores based on the vectors, rather than assuming
'orthoganlity. This will give off-diagonal terms in the Eigenvalues matrix.
'This step is only really necessary when calculating models with large (a>10?)
'dimensions.

1900    input " Want to calculate values based on the vector?(y=1,n=0)",reply
1910    if reply = 0 then 2280
2000    lambda = F [#] trans(F)         'calc new eigenvalues based on vectors
'Output Lambda, the new eigenvalues
2010    input " Enter name for values based on the vectors:", $sname
2020    open "C", #1,$sname
2030    print #1, "new eigenvalues"
2040    for i=0 to a-1
2050     printline 24:print " New eigenvalues, row #: ", i+1, lambda(i)
2060     print #1, i+1, lambda(i)
2070    next i

2080    invertdp lambda                 'and invert for calc of new scores
2090    L = X [#] trans(F) [#] lambda           'calculate new scores based on vectors
'print out the new scores
2100    print #1, "New scores based on vectors"
2110    for i=0 to a-1
         printline 24:print "New scores row #: ", i+1, L(i)
2120     print #1, i+1, L(i)
2130    next i
2140    close #1
2150    D= L [#] lambda
2160    input "other data file, based on vectors :", $sname

2170    for i= 0 to a-1
2180            string sname, 0
2190            open "c", #1, $sname
2200            for j=0 to p-1
2210            pt= sw-j*((sw-ew)/p)
2220            SD= D(i,j)
2230            print #1,pt, SD
2240            next j
2250            close #1
2260    next i

2270    printline 24:print "Calculated new data based on vectors"
5000    end
```

APPENDIX B

OVEN COOLING PROGRAM

```
$NOTRUNCATE
c..TEMPERATURE CONTROLLING PROGRAM FOR THE HSU GROUP
c.......08/05/91.revised 1/6/92

c.......COMMON  STATEMENTS.....................................
        common fname
        common/jen/temp,volwri,zonwri,gnwri,tempwri,frewri
        common/jen2/done,timwri,fwrite
        common/fi/oh,om,os,od,setgn,rh,rm,rs,rd,only2,only3

c.......VARIABLES.....................................
        character fname*8
c....new variables for multistep.....
        integer step,s,isot,q
        dimension aimt(1,20), srt(1,20), isot(4,20),rate(1,20)
        integer answ, freq, done, freq2,fwrite
        integer timwri,frewri,tempwri,volwri,zonwri,gnwri
        integer write,choice,count,setgn,num,only2,only3
        integer only4,only5,avg
        integer  hh,mm,ss,hd,rh,rm,rs,rd,oh,om,os,od
        integer ih,im,is,id,ah,am,as,ad,tim,atim
        real aimt, srt, temp, diff, dtasrt,voltavg,totvolt
        real zone1,zone2,zone3,zone4,zone5,zone6,zone7,zone8
c       new variables for controlled cooling
        real rate,deltemp2,deltim1,rate2,temp1,tmin,temp2
         real diff1, diff2,deltemp1,rate3
        integer initim,tottim,time,time1,time2

c.......MAIN  PROGRAM.....................................

c.......INITIALIZE  DONE  TO  NO  (0).....................
c.........."DONE" ALLOWS THE ZONES TO BE SET ONLY ONCE, THEN.
c.........FOR EACH FOLLOWING LOOP, THE PROGRAM SKIPS OVER...
c.........THE ZONE INITIALIZATIONS AND ZONE STATEMENTS......
        call select_board(1)
        call reset_dt(1)
        call enable_for_output(0)
        call output_digital_value(0,16,0)

        print *, '       ************************************'
        print *, '       HEATING PROGRAM FOR THE HSU GROUP'
        print *, '       ************************************'
        print *, '                                                                '
        print *, 'A few reminders before we start: '
        print *, '1)     To prevent destroying the computer:'
        print *, '       Make sure input and output wires of the'
        print *, '       solid state relay are connected correctly'
        print *, ' (input to port 0 on DT2805 board)'
        print *, '2)     Be sure to check that the offset'
```

```
      print *, '       of the amplifier is set to plus 250mV and'
      print *, '       gain is set to 20. The amplifier is'
      print *, ' to port 2 on the board.'
      print *, '3)     There must be a load on the output,'
      print *, '       otherwise the Output LED will already be'
      print *, '       on when the relay is plugged in.'
      print *, '4)     The manual for this program is stored'
      print *, '       under <manual.for>.'
      print *, '----------------------------------------'
      write(*,'(A\)')' TYPE ANY NUMBER THEN ENTER TO GO ON '
      read *,num
      print *, 'Just a note: If you so choose, you may see'
      print *, 'the Zones of your particular heating.'
      print *, '"Zones" are the temperature at which'
      print *, 'frequency changes.'
      print *, '----------------------------------------'
      print *, 'Now we may begin...'
      print *, 'What would you like to call your file?'
      print *, '(File includes Time, Temperature, Frequency'
      print *, ' and Computer Gain for each call)'
      print *, 'There is a max of 8 characters for the name'
      print *, 'Please use single quotes: "filename"'
      read *, fname

c.....OPEN  FILE.....
      open(unit=1,file=fname,status='unknown')
c.....WRITE HEADER IN FILE.....
      5 format(8x,A,13x,A,13x,A,7x,A,7x,A)
      write(1,5)  'Time','Temp','Freq','Gain','t(min)'
c....Loop for multistep.....
            print *, 'Step annealing can be done'
            print *, 'How many steps do you wish? (less than 20)'
            read *, s
            step=1
      do 20 step =1,s
      10 print *, 'At what temperature would you like'
            print *, 'to start recording data for step ',step, '?'
            read *, srt(1,step)
            print *, 'What is the goal temperature ',step, '?'
            read *, aimt(1,step)
            print *,'At what rate do you want to go (C/min)'
            read *, rate(1,step)
            print *, 'How long an isotherm do you want for this'
            print *, ' step (hh,mm,ss,dd)?'
            read *,isot(1,step),isot(2,step),isot(3,step),isot(4,step)
      15 print *, 'Are you sure these are correct? y=1/n=0'
            read *, answ
            if (answ.ne.1) goto 10
      20 continue

c.....SCREEN INFORMATION CHOICES.....
      25 print *, 'Do you want all information shown on'
            print *, 'the screen(y=1/n=0)?'
```

```
        read *, choice
        if (choice .eq. 1) goto 31
        if (choice .eq. 0) goto 30
30 print *, 'What would you like to see on the screen?'
        print *, 'Frequency(y=1/n=0)?'
        read *, frewri
        if ((frewri .ne. 0) .and. (frewri .ne. 1)) goto 30
        print *, 'Temperature(y=1/n=0)?'
        read *, tempwri
        if ((tempwri .ne. 1) .and. (tempwri .ne. 0)) goto 30
        print *, 'Time(y=1/n=0)?'
        read *, timwri
        if ((timwri .ne. 1) .and. (timwri .ne. 0)) goto 30
        print *, 'Zones(y=1/n=0)?'
        read *, zonwri
        if ((zonwri .ne. 1) .and. (zonwri .ne. 0)) goto 30
        print *, 'voltage(y=1/n=0)?'
        read *, volwri
        if ((volwri .ne. 1) .and. (volwri .ne. 0)) goto 30
        print *, 'Gain(y=1/n=0)?'
        read *, gnwri
        if ((gnwri .ne. 1) .and. (gnwri .ne. 0)) goto 30
goto 16
31 frewri=1
timwri=1
tempwri=1
volwri=1
zonwri=1
        gnwri=1
        fwrite=0

c.....ASSIGNS THE DATA STARTING POINT TO THE .....
c.....HEATING STARTING POINT.....
c       srt=dtasrt
c       12 call tempad
c       srt=temp
c       if (aimt .le. srt) goto 13
c       if (aimt .gt. srt) goto 14
c       13 print *, 'The current temperature of your sample is'
c       print *, 'greater than your aim temperature. Please'
c       print *, 're-enter.'
c       goto 6
c       14 if (srt .le. dtasrt) goto 16
c       if (srt .gt. dtasrt) goto 15
c       15 print *, 'Your current temperature is greater than'
c       print *, 'the temperature at which you wanted to'
c       print *, 'start recording data. Please start over.'
c       goto 6

c.....FIND STARTING TIME.....
16 call gettim (hh,mm,ss,hd)
        oh=hh
        om=mm
        os=ss
```

```
        od=hd

c.....START MULTISTEP LOOP.....
        do 75 q=1, s
        done=0
        only2=0
        only3=0
        only4=0
        only5=0
        count=0

c.....BEGINNING OF MAIN LOOP.....

35      count=count+1
        print *,'step:',q
        print'(t5,A,i5)','Count:',count

c.....READ IN CURRENT TEMPERATURE.....
        call tempad
        call timchk
c..for heating.without a controlled rate.....
45      if(aimt(1,q) .gt. srt(1,q)) then
50      call heat(aimt(1,q),srt(1,q))
c...for cooling.at an input rate.....
        else
55      call cool (aimt(1,q),srt(1,q),rate(1,q))
        goto 70
        endif

c....CHECK FOR ISOTHERMAL
        if(abs(temp-aimt(1,q)).LE.(.2)) goto 70
65      goto 35
70      call ISO(isot,q,aimt(1,q))
75      continue

c.....REWIND AND CLOSE SEQUENTIAL FILE UNIT #1.....
        rewind(1)
        close (1)
100     end


        SUBROUTINE HEAT(aimt,srt)
c.....This subroutine finds the right frequency given
c.....current  temperature.....

c.....COMMON  STATEMENTS.....
        common fname
        common/jen/temp,volwri,zonwri,gnwri,tempwri,frewri
        common/jen2/done,timwri,fwrite
        common/fi/oh,om,os,od,setgn,rh,rm,rs,rd,only2,only3

c.....VARIABLES.....
        real acc,offval,temp,aimt,srt
        real zone1,zone2,zone3,zone4,zone5,zone6,zone7,zone8
```

```
      integer zonwri,done,freq,only2,only3,fwrite
      integer only4,only5
      parameter (acc=.1,offval=.75)
      freq=1
c.....FREQ WILL LATER BE CHANGED. 1 IS USED AS A FLAG ONLY..
      if ((done.ne.0) .and. (only2.eq.1)) goto 110
      if ((done.ne.0) .and. (only3.eq.1)) goto 120
      if ((done.ne.0).and.(only4.eq.1)) goto 130
      if ((done.ne.0).and.(only5.eq.1)) goto 140
c .....IF DONE = 1 THEN ZONES ARE ALREADY SET; SKIP OVER
c.....ZONE..CALCULATIONS.....
c.......ZONE INITIALIZATIONS TO SOME HIGH NUMBER.....
      zone1=10000
      zone2=10000
      zone3=10000
      zone4=10000
      zone5=10000
      zone6=10000
      zone7=10000
      zone8=10000

c.......ZONE  CALCULATIONS.....
      print *,'aimt',aimt,' srt: ',srt,' temp: ',temp
      diff = (aimt-srt)
      if (abs(diff) .le. acc) goto 130
      zone1 = (srt + (offval * diff))
      diff = aimt-zone1
      if (abs(diff) .le. acc) goto 130
      zone2 = (zone1 +(offval * diff))
      diff = aimt-zone2
      if (abs(diff).le. acc) goto 110
      zone3 = (zone2 +(offval * diff))
      diff = aimt-zone3
      if (abs(diff).le.acc) goto 120
      zone4 = (zone3 +(offval * diff))
      diff = aimt-zone4
      if (abs(diff).le.acc) goto 130
      zone5 = (zone4 +(offval * diff))
      diff = aimt-zone5
      if (abs(diff).le.acc) goto 140
      zone6 = (zone5 +(offval * diff))
      diff = aimt-zone6
      if (abs(diff).le.acc) goto 145
      zone7 = (zone6 +(offval * diff))
      diff = aimt-zone7
      if (abs(diff).le.acc) goto 145
      zone8 = (zone7 +(offval * diff))

c....110.(38)IS NEEDED WHEN THERE ARE ONLY TWO ZONES.....
      110 done = 1
      only2 = 1
      if (temp .LE. zone1) freq=113
      if (temp .gt. zone1) freq=80
      if (temp .GT. zone2) freq=0
```

```
        goto 150

c....120.(39)IS NEEDED WHEN THERE ARE ONLY THREE ZONES.....
        120 done = 1
        only3 = 1
        if (temp .LE. zone1) freq=340
        if (temp .gt. zone1) freq=113
        if (temp .gt. zone2) freq=80
        if (temp .GT. zone3) freq=0
        goto 150

c.....THIS IS THE NORMAL MODE; MORE THAN THREE ZONES...
        130 done = 1
        only4=1
        if (temp .LE. zone1) freq=409
        if (temp .GT. zone1) freq=227
        if (temp .GT. zone2) freq=113
        if (temp .GT. zone3) freq=80
        if (temp .GT. zone4) freq=0
        if (temp .GT. zone5) freq=0
        if (temp .GT. zone6) freq=0
        if (temp .GT. zone7) freq=0
        if (temp .GT. zone8) freq=0
        goto 150
c       This is for more than 4 zones
        140   done=1
        only5=1
        if (temp .LE. zone1) freq=409
        if (temp .GT. zone1) freq=340
        if (temp .GT. zone2) freq=186
        if (temp .GT. zone3) freq=92
        if (temp .GT. zone4) freq=0
        if (temp .GT. zone5) freq=0
        if (temp. GT. zone6) freq=0
        if (temp .GT. zone7) freq=0
        if (temp .GT. zone8) freq=0
        goto 150
c       This is for more than 5 zones
        145     done=1
        if (temp .LE. zone1) freq=450
        if (temp .GT. zone1) freq=409
        if (temp .GT. zone2) freq=340
        if (temp .GT. zone3) freq=272
        if (temp .GT. zone4) freq=113
        if (temp .GT. zone5) freq=0
        if (temp .GT. zone6) freq=0
        if (temp .GT. zone7) freq=0
        if (temp .GT. zone8) freq=0
        150     if (zonwri.eq.1) goto 165
        if (zonwri.eq.0) goto 170
        155     format (t5,A,f20.7,f20.7,f20.7)
        160     format (t5,A,f20.7,f20.7)
        165     write (*,155) 'Zones 1-3',zone1,zone2,zone3
        write (*,155) 'Zones 4-6',zone4,zone5,zone6
```

```
        write (*,160) 'Zones 7-8', zone7,zone8
        170     call freqset (freq)
        199 end


        SUBROUTINE FREQSET(freq)
$NOTRUNCATE
c.....This controls turning on & off of heater based on the
c.....frequency values in the following way :
c.....freq=0,  0 seconds, freq=23, .05 seconds
c       freq=46, .10 seconds, freq=113, .25 seconds
c       freq=227, .50 seconds,freq=272, .60 seconds
c       freq=340, .75 seconds, freq=409, .90 seconds

c.....COMMON STATEMENTS
        common fname
        common/jen/temp,volwri,zonwri,gnwri,tempwri,frewri
        common/jen2/done,timwri,fwrite
        common/fi/oh,om,os,od,setgn,rh,rm,rs,rd,only2,only3

c.....VARIABLES
        integer freq,freq2,setgn,rh,rm,rs,rd
        integer hh,mm,ss,hd,timwri,frewri,fwrite
        real temp,tmin
c       THis flag, fwrite saves only every 10th data point
c       fwrite = fwrite+1
210     if (freq.eq.0) goto 230
        call enable_for_output (0)

c.....TURN ON HEATER FOR DESIRED DURATION
        call output_digital_value(0,16,255)
        do 220 k=1,freq
c.....loop to take up time
        call enable_for_output (0)
        call gettim(hh,mm,ss,hd)
220     continue
230     call enable_for_output(0)

c.....SHUT OFF HEATER FOR REMAINING TIME OF SECOND
        call output_digital_value(0,16,0)
        freq2=454-freq
        do 240 m=1,freq2
        call enable_for_output(0)
        call gettim(hh,mm,ss,hd)
240     continue

c.....PRINTING OPTIONS
        if (frewri.eq.1) goto 245
        if (frewri.eq.0) goto 246
245     print  '(T5,A,i3)','Freq:',freq
246     if (timwri.eq.1) goto 247
        if (timwri.eq.0) goto 249
247     print'(t5,i2,A,i2,A,i2,A,i2)',hh,':',mm,':',ss,':',hd
249     tmin=((rh*60*60*100)+(rm*60*100)+(rs*100)+rd)/6000.0
```

```
c       if((fwrite/5.0) .NE.(int(fwrite/5.))) goto 298

c.....WRITE INFO TO FILE
250     format(3x,i3,A,i2,A,i2,A,i2,5x,F12.8,8x,i4,8x,i4,f12.4)
255     write (1,250) rh,':',rm,':',rs,':',rd,temp,freq,setgn,tmin
298     print  *,'.....'
299     end



        SUBROUTINE TEMPAD
$NOTRUNCATE
c.......The goal of this subroutine will be to read the adc.
c.......value from the thermocouple, convert this value to..
c.......voltage,and convert voltage to temperature.....

c.......VARIABLES.....
        common fname
        common/jen/temp,volwri,zonwri,gnwri,tempwri,frewri
        common/jen2/done,timwri,fwrite
        common/fi/oh,om,os,od,setgn,rh,rm,rs,rd,only2,only3
        integer trans,setgn,trans2,volwri,zonwri,gnwri,tempwri
        integer fwrite,avg
        real voltavg,totvolt
        real fvl,volt,volt2,temp,trans3,setgn2,atemp,btemp

c.......MAIN SECTION OF SUBROUTINE TEMPAD.....
        totvolt=0
        call adc_value(2,1,trans)
300     if ((trans.gt.400) .and. (trans.le.4096)) goto 310
        if ((trans.le.400) .and. (trans.ge.40)) goto 320
        if ((trans.lt.40) .and. (trans.ge.8)) goto 330
        if ((trans.lt.8) .and. (trans .ge.1)) goto 340
        if (trans.eq.0) goto 350
310     setgn=1
        goto 365
320     setgn=10
        goto 365
330     setgn=100
        goto 365
340     setgn=500
        goto 365
350     print '(t5,A)', 'Adc value has been measured at zero.'
360     goto 399

c       ADD LOOP TO AVG 50 VOLTAGE READINGS TO COMPUTE TEMP
365     do 391 avg=1,50
370     if (gnwri .eq. 1) goto 380
        if (gnwri .eq. 0) goto 390
380     print '(T5,A,i5)', 'gain=',setgn
390     call adc_value(2,setgn,trans2)
        print *, 'trans2: ',trans2
        trans3=trans2
        volt=(trans3*10.0)/4096.0
```

```
      setgn2=setgn
      volt2=(volt/setgn2)
      totvolt=totvolt+volt2
391   continue
      voltavg=totvolt/50
c.....VOLTAGE IS NOW IN VOLTS.....
      fvl=(voltavg*1000.0)
c     fvl=(volt2      *1000.0)
c.....VOLTAGE IS NOW IN MILLIVOLTS.....
c     new calibration 10/25/91 20-151C
      atemp=((-217.27+(1.1776*fvl)-(.0014451*fvl*fvl)))
      btemp=(.000000851053*fvl*fvl*fvl)
      temp=(atemp+btemp)
      if (volwri .eq. 1) goto 392
      if (volwri .eq. 0) goto 399
      392     print '(t5,A,f12.8)', 'voltage(millivolts)=', fvl
      if (tempwri .eq. 1) goto 393
      if (tempwri .eq. 0) goto 394
      393 print *, 'temp(C)=', temp
      394 return
      399 end

      SUBROUTINE TIMCHK
c     This subroutine computes the time difference between
c     starting time and the current time by calling time
c     from the internal clock.
      integer  hh,mm,ss,hd,rh,rm,rs,rd,oh,om,os,od
      common fname
      common/jen/temp,volwri,zonwri,gnwri,tempwri,frewri
      common/jen2/done,timwri,fwrite
      common/fi/oh,om,os,od,setgn,rh,rm,rs,rd,only2,only3
      integer fwrite
      call gettim (hh,mm,ss,hd)
      rh=(hh-oh)
      rm=(mm-om)
      rs=(ss-os)
      rd=(hd-od)
      if (rd.ge.0) goto 400
      rd=(100+rd)
      rs=rs-1
      400 if (rs.ge.0) goto 410
      rs=(60+rs)
      rm=rm-1
      410 if (rm.ge.0) goto 420
      rm=(60+rm)
      rh=rh-1
      420 end

      SUBROUTINE ISO(isot,q,aimt)
$NOTRUNCATE
c....This subroutine holds the temperature steady for a c....given amount of time
      common fname
      common/jen/temp,volwri,zonwri,gnwri,tempwri,frewri
      common/jen2/done,timwri,fwrite
```

```
      common/fi/oh,om,os,od,setgn,rh,rm,rs,rd,only2,only3
      real acc,temp,diff,aimt
      dimension isot(4,20)
      integer tim,atim,ah,am,as,ad,hh,mm,ss,dd,freq,freq2
      integer rh,rm,rs,rd,ih,im,is,id,setgn
      integer isot,q,fwrite
      parameter (acc=.1)
      call timchk
      print *,'Isotherm started at',rh,':',rm,':',rs,':',rd

c     CALCULATE ISOTHERMAL TIME
      ih=isot(1,q)
      im=isot(2,q)
      is=isot(3,q)
      id=isot(4,q)
      ah=rh+ih
c     print *,'ah=',ah
      am=rm+im
c     print *,'am=',am
      as=rs+is
c     print *,'as=',as
      ad=rd+id
530   if(ad.lt.100) goto 550
      ad=ad-100
      as=as+1
550   if(as.lt.60) goto 560
      as=as-60
      am=am+1
560   if (am.lt.60) goto 570
      am=am-60
      ah=ah+1
c     PUT TIME & ISOTIME INTO INTEGER VALUES
570   tim=(rh*60*60*100)+(rm*60*100)+(rs*100)+rd
      atim=(ah*60*60*100)+(am*60*100)+(as*100)+ad
      print *, 'tim',tim
      print *, 'atim',atim

c     LOOP TO CHECK TEMP & KEEP STEADY FOR ISOTHERM
      do 580 t=tim,atim
      call timchk
      print  *,'Time',  rh,':',rm,':',rs,':',rd
      tim=(rh*60*60*100)+(rm*60*100)+(rs*100)+rd
      call tempad
      diff=temp-aimt
      if (abs(diff).le.acc) freq=0
      if (diff.ge.acc) freq=0
      if ((diff.gt.(-.2)).AND.(diff.le.(-.1))) freq=92
      if ((diff.gt.(-.4)).AND.(diff.le.(-.2))) freq=120
      if ((diff.gt.(-.7)).AND.(diff.le.(-.4))) freq=150
      if ((diff.gt.(-.9)).AND.(diff.le.(-.7))) freq=184
      if ((diff.le.(-.9))) freq=272
      call freqset(freq)
      if (tim.ge.atim) goto 599
580   continue
```

```
599     end


        SUBROUTINE COOL(aimt,srt,rate)
c.....This gives cooling at rates given by user

c....COMMON STATEMENTS
        common fname
        common/jen/temp,volwri,zonwri,gnwri,tempwri,frewri
        common/jen2/done,timwri,fwrite
        common/fi/oh,om,os,od,setgn,rh,rm,rs,rd,only2,only3

c....VARIABLES
        integer initim,tottim,freq,time,t,time1,time2
        integer freq2,setgn,rh,rm,rs,rd,fwrite
        real aimt,srt,rate,deltemp1,temp,deltim1,diff1,rate2
        real temp2,deltemp,diff2,rate3
        real temp1

c ....SETUP INITIAL VALUES
        print *,'rate:';rate
        rate2=rate/(60*100)
        print *, 'rate2:', rate2
        call TIMCHK
        time1 = (rh*60*60*100)+(rm*60*100)+(rs*100)+rd
        initim=(rh*60*60*100)+(rm*60*100)+(rs*100)+rd
        tottim=initim+((srt-aimt)/rate)*60*100
        call TEMPAD
        temp1=temp
                temp2=temp
                time2=0

c       LOOP FOR COOLING AT RATE DETERMINED BY THE ACTUAL TIME
c       AND TEMPERATURE DIFFERENCES
        do 600 t=initim,tottim
        call TIMCHK
        time = (rh*60*60*100)+(rm*60*100)+(rs*100)+rd
        deltim2=time-time1
                diff1=time-time2
        if(int(deltim).eq.0) then
        diff2=100
        else
        diff2=deltim2
        endif
        call TEMPAD
c....CALCULATE THE RATE AS POSITIVE #
        deltemp=temp1-temp
                deltemp1=temp2-temp
                rate=deltemp/diff2
                rate3=deltemp1/diff1
        print *,'deltim:',deltim2,'deltemp:',deltemp
        print *,'rate:',rate

        if((rate.LT.rate2).AND.(rate3.LT.rate2))    freq=0
```

```
      if((rate.LT.rate2).AND.(rate3.LT.rate2))      freq=0
      if((rate.GT.(.10*rate2)).AND. (rate3.GT.(.10*rate2))) freq=46
      if((rate.GT.(.20*rate2)).AND.(rate3.GT.(.20*rate2))) freq=64
      if((rate.GT.(.40*rate2)).AND.(rate3.GT.(.40*rate2))) freq=80
      if((rate.GT.(.60*rate2)).AND.(rate3.GT.(.60*rate2))) freq=100
      if((rate.GT.(.80*rate2)).AND.(rate3.GT.(.80*rate2))) freq=120
      if ((rate.GT.(rate2)).AND.(rate3.GT.rate2))  freq=150
      if((time.GE.tottim).AND. (temp.LE.aimt)) goto 699
      610     call FREQSET(freq)
              time2=time1
              temp2=temp1
      temp1=temp
      time1=time
600   continue
699   end
```

BIBLIOGRAPHY

Alexander, L. E.; *X-Ray Diffraction Methods in Polymer Science*; Robert E. Krieger: Malabar, FL, 1969.

Antoon, M. K.; D'Esposito, L.; Koenig, J. L. *Appl. Spectrosc.*, **1979**, *33*, 351.

Bartenev, G. M.; Remizova, A. A.; Kuleshov, I. V.; Martynov, M. A.; Sarminskaya, T. N. *Polym. Sci., USSR*, **1975**, *17*, 2381.

Bassett, D. C.; *Principles of Polymer Morphology*; Cambridge University: London, 1981.

Boerio, F. J.; Koenig, J. L. *J. Polym. Sci.*, **1971**, *A2*, 1517.

Bongianni, W. *Ferroelectrics*, **1990**, *103*, 57.

Bourgaux-Leonard, C.; Legrand, J. F.; Renault, A.; Delzenne, P. *Polymer*, **1991**, *32*, 597.

Burchell, D. J.; Hsu, S. L. *Polymer*, **1981**, *22*, 907.

Danz, R. *Polym. Bull.*, **1982**, *7*, 497.

Das-Gupta, D. K. *Ferroelectrics*, **1991**, *118*, 165.

Davis, G. T.; *The Applications of Ferroelectric Polymers;* T. T. Wang, J. M. Herbert and A. M. Glass, ed.; Chapman and Hall: New York, 1988; p 37.

Davis, G. T.; McKinney, J. E.; Broadhurst, M. G.; Roth, S. C. *J. Appl. Phys.*, **1978**, *49*, 4998.

Doll, W. W.; Lando, J. B. *J. Macromol. Sci.- Phys.*, **1968**, *B2*, 219.

Farmer, B. L.; Hopfinger, A. J.; Lando, J. B. *J. Appl. Phys.*, **1972**, *49*, 1232.

Fernandez, M. V.; Suzuki, A.; Chiba, A. *Macromolecules*, **1987**, *20*, 1806.

Furukawa, T. *IEEE Trans. El. Ins.*, **1989**, *24*, 375.

Furukawa, T.; Wang, T. T.; *The Applications of Ferroelectric Polymers;* T. T. Wang, J. M. Herbert and A. M. Glass, ed.; Chapman and Hall: New York, 1988; p 64.

Green, J. S.; Farmer, B. L.; Rabolt, J. F. *J. Appl. Phys.*, **1986**, *60*, 2690.

Hasegawa, R.; Takahashi, Y.; Chatani, Y.; Tadokoro, H. *Polymer J.*, **1972**, *3*, 600.

Hendra, P.; Jones, C.; Warnes, G.; *Fourier Transform Raman Spectroscopy: Instrumental and Chemical Applications*; Ellis Horwood: New York, 1991.

Hermans, J. J.; Hermans, P. H.; Vermaas, D.; Weidinger, A. *Rec. Trav. Chim.*, **1946**, *65*, 427.

Higashihata, Y.; Sako, J.; Yagi, T. *Ferroelectrics*, **1981**, *32*, 85.

Ikeda, S.; Shimojima, Z.; Kutani, M. *Ferroelectrics*, **1990**, *109*, 297.

Janke, A.; Künstler, W.; Geiss, D.; Danz, R.; Stark, W.; *Morphology of Polymers;* B. Sedlacek, ed.; Walter de Gruyter & Co.: New York, 1986; p 673.

Jasse, B.; Koenig, J. L. *J. Macromol. Sci.-Rev. Macromol. Chem.*, **1979**, *C17*, 61.

Karasawa, N.; Goddard, W. A., III *Macromolecules*, **1992**, *25*, 7268.

Kim, K. J.; Reynolds, N. M.; Hsu, S. L. *Macromolecules*, **1989**, *22*, 4395.

Kim, K. J.; Reynolds, N. M.; Wang, Y. K.; Antolin, K.; Hsu, S. L.; Stidham, H. D. *submitted.*

Kobayashi, M.; Tashiro, K.; Tadokoro, H. *Macromolecules*, **1975**, *8*, 158.

Koga, K.; Nakano, N.; Hattori, T.; Ohigashi, H. *J. Appl. Phys.*, **1990**, *67*, 965.

Koga, K.; Ohigashi, H. *J. Appl. Phys.*, **1986**, *59*, 2142.

Lando, J. B.; Doll, W. W. *J. Macromol. Sci.-Phys.*, **1968**, *B2*, 205.

Latour, M.; Almairac, R.; Moreira, R. L. *IEEE Trans. Electrical Insul.*, **1989**, *24*, 443.

Legrand, J. F. *Ferroelectrics*, **1989**, *91*, 303.

Li, G. R.; Kagami, N.; Ohigashi, H. *J. Appl. Phys.*, **1992**, *72*, 1056.

Lopez Cabarcos, E.; Gonzalez Arche, A.; Baltá Calleja, F. J.; Bösecke, P.; Röber, S.; Bark, M.; Zachmann, H. G. *Polymer*, **1991**, *32*, 3097.

Lovinger, A. J. *Polymer*, **1980**, *21*, 1317.

Lovinger, A. J. *J. Polym. Sci., Polym. Phys. Ed.*, **1980**, *18*, 793.

Lovinger, A. J. *Polymer*, **1981**, *22*, 412.

Lovinger, A. J. *Macromolecules*, **1981**, *14*, 225.

Lovinger, A. J.; *Developments in Crystalline Polymers-1;* D. C. Bassett, ed.; Applied Science: London, 1982; p 195.

Lovinger, A. J.; Davis, D. D.; Cais, R. E.; Kometani, J. M. *Polymer*, **1987**, *28*, 617.

Lovinger, A. J.; Davis, G. T.; Furukawa, T.; Broadhurst, M. G. *Macromolecules*, **1982**, *15*, 323.

Lovinger, A. J.; Furukawa, T.; Davis, G. T.; Broadhurst, M. G. *Polymer*, **1983**, *24*, 1233.

Lovinger, A. J.; Furukawa, T.; Davis, G. T.; Broadhurst, M. G. *Polymer*, **1983**, *24*, 1225.

Lu, F. J.; Hsu, S. L. *Macromolecules*, **1986**, *19*, 326.

Maliknowski, E. R. *Anal. Chim. Acta*, **1982**, *134*, 129.

Maliknowski, E. R.; Howery, D. G.; *Factor Analysis in Chemistry*; Wiley-Interscience: New York, 1980.

Mancarella, C.; Martuscelli, E. *Polymer*, **1977**, *18*, 1240.

Mandelkern, L.; *Crystallization of Polymers*; McGraw-Hill: New York, 1964.

Marand, H.; Stein, R. S. *J. Poly. Sci., Polym. Phys. Ed.*, **1989**, *27*, 1089.

Marand, H.; Stein, R. S. *Macromolecules*, **1989**, *22*, 444.

Marand, H. L., Ph.D. Dissertation, University of Massachusetts, **1988**.

Marand, H. L.; Stein, R. S.; Stack, G. M. *J. Polym. Sci., Polym. Phys. Ed.*, **1988**, *26*, 1361.

Moreira, R. L.; Almairac, R.; Latour, M. *J. Phys.: Condens. Matter*, **1989**, *1*, 4273.

Moreira, R. L.; Saint-Gregoire, P.; Latour, M. *Phase Transitions*, **1989**, *14*, 243.

Moreira, R. L.; Saint-Gregoire, P.; Lopez, M.; Latour, M. *J. Polym. Sci., Polym. Phys. Ed.*, **1989**, *27*, 709.

Nakamura, S.; Sasaki, T.; Funamoto, J.; Matsuzuki, K. *Die Makromol. Chemie*, **1975**, *176*, 3471.

Nalwa, H. S. *J.M.S.-Rev. Macromol. Chem. Phys.*, **1991**, *C31*, 341.

Ohigashi, H.; Kagami, N.; Li, G. R. *J. Appl. Phys.*, **1992**, *71*, 506.

Oka, Y.; Murata, Y.; Koizumi, N. *Polymer J.*, **1986**, *18*, 417.

Osaki, S.; Ishida, Y. *J. Polym. Sci., Polym. Phys. Ed.*, **1975**, *13*, 1071.

Ozawa, T. *Polymer*, **1971**, *12*, 150.

Prest, W. M., Jr.; Luca, D. J. *J. Appl. Phys.*, **1975**, *46*, 4136.

Prest, W. M., Jr.; Luca, D. J. *J. Appl. Phys.*, **1978**, *49*, 5042.

Reynolds, N. M., Ph.D. Dissertation, University of Massachusetts, **1990**.

Reynolds, N. M.; Kim, K. J.; Chang, C.; Hsu, S. L. *Macromolecules*, **1989**, *22*, 1092.

Russell, T. P.; Koberstein, J. T. *J . Polymer Sci., Polym. Phys. Ed.*, **1985**, *23*, 1109.

Samuels, R. J.; *Structured Polymer Properties*; Wiley-Interscience: New York, 1974.

Servet, B.; Broussoux, D.; Micheron, F. *J. Appl. Phys.*, **1981**, *52*, 5926.

Sessler, G. M.; Das-Gupta, D. K.; DeReggi, A. S.; Eisenmenger, W.; Furukawa, T.; Giacometti, J. A.; Gerhard-Multhaupt, R. *IEEE Trans. Electr. Insul.*, **1992**, *27*, 872.

Shimada, T.; Zachariades, A. E.; Mead, W. T.; Porter, R. S. *J. Crystal Growth*, **1980**, *48*, 334.

Shurvell, H. F.; Bulmer, J. T.; *Vibrational Spectra and Structure;* J. R. Durig, ed.; Elsevier Scientific: New York, 1977; p 91.

Stack, G. M.; Ting, R. Y. *J. Polym. Sci., Polym. Phys. Ed.*, **1988**, *26*, 55.

Stein, R. S. *J. Polym. Sci.*, **1958**, *31*, 327.

Tanaka, H.; Yukawa, H.; Nishi, T. *Macromolecules*, **1988**, *21*, 2469.

Tashiro, K.; Itoh, Y.; Kobayashi, M.; Tadokoro, H. *Macromolecules*, **1985**, *18*, 2600.

Tashiro, K.; Kobayashi, M. *Polymer*, **1986**, *27*, 667.

Tashiro, K.; Kobayashi, M. *Rep. Prog. Polym. Phys. Jpn.*, **1987**, *30*, 119.

Tashiro, K.; Kobayashi, M. *Polymer*, **1988**, *29*, 426.

Tashiro, K.; Kobayashi, M. *Phase Transitions*, **1989**, *18*, 213.

Tashiro, K.; Takano, K.; Kobayashi, M.; Chatani, Y.; Tadokoro, H. *Polymer*, **1981**, *22*, 1312.

Tashiro, K.; Takano, K.; Kobayashi, M.; Chatani, Y.; Tadokoro, H. *Ferroelectrics*, **1984**, *57*, 297.

Tashiro, K.; Takano, K.; Kobayashi, M.; Chatani, Y.; Tadokoro, H. *Polymer*, **1984**, *25*, 195.

Walsiak, A. *Chemtracts-Macro. Chem.*, **1991**, *2*, 211.

Weinhold, S.; Litt, M. H.; Lando, J. B. *Macromolecules*, **1980**, *13*, 1178.

Welch, G. J.; Miller, R. L. *J. Polym. Sci., Polym. Phys. Ed.*, **1976**, *14*, 1683.

Wunderlich, B.; *Macromolecular Physics Vol.1*; Academic Press: New York, 1973.

Wunderlich, B.; *Macromolecular Physics Vol. 2*; Academic Press: New York, 1976.

Yadav, Y. S.; Jain, P. C. *J. Macromol. Sci.-Phys.*, **1986**, *B25*, 335.

Yagi, T.; Tatemoto, M. *Polymer J.*, **1979**, *11*, 429.

Yagi, T.; Tatemoto, M.; Sako, J. *Polym. J.*, **1980**, *12*, 209.

Zbinden, R.; *Infrared Spectroscopy of High Polymers*; Academic Press: New York, 1964.